

Scientific Imaging Sensors

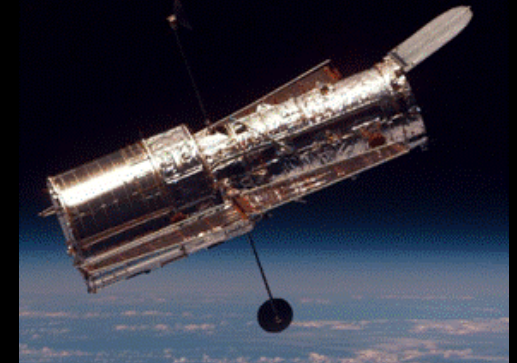


A Short Course presented at the
“Detectors for Astronomy” workshop
Garching, Germany



12 October 2009

James W. Beletic and Markus Loose





2009 Nobel Prize in Physics awarded to the inventors of the CCD

In 1969, Willard S. Boyle and George E. Smith invented the first successful imaging technology using a digital sensor, a CCD (charge-coupled device). The two researchers came up with the idea in just an hour of brainstorming.



Bell Labs researchers Willard Boyle (left) and George Smith (right) with the charge-coupled device.

Photo taken in 1974. Photo credit: Alcatel-Lucent/Bell Labs.



The Nobel Prize in Physics 2009

"for the invention of an imaging semiconductor circuit – the CCD sensor"



Willard S. Boyle



George E. Smith

Credits and sincere thanks to all contributing parties

Presentations from the workshop entitled “Scientific Detectors for Astronomy 2005”

- CCDs: Barry Burke, Paul Jorden, Paul Vu
- CMOS: Markus Loose, Alan Hoffman, Vyshnavi Suntharalingham
- Pan-STARRS: John Tonry

For reference, see workshop proceedings: *Scientific Detectors for Astronomy 2005*, Jenna E. Beletic, James W. Beletic and Paola Amico (editors), Springer, (2006).

Other sources

- Slide set used in presentations at the NATO Advanced Studies Institute – Corsica (2002)
For reference, see: “Optical and infrared detectors for astronomy: basic principles to state-of-the-art”, James W. Beletic, chapter in book from the NATO Summer School: *Optics in Astrophysics*, Renaud Foy (editor), NATO Sciences Series II, Springer (2004).
- James Janesick CCD Course Notes
- “Substrate Removed HgCdTe-Based Focal Plane Arrays for Short Wavelength Infrared Astronomy”, by Eric Piquette et al (2007)
- Wikipedia and other Internet sites
- Individual slides as identified in the presentation

Disclaimer

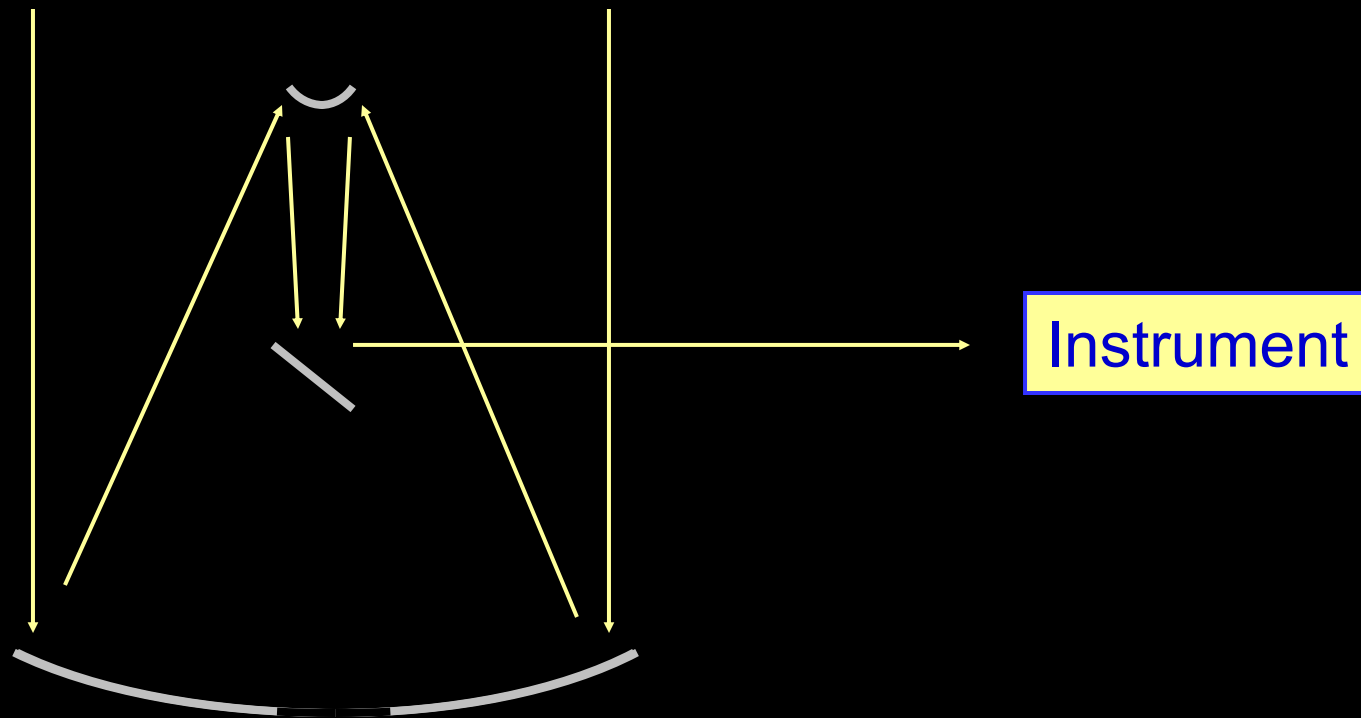
- All information presented in this slide set is accurate according to the best knowledge of the authors (James Beletic and Markus Loose). Any errors in content or presentation are solely due to the authors, and not the persons listed above.

Optical and Infrared Astronomy (0.3 to 25 μm)

Two basic parts

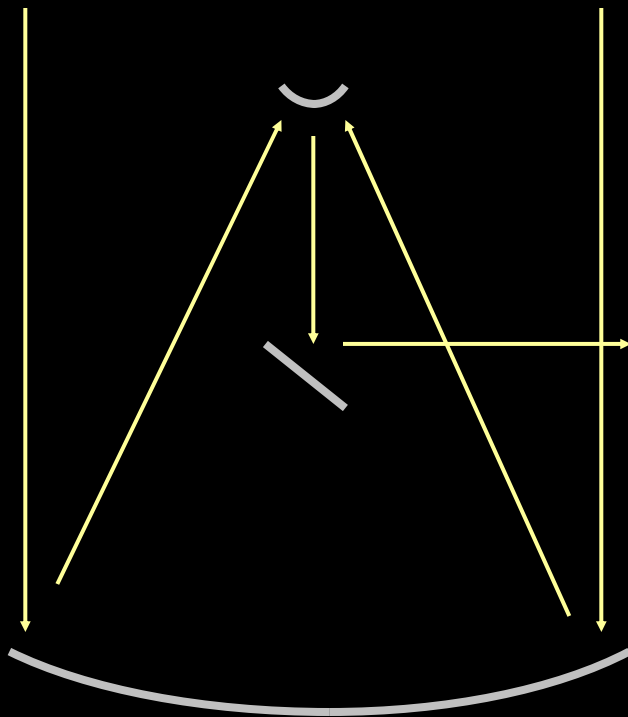
Telescope to collect and focus light

Instrument to measure light



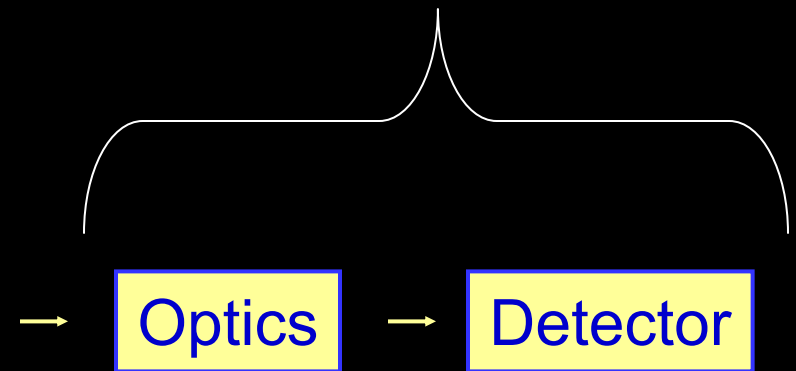
Optical and Infrared Astronomy (0.3 to 25 μm)

Telescope to collect and focus light

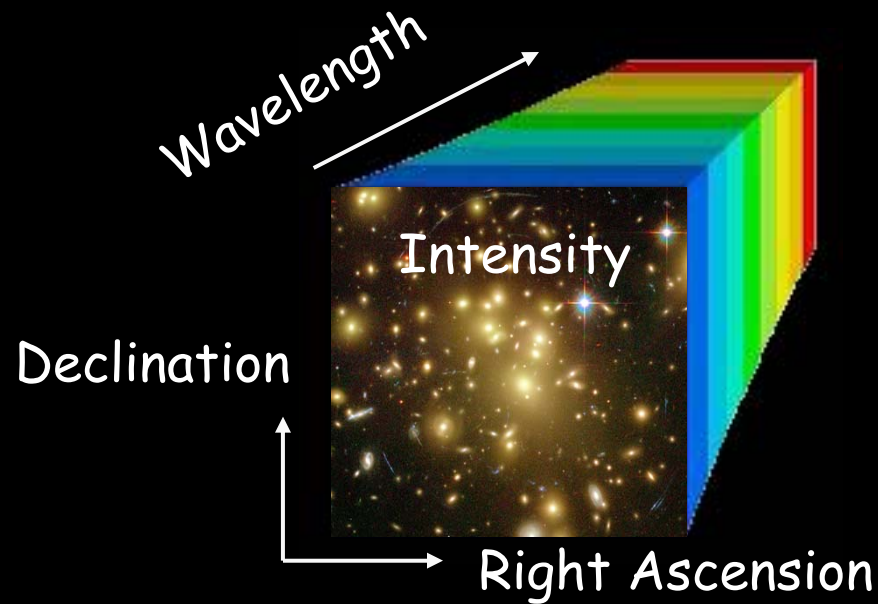


Adaptive
Optics

Instrument to measure light



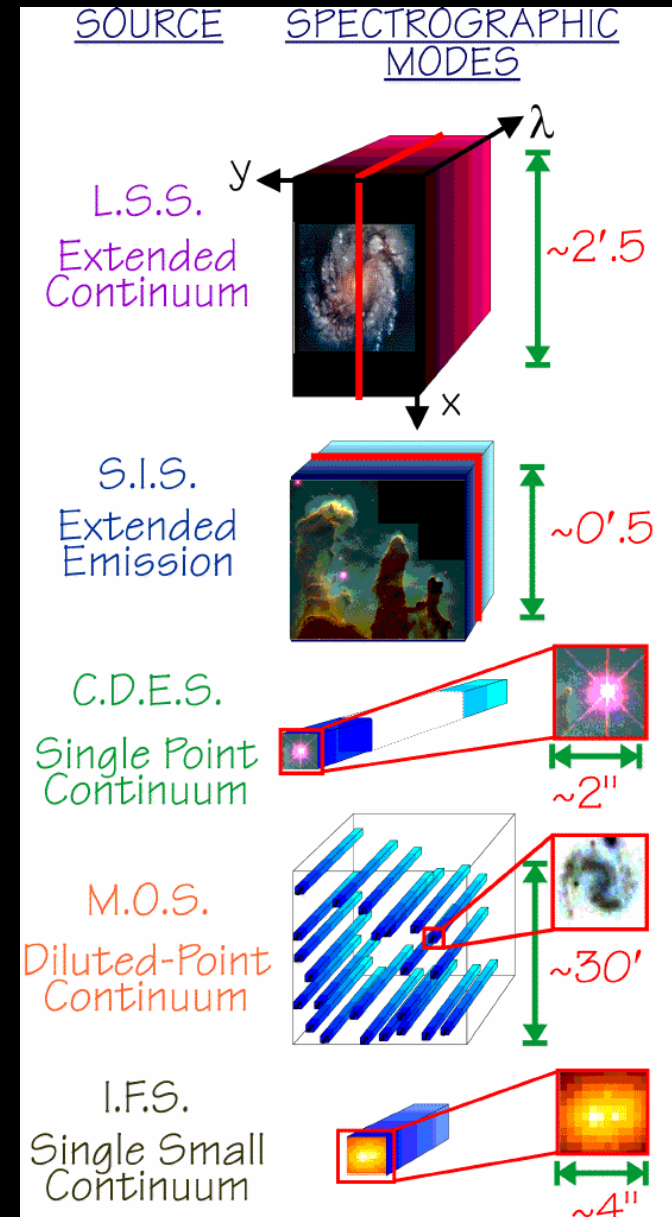
Instrument goal is to measure a 3-D data cube



But most detectors are 2-dimensional !

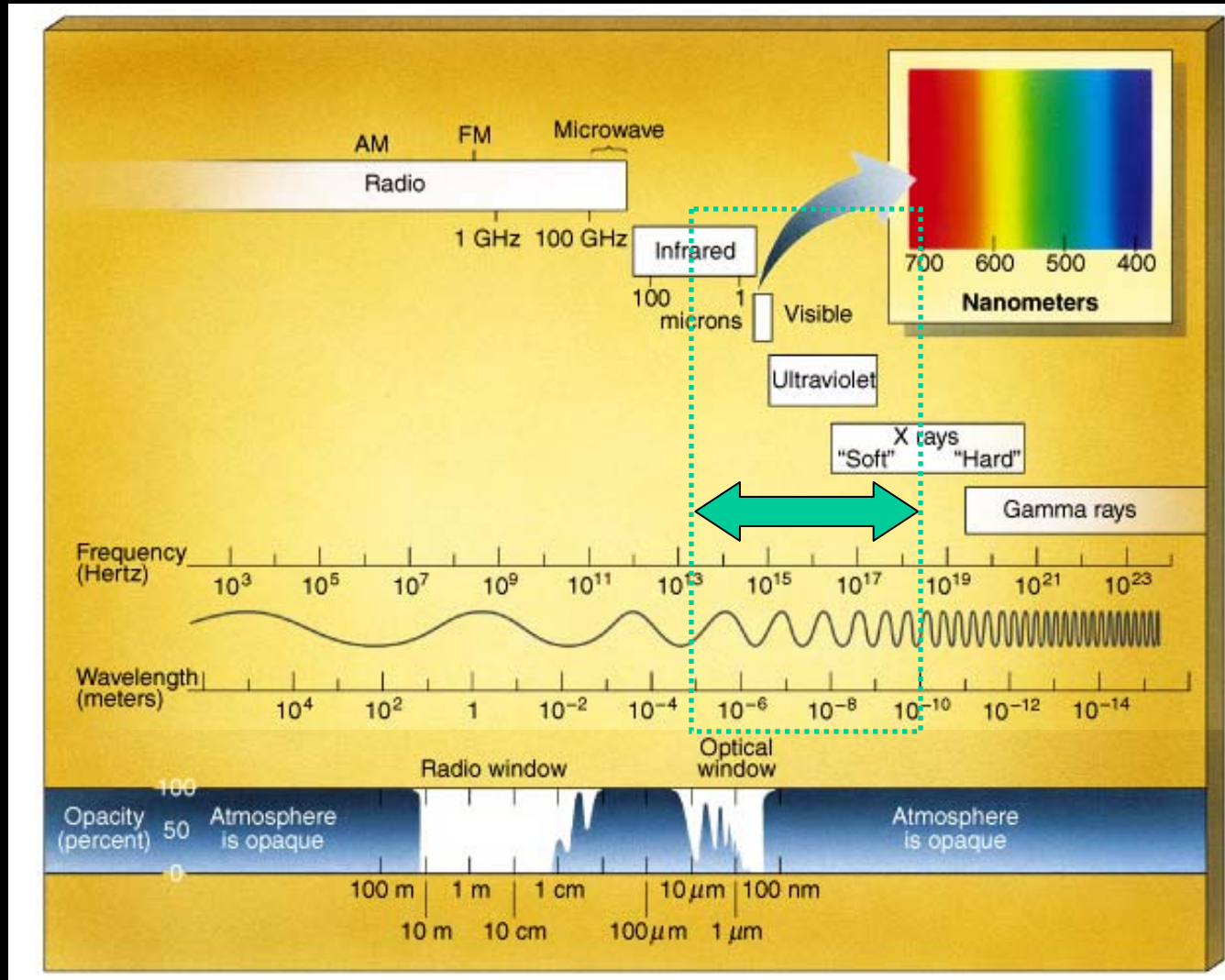
- Detectors are **BLACK & WHITE**
- Can not measure color
- Only measure intensity

Optics of the instrument are used to map a portion of the 3-D data cube onto the 2-D detector

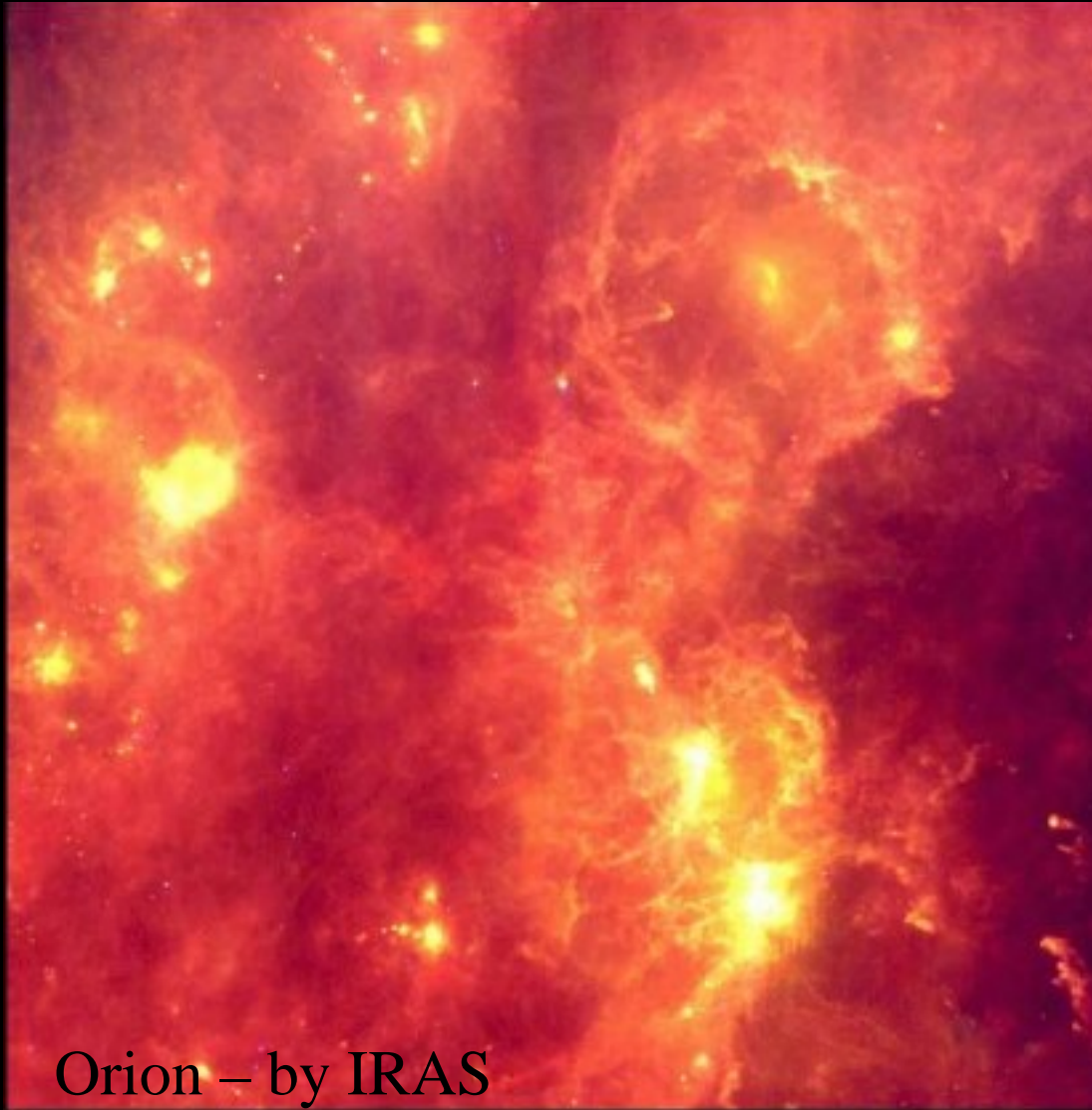


With appropriate apologies to Foveon and 3rd Gen IR

The Electromagnetic Spectrum

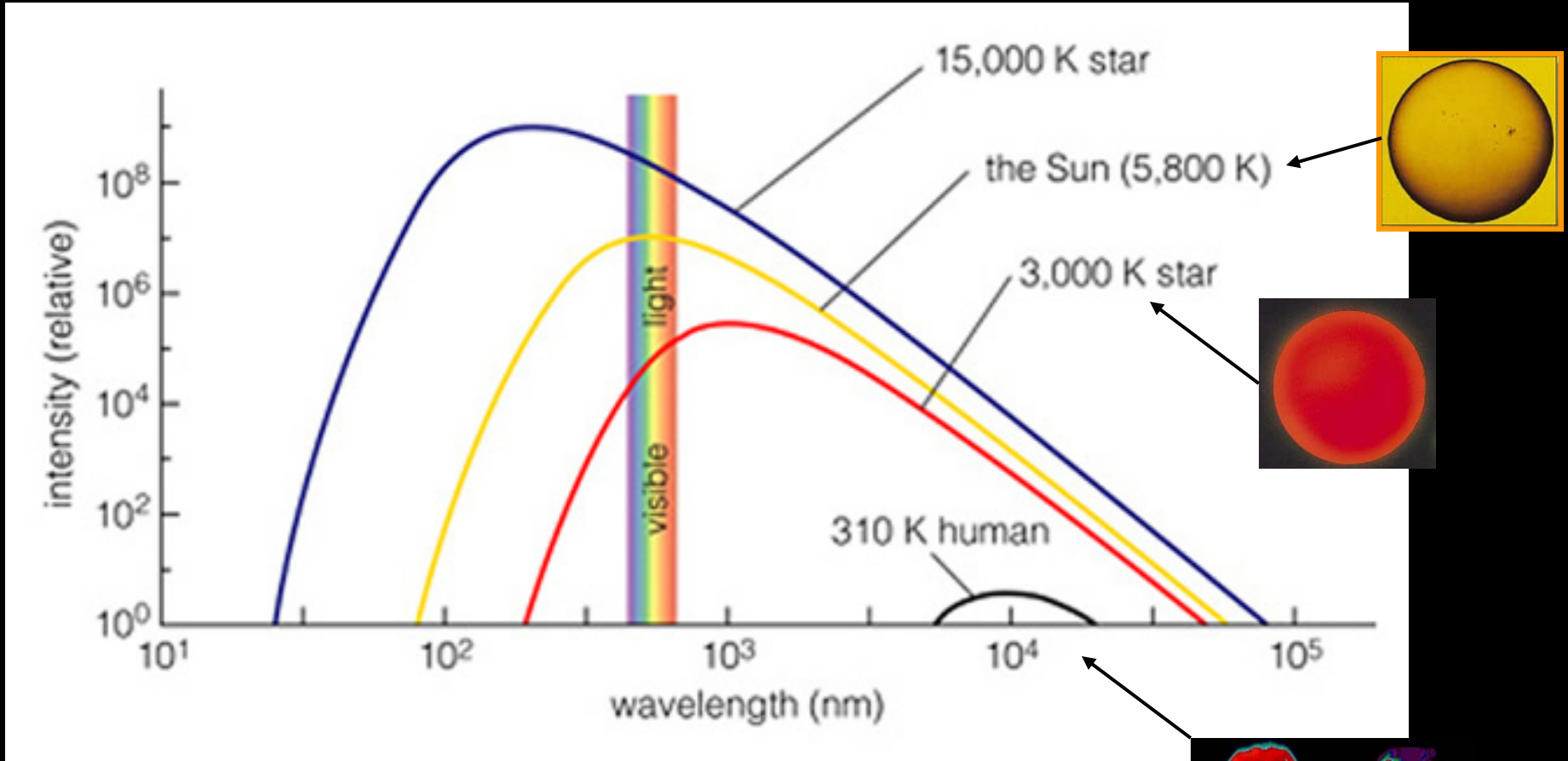


Orion - In visible and infrared light



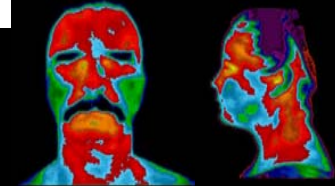
Orion - by IRAS

Temperature and Light



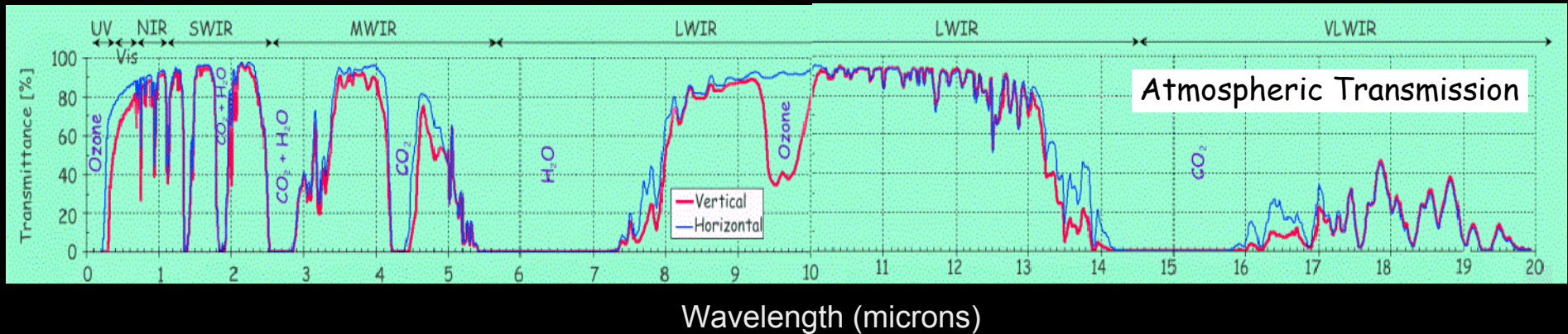
Ultraviolet

Infrared



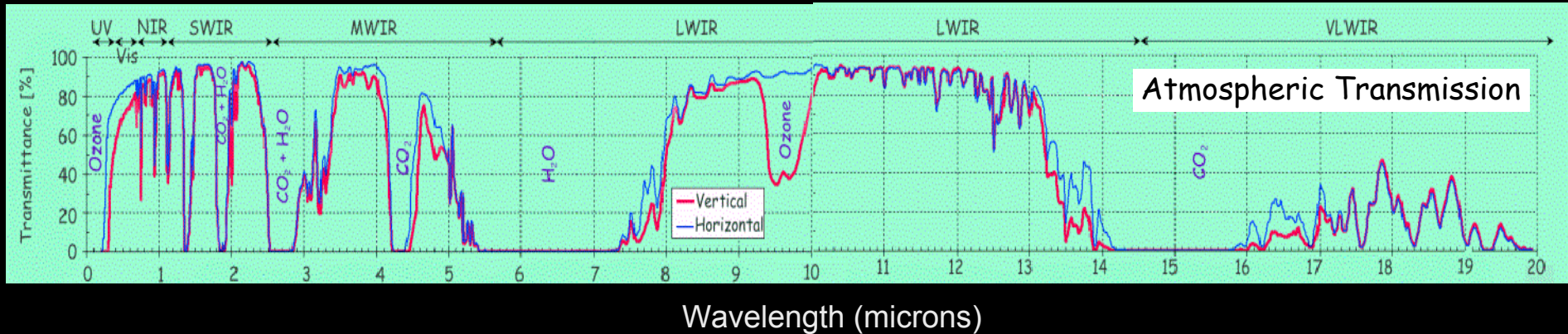
Atmospheric transmission

Not all of the light gets through atmosphere to ground-based telescopes

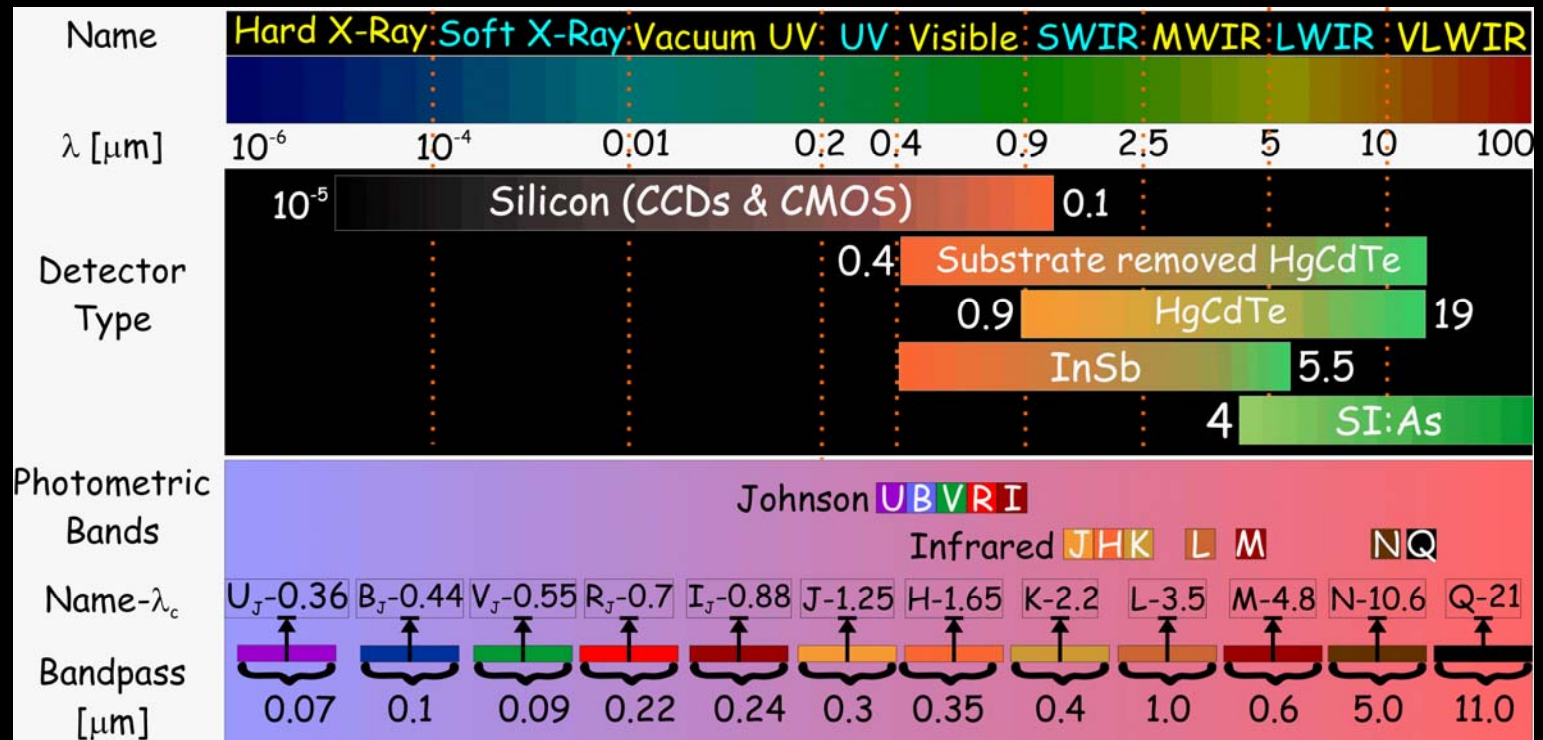


Spectral Bands

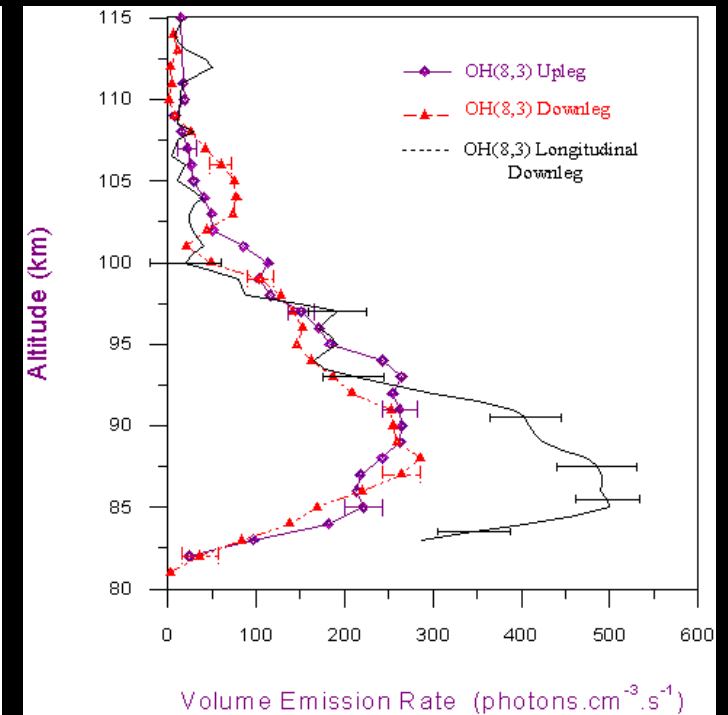
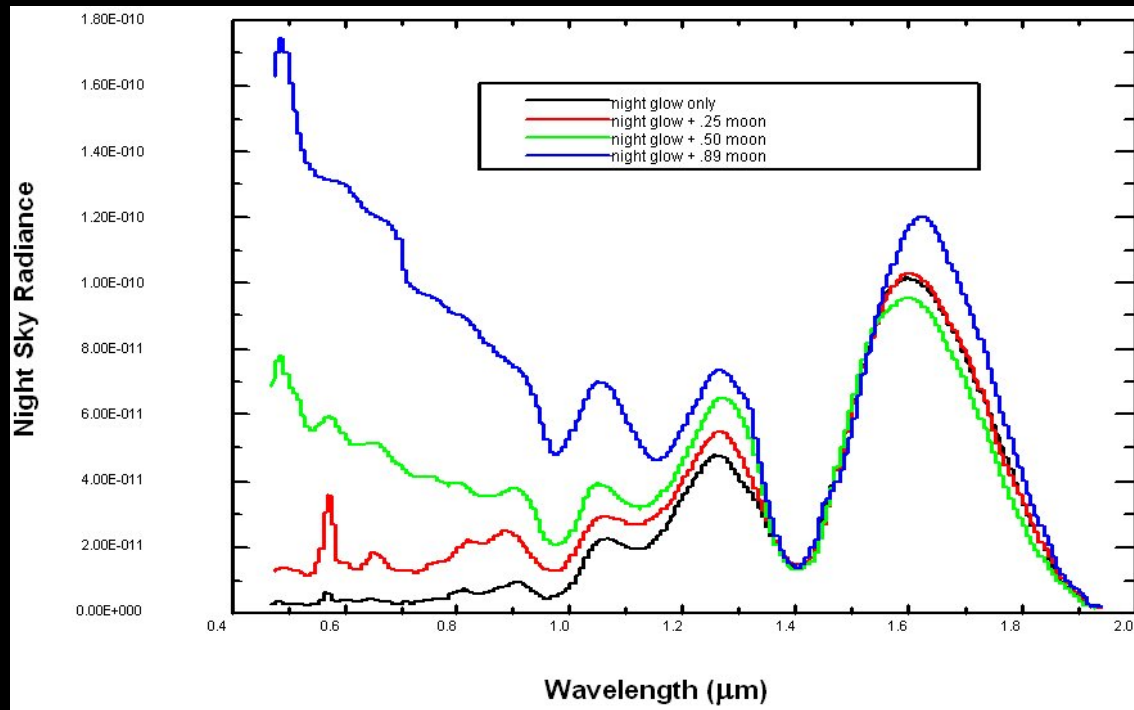
Defined by atmospheric transmission & detector material properties



Detector Zoology

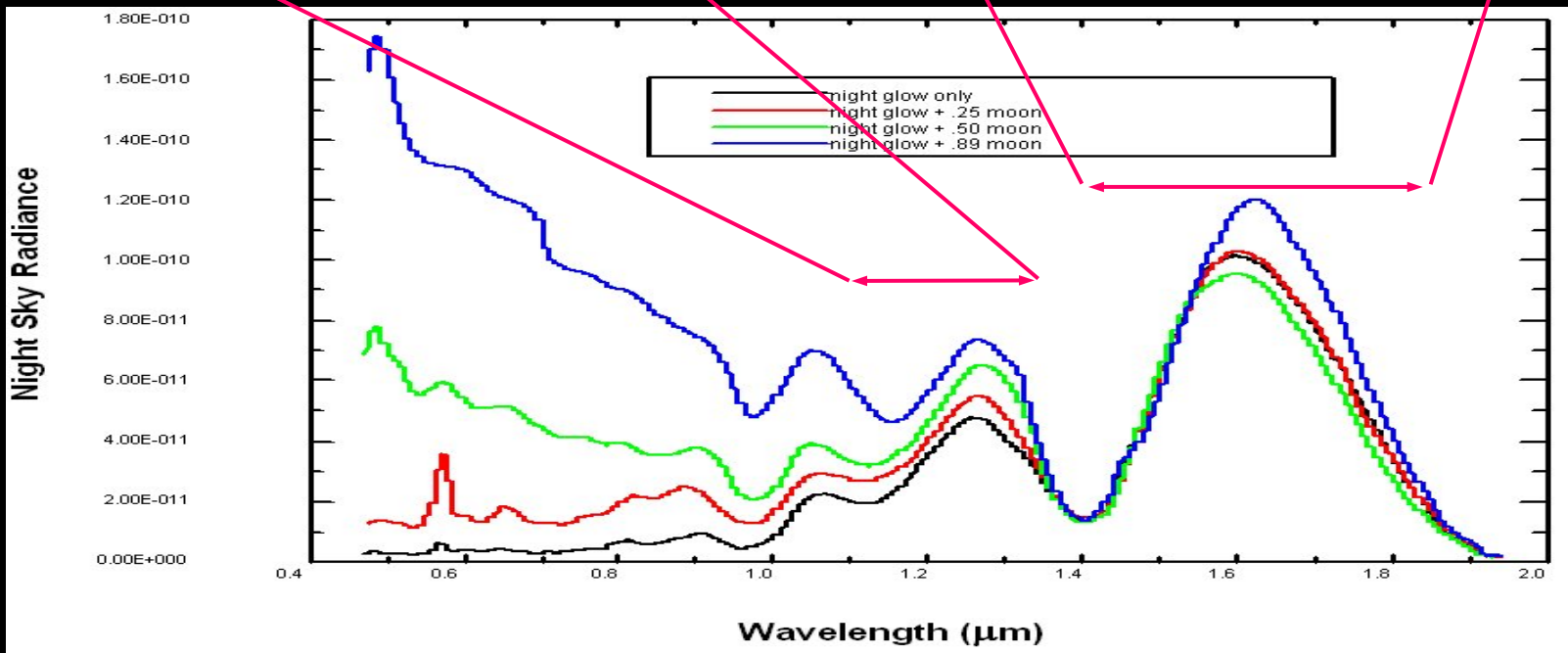
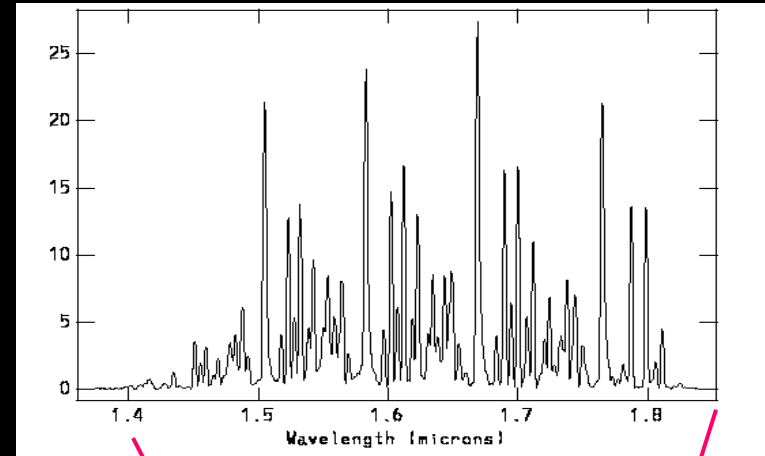
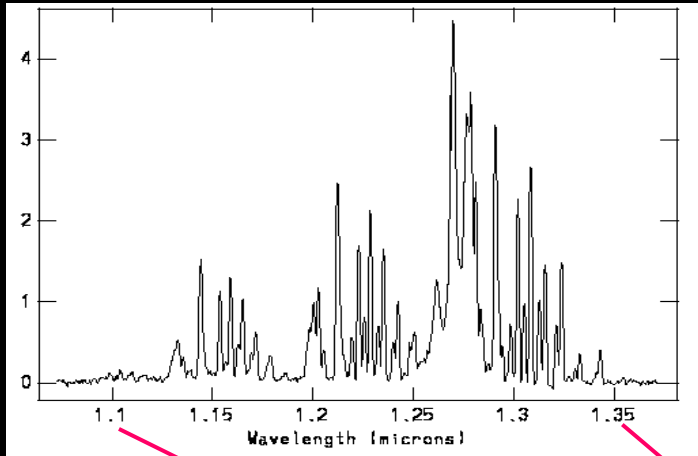


OH airglow (1.0-1.9 μm)



- OH provides a constant source of illumination in the near infrared
- OH created by the reaction: $\text{H} + \text{O}_3 \rightarrow \text{OH} + \text{O}_2$
- Thin emitting layer at ~85 km altitude
- Daytime intensity is 3x nighttime intensity, and intensity drops 40% during the night

OH airglow (1.0-1.9 μm)



Energy of a photon

$$E = h\nu$$

h = Planck constant (6.63×10^{-34} Joule·sec)
 ν = frequency of light (cycles/sec) = λ/c

Wavelength (μm)	Energy (eV)	Band
0.3	4.13	UV
0.5	2.48	Vis
0.7	1.77	Vis
1.0	1.24	NIR
2.5	0.50	SWIR
5.0	0.25	MWIR
10.0	0.12	LWIR
20.0	0.06	VLWIR

Note Bene:
IR Industry definitions
NOT the same for astronomers!

- Energy of photons is measured in electron-volts (eV)
- eV = energy that an electron gets when it “falls” through a 1 volt potential difference.

JWST - James Webb Space Telescope

15 Teledyne 2Kx2K infrared arrays on board (~63 million pixels)



- International collaboration
- 6.5 meter primary mirror and tennis court size sunshield
- 2014 launch on Ariane 5 rocket
- L2 orbit (1.5 million km from Earth)

H2RG qualified to TRL-6
and SIDECAR ASIC
qualified to TRL-9

JWST will find the “first light” objects after the Big Bang, and will study how galaxies, stars and planetary systems form

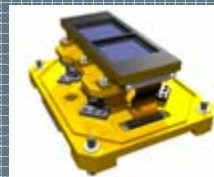
FGS (Fine Guidance Sensors)



3 individual MWIR 2Kx2K

- Acquisition and guiding
- Images guide stars for telescope stabilization
- Canadian Space Agency

NIRSpec (Near Infrared Spectrograph)



1x2 mosaic of MWIR 2Kx2K

- Spectrograph
- Measures chemical composition, temperature and velocity
- European Space Agency / NASA

NIRCam (Near Infrared Camera)



Two 2x2 mosaics
of SWIR 2Kx2K

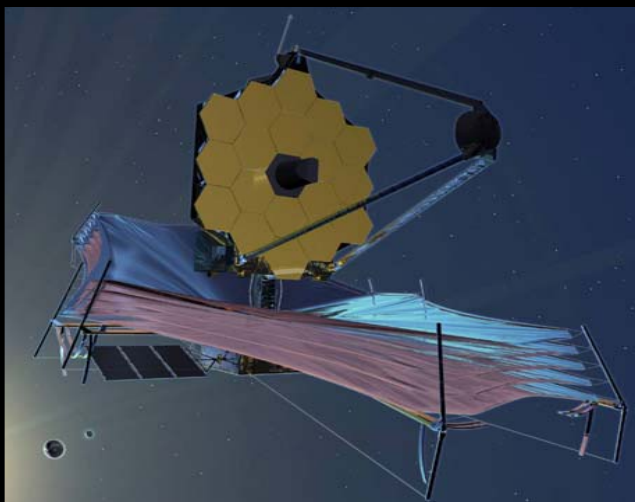
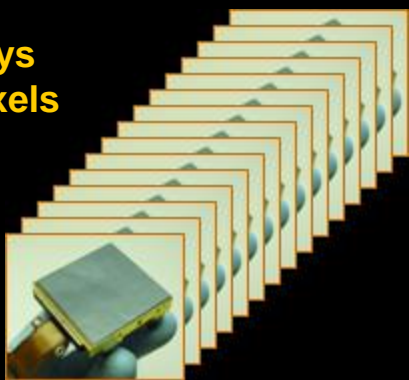
Two individual
MWIR 2Kx2K

- Wide field imager
- Studies morphology of objects and structure of the universe
- U. Arizona / Lockheed Martin

An electron-volt (eV) is extremely small

WFC3/IR

15 H2RG
2K×2K arrays
63 million pixels



$$1 \text{ eV} = 1.6 \cdot 10^{-19} \text{ J (J = joule)}$$

$$1 \text{ J} = \text{N} \cdot \text{m} = \text{kg} \cdot \text{m} \cdot \text{sec}^{-2} \cdot \text{m}$$

$$1 \text{ kg raised 1 meter} = 9.8 \text{ J} = 6.1 \cdot 10^{19} \text{ eV}$$

- The energy of a photon is **VERY** small
 - Energy of SWIR (2.5 μm) photon is 0.5 eV
- In 5 years, JWST will take ~1 million images
 - 1000 sec exp., 15 H2RGs, 90% duty cycle
 - Photons / H2RG image $\approx 3.6 \times 10^{10}$ photons
 - 5% pixels at 85% full well
 - 10% " at 40% full well
 - 10% " at 10% full well
 - 75% " at 1% full well

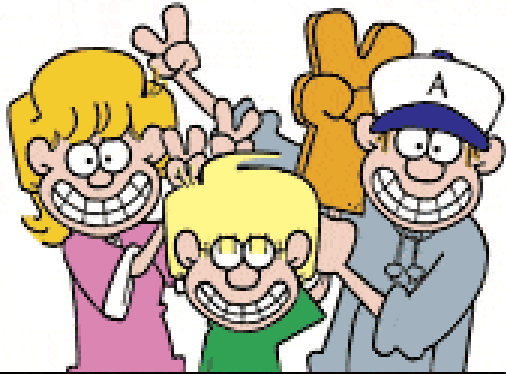
Full well
85,000 e-

– Total # SWIR photons detected $\approx 3.6 \times 10^{16}$
 – Total energy detected $\approx 1.8 \times 10^{16}$ eV

- Drop peanut M&M[®] candy (~2g) from height of 15 cm (~6 inches)
 - Potential energy $\approx 1.8 \times 10^{16}$ eV

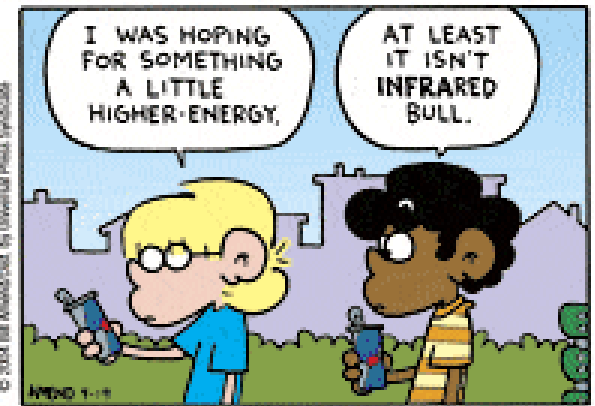
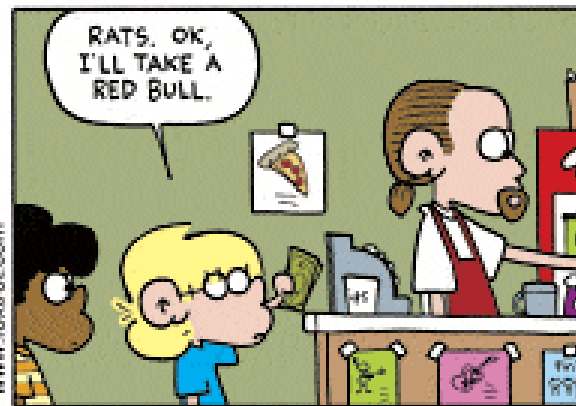
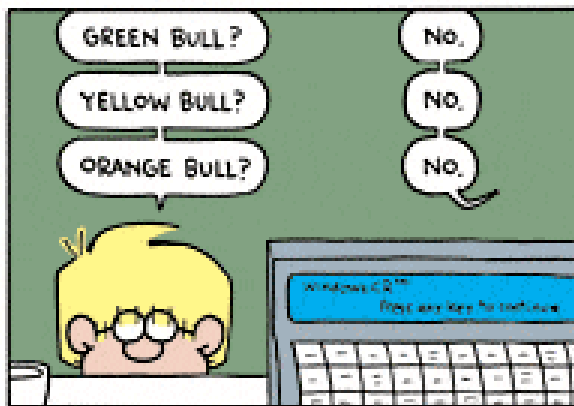
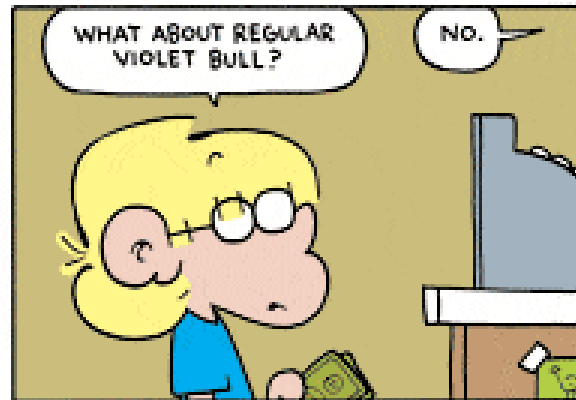
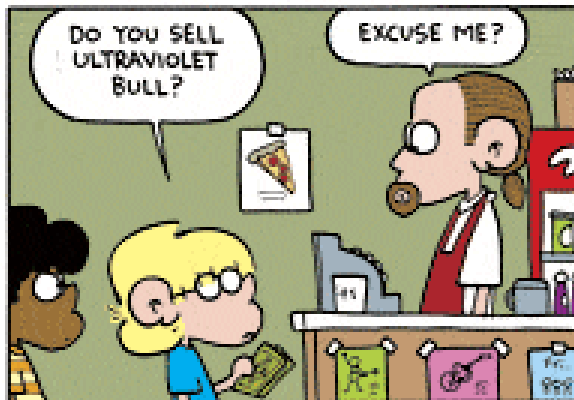
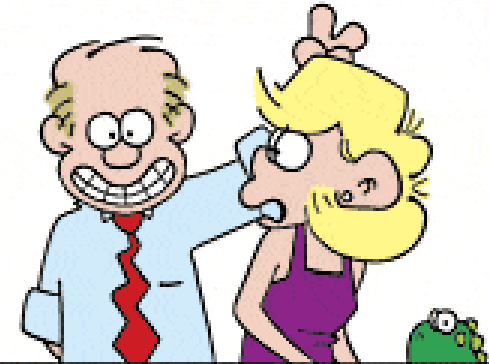
15 cm peanut M&M[®] drop is equal to the energy detected during 5 year operation of the James Webb Space Telescope!





FoxTrot

by Bill Amend

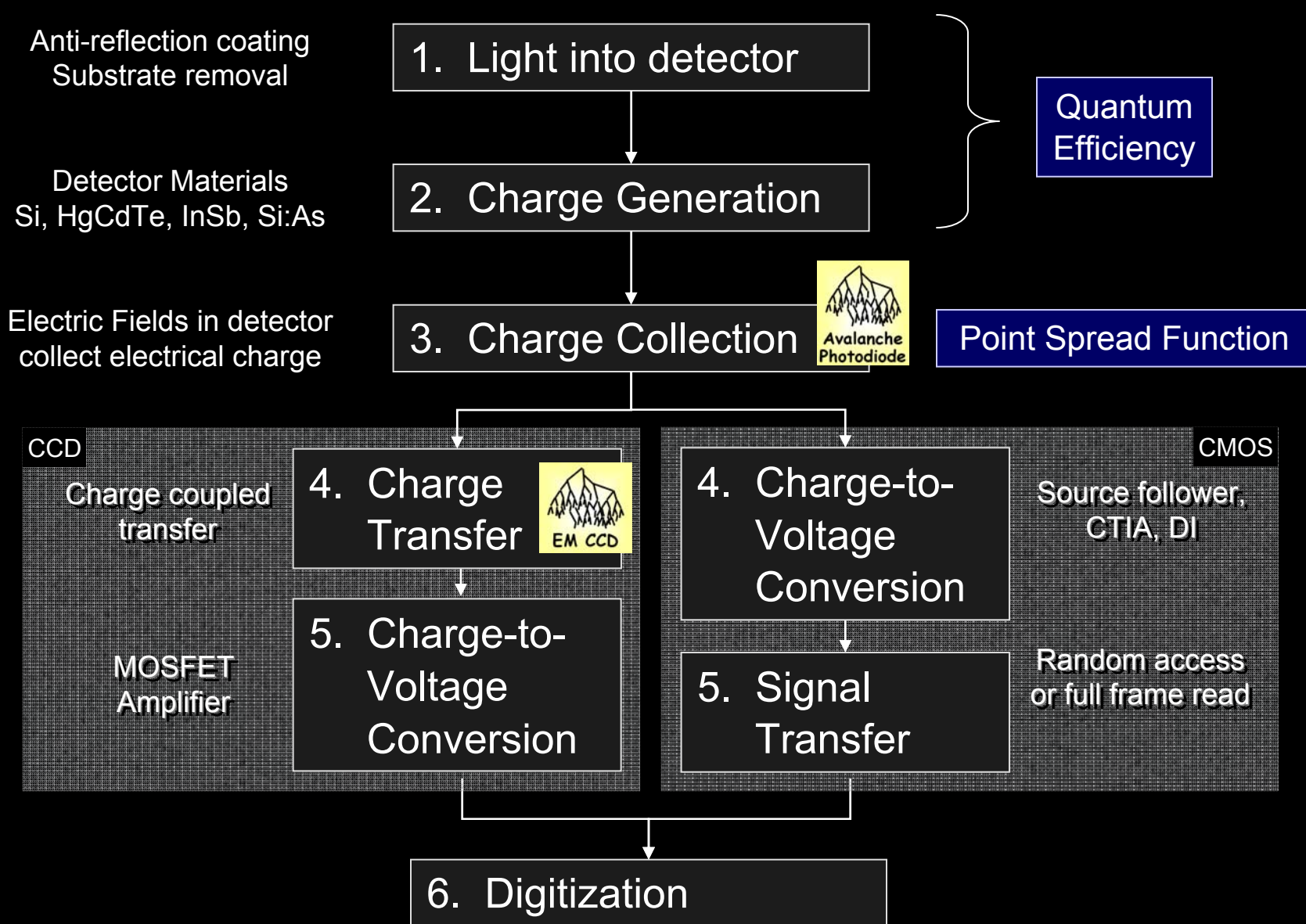


The Ideal Detector

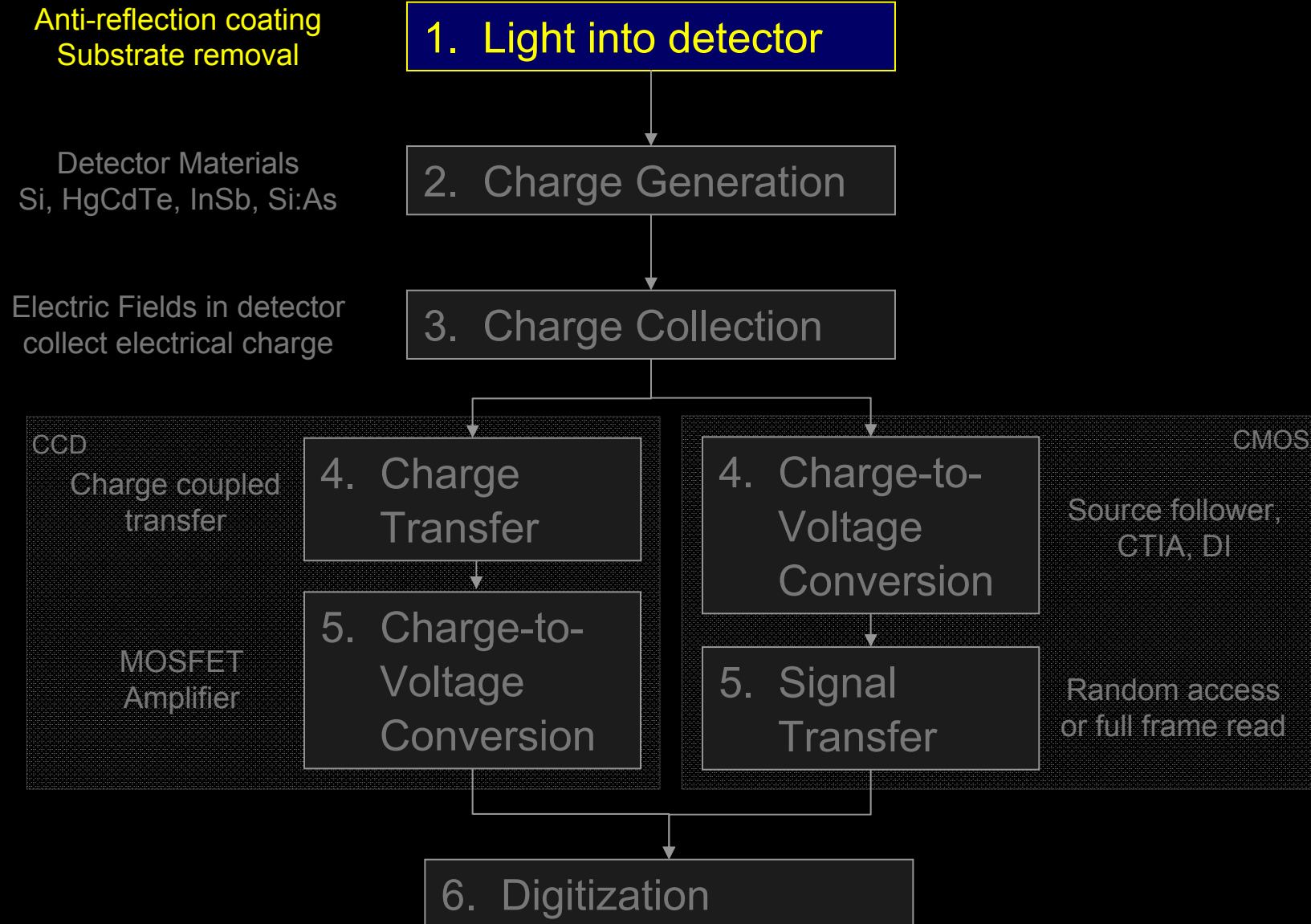
- Detect 100% of photons
 - Each photon detected as a delta function
 - Large number of pixels
 - Time tag for each photon
 - Measure photon wavelength
 - Measure photon polarization
- ✓ Up to 98% quantum efficiency
 - ✓ One electron for each photon
 - ✓ ~1,400 million pixels ($>10^9$)
 - ✗ No - framing detectors
 - ✓ APDs & event driven readout
 - ✗ No – defined by filter
 - ✓ Foveon, 3rd Gen IR
 - ✗ No – defined by filter
 - Can place filter on detector

Plus READOUT NOISE and other “features”

6 steps of optical / IR photon detection



6 steps of optical / IR photon detection

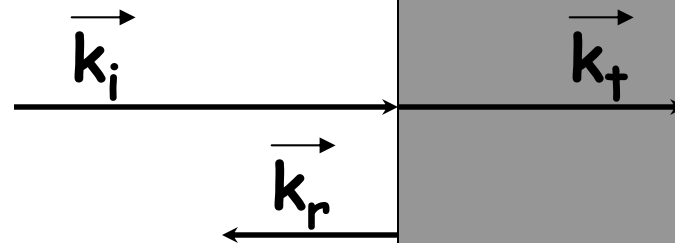


1st Step: Get light into the detector

Anti-reflection coatings

Velocity of light = c / n
 c = speed of light in a vacuum
 n = index of refraction of medium

Light incident from this medium
 n_i = index of refraction



Light transmitted into this medium
 n_t = index of refraction

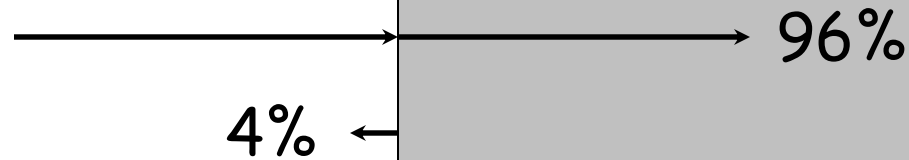
For transmission directly into interface (angle of incidence = 0°)

$$R = \text{fraction of incident energy reflected} \\ = \left(\frac{n_t - n_i}{n_t + n_i} \right)^2$$

Loss at a surface

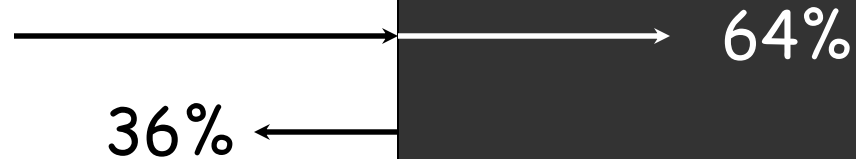
Air $n_i = 1.00$

Glass $n_t = 1.5$



Air $n_i = 1.00$

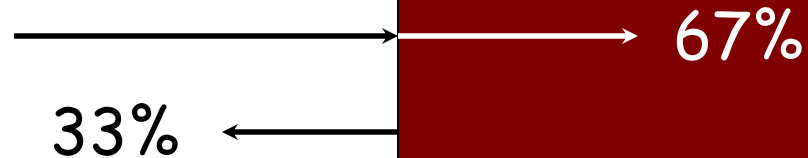
Silicon $n_t \sim 4$



Turns an 8-m telescope into an 6.4-m !

Air $n_i = 1.00$

HgCdTe $n_t = 3.7$



Turns an 8-m telescope into a 6.5-m !

Single layer anti-reflection coatings (angle of incidence = 0°)

Incident from this medium

n_i

\vec{k}_i

\vec{k}_r

n_{layer}

\vec{k}_{layer}

\vec{k}_{2r}

Transmitted into this medium

n_t

\vec{k}_t

$\lambda / 4$

$$R = \left[\frac{n_i n_t - n_{\text{layer}}^2}{n_i n_t + n_{\text{layer}}^2} \right]^2$$

If $n_{\text{layer}}^2 = n_i n_t \Rightarrow$ 0% reflected, 100% transmitted !

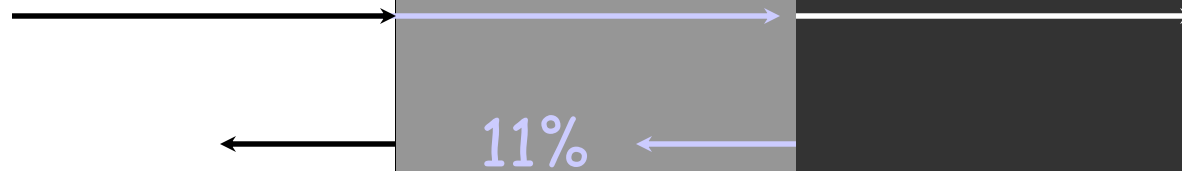
Ideal CCD anti-reflection coating

Air

$$n_i = 1$$

$$n_{\text{layer}} = 2$$

Silicon $n_t = 4$



100%

11%

$$\lambda / 4$$

$$R = \left(\frac{1 \cdot 4 - 2^2}{1 \cdot 4 + 2^2} \right)^2 = 0$$

Actual CCD anti-reflection coating

Air $n_i = 1.00$

Hafnium Oxide
 $n_{\text{layer}} \sim 2$

Silicon $n_t = 4$

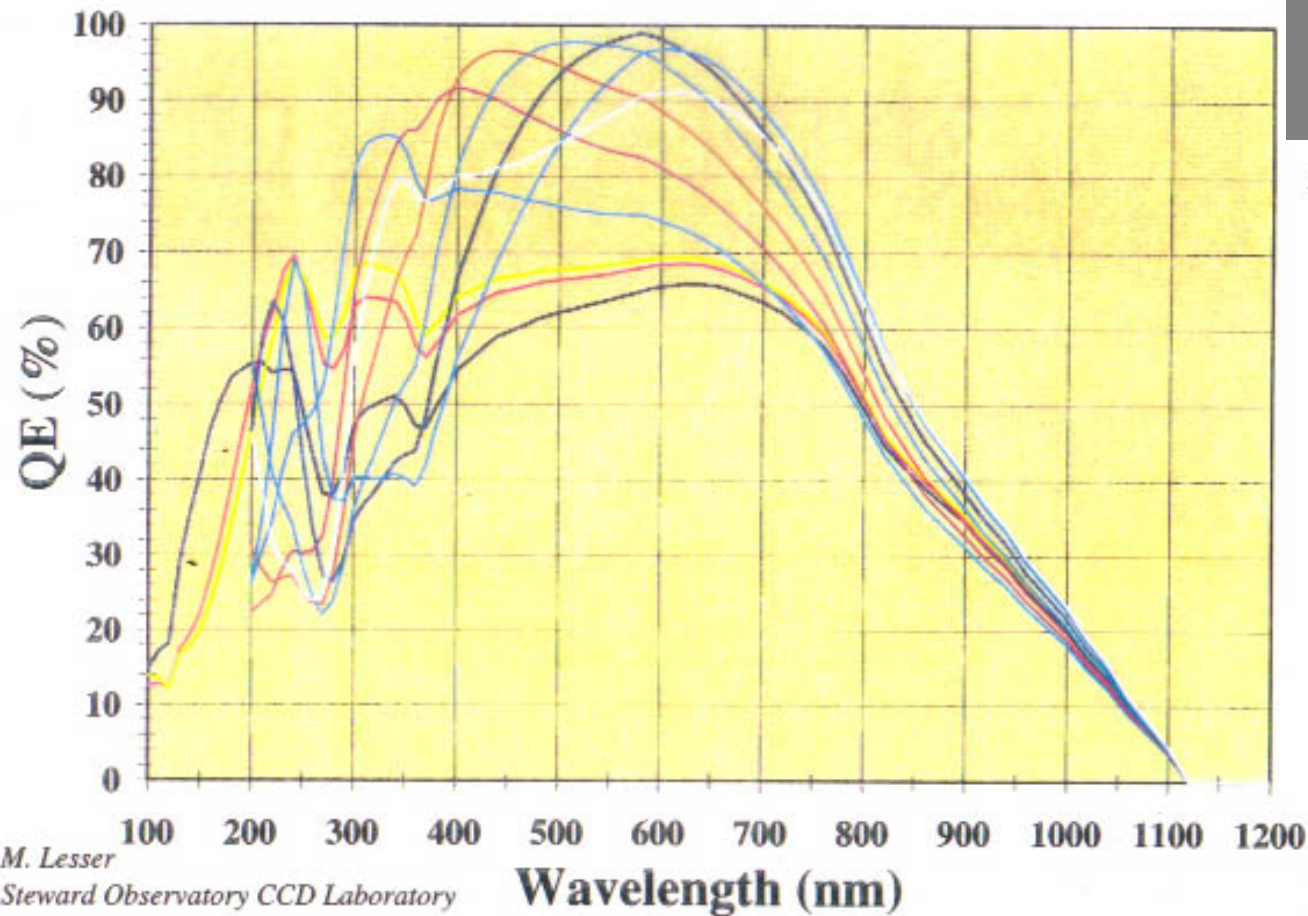
99%



$$R = \left[\frac{1 \cdot 4 - 2.0^2}{1 \cdot 4 + 2.0^2} \right]^2 \sim 0\%$$

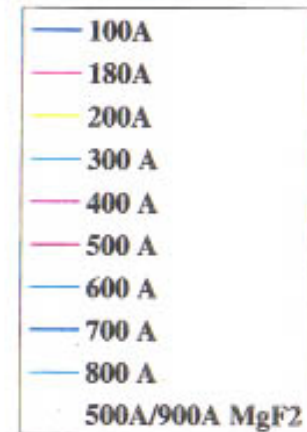
Quarter wave HfO_2 at 560 nm is $0.25(560)/2 = 70$ nm

Predicted CCD Quantum Efficiency Hafnium Oxide AR Coatings



For fixed spectra,
can use a variable
single layer AR
coating for max.
transmission at all
wavelengths

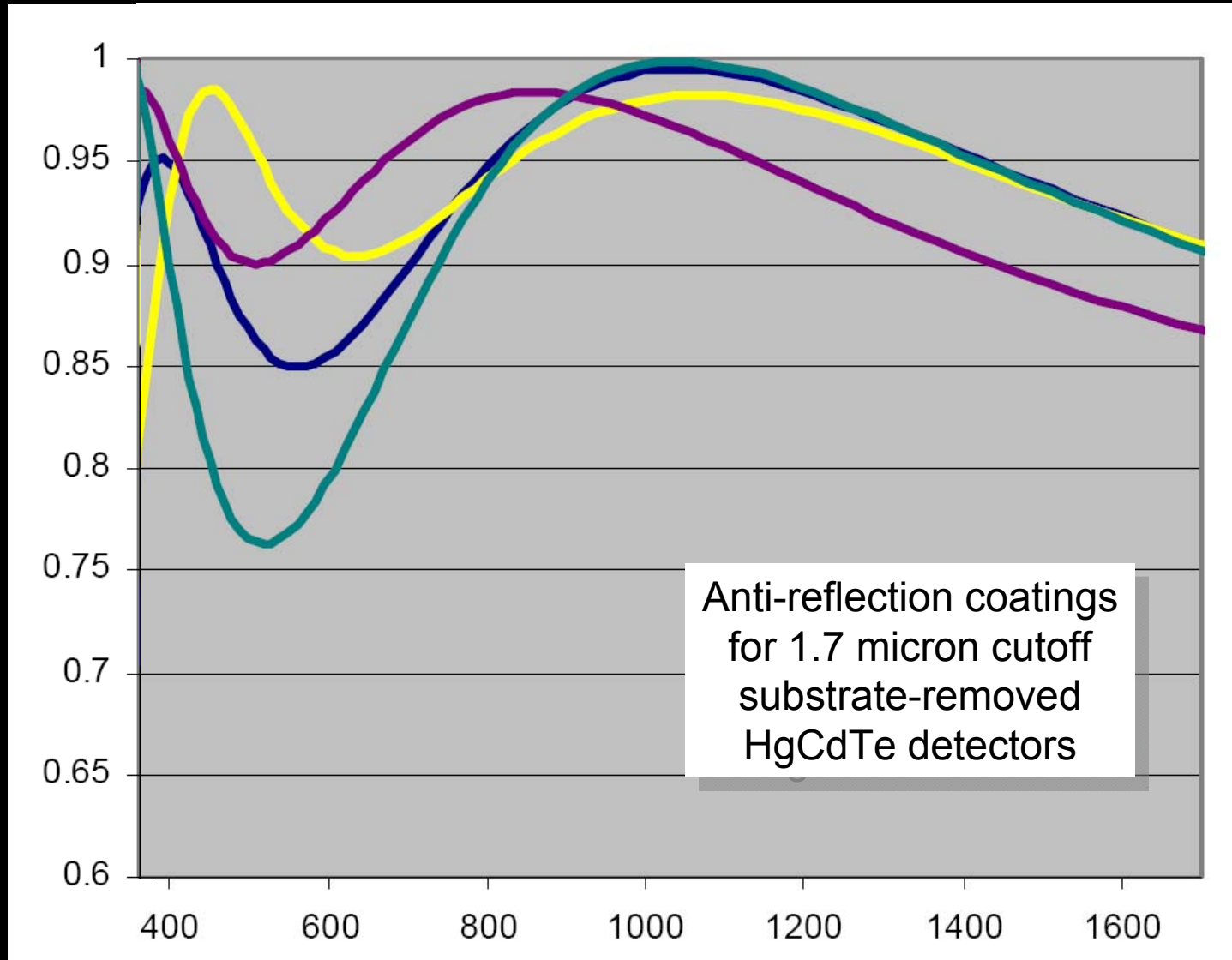
Coating Thickness



Quarter wave HfO_2 at 560 nm is $0.25(560)/2 = 70 \text{ nm}$ (700 Å)

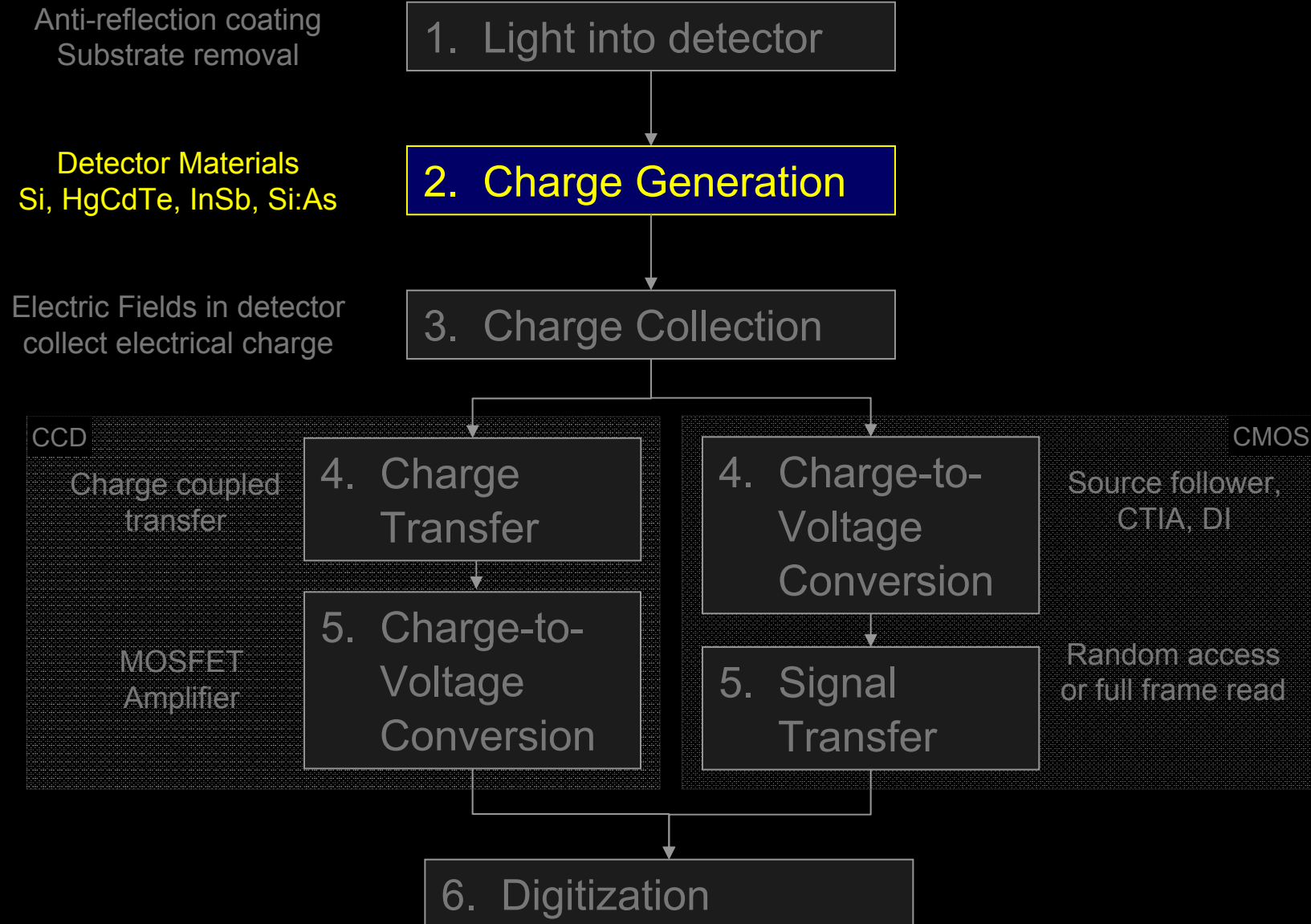
Example Anti-reflection coating for HgCdTe

Transmission into the HgCdTe detector

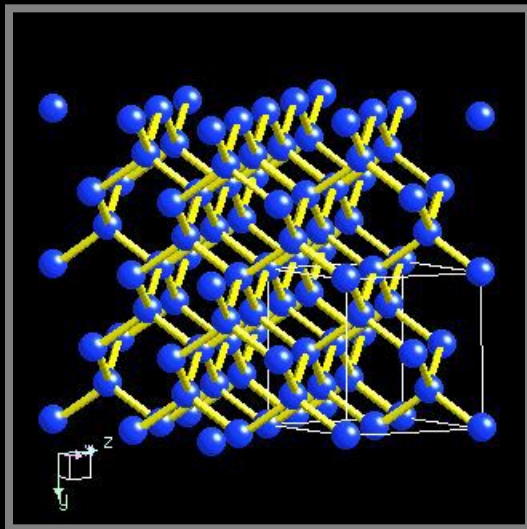
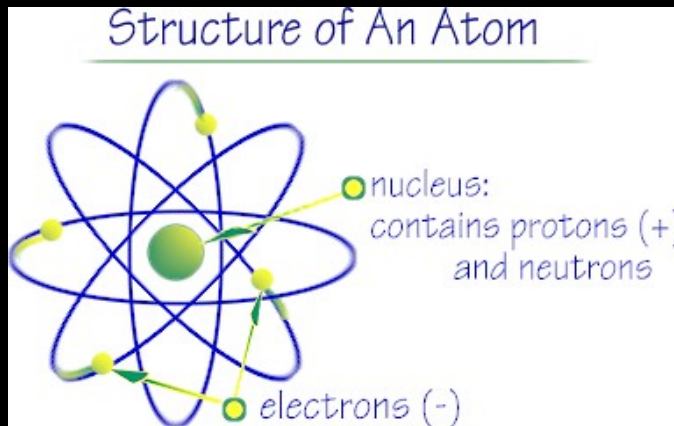


Wavelength (nm)

6 steps of optical / IR photon detection



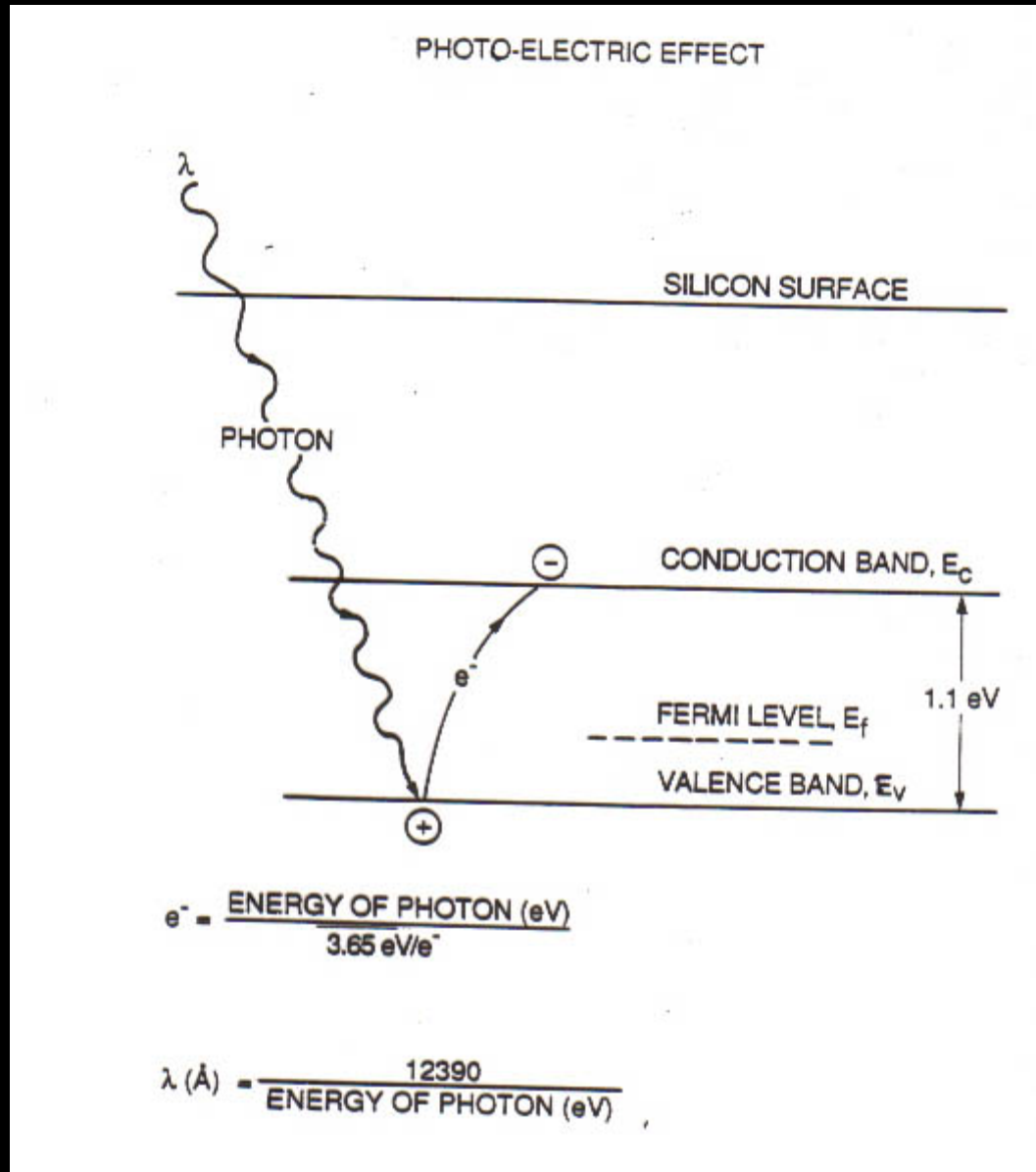
Crystals are excellent detectors of light



Silicon crystal lattice

- Simple model of atom
 - Protons (+) and neutrons in the nucleus with electrons orbiting
- Electrons are trapped in the crystal lattice
 - by electric field of protons
- Light energy can free an electron from the grip of the protons, allowing the electron to roam about the crystal
 - creates an “electron-hole” pair.
- The photocharge can be collected and amplified, so that light is detected
- The light energy required to free an electron depends on the material.

Charge Generation



Silicon CCD

Similar physics for
IR materials

Periodic Table

1 H Hydrogen 1.0																	2 He Helium 4.0
3 Li Lithium 6.9	4 Be Beryllium 9.0											5 B Boron 10.8	6 C Carbon 12.0	7 N Nitrogen 14.0	8 O Oxygen 16.0	9 F Fluorine 19.0	10 Ne Neon 20.2
11 Na Sodium 23.0	12 Mg Magnesium 9.0											13 Al Aluminum 27.0	14 Si Silicon 28.1	15 P Phosphorus 31.0	16 S Sulfur 32.1	17 Cl Chlorine 35.5	18 Ar Argon 40.0
19 K Potassium 39.1	20 Ca Calcium 40.2	21 Sc Scandium 45.0	22 Ti Titanium 47.9	23 V Vanadium 50.9	24 Cr Chromium 52.0	25 Mn Manganese 54.9	26 Fe Iron 55.9	27 Co Cobalt 58.9	28 Ni Nickel 58.7	29 Cu Copper 63.5	30 Zn Zinc 65.4	31 Ga Gallium 69.7	32 Ge Germanium 72.6	33 As Arsenic 74.9	34 Se Selenium 79.0	35 Br Bromine 79.9	36 Kr Krypton 83.8
37 Rb Rubidium 85.5	38 Sr Strontium 87.6	39 Y Yttrium 88.9	40 Zr Zirconium 91.2	41 Nb Niobium 92.9	42 Mo Molybdenum 95.9	43 Tc Technetium 99	44 Ru Ruthenium 101.0	45 Rh Rhodium 102.9	46 Pd Palladium 106.4	47 Ag Silver 107.9	48 Cd Cadmium 112.4	49 In Indium 114.8	50 Sn Tin 118.7	51 Sb Antimony 121.8	52 Te Tellurium 127.6	53 I Iodine 126.9	54 Xe Xenon 131.3
55 Cs Caesium 132.9	56 Ba Barium 137.4	57-71 Lanthanides	72 Hf Hafnium 178.5	73 Ta Tantalum 181.0	74 W Tungsten 183.9	75 Re Rhenium 186.2	76 Os Osmium 190.2	77 Ir Iridium 192.2	78 Pt Platinum 195.1	79 Au Gold 197.0	80 Hg Mercury 200.6	81 Tl Thallium 204.4	82 Pb Lead 207.2	83 Bi Bismuth 209.0	84 Po Polonium 210.0	85 At Astatine 210.0	86 Rn Radon 222.0
87 Fr Francium 223.0	88 Ra Radium 226.0	89-103 Actinides	104 Rf Rutherfordium 261	105 Db Dubnium 262	106 Sg Seaborgium 263	107 Bh Bohrium 262	108 Hs Hassium 265	109 Mt Meitnerium 266	110 Uun Ununnilium 272								

Types of Elements Key:

- Alkali metals
- Alkaline earth metals
- Transition metals
- Lanthanides
- Actinides
- Poor metals
- Semi-metals
- Non-metals
- Noble gases

57 La Lanthanum 138.9	58 Ce Cerium 140.1	59 Pr Praseodymium 140.9	60 Nd Neodymium 144.2	61 Pm Promethium 147.0	62 Sm Samarium 150.4	63 Eu Europium 152.0	64 Gd Gadolinium 157.3	65 Tb Terbium 158.9	66 Dy Dysprosium 162.5	67 Ho Holmium 164.9	68 Er Erbium 167.3	69 Tm Thulium 168.9	70 Yb Ytterbium 173.0	71 Lu Lutetium 175.0
89 Ac Actinium 132.9	90 Th Thorium 232.0	91 Pa Protactinium 231.0	92 U Uranium 238.0	93 Np Neptunium 237.0	94 Pu Plutonium 242.0	95 Am Americium 243.0	96 Cm Curium 247.0	97 Bk Berkelium 247.0	98 Cf Californium 251.0	99 Es Einsteinium 254.0	100 Fm Fermium 253.0	101 Md Mendelevium 258.0	102 No Nobelium 254.0	103 Lr Lawrencium 257.0

Periodic Table

II III IV V VI

1 H Hydrogen 1.0																	2 He Helium 4.0
3 Li Lithium 6.9	4 Be Beryllium 9.0											5 B Boron 10.8	6 C Carbon 12.0	7 N Nitrogen 14.0	8 O Oxygen 16.0	9 F Fluorine 19.0	10 Ne Neon 20.2
11 Na Sodium 23.0	12 Mg Magnesium 24.3											13 Al Aluminum 27.0	14 Si Silicon 28.1	15 P Phosphorus 31.0	16 S Sulfur 32.1	17 Cl Chlorine 35.5	18 Ar Argon 40.0
19 K Potassium 39.1	20 Ca Calcium 40.2	21 Sc Scandium 45.0	22 Ti Titanium 47.9	23 V Vanadium 50.9	24 Cr Chromium 52.0	25 Mn Manganese 54.9	26 Fe Iron 55.9	27 Co Cobalt 58.9	28 Ni Nickel 58.7	29 Cu Copper 63.5	30 Zn Zinc 65.4	31 Ga Gallium 69.7	32 Ge Germanium 72.6	33 As Arsenic 74.9	34 Se Selenium 79.0	35 Br Bromine 79.9	36 Kr Krypton 83.8
37 Rb Rubidium 85.5	38 Sr Strontium 87.6	39 Y Yttrium 88.9	40 Zr Zirconium 91.2	41 Nb Niobium 92.9	42 Mo Molybdenum 95.9	43 Tc Technetium 99	44 Ru Ruthenium 101.0	45 Rh Rhodium 102.9	46 Pd Palladium 106.4	47 Ag Silver 107.9	48 Cd Cadmium 112.4	49 In Indium 114.8	50 Sn Tin 118.7	51 Sb Antimony 121.8	52 Te Tellurium 127.6	53 I Iodine 126.9	54 Xe Xenon 131.3
55 Cs Caesium 132.9	56 Ba Barium 137.4	57-103 Lanthanides	72 Hf Hafnium 178.5	73 Ta Tantalum 181.0	74 W Tungsten 183.9	75 Re Rhenium 186.2	76 Os Osmium 190.2	77 Ir Iridium 192.2	78 Pt Platinum 195.1	79 Au Gold 197.0	80 Hg Mercury 200.6	81 Tl Thallium 204.4	82 Pb Lead 207.2	83 Bi Bismuth 209.0	84 Po Polonium 210.0	85 At Astatine 210.0	86 Rn Radon 222.0
87 Fr Francium 223.0	88 Ra Radium 226.0	89-103 Actinides	104 Rf Rutherfordium 261	105 Db Dubnium 262	106 Sg Seaborgium 263	107 Bh Bohrium 262	108 Hs Hassium 265	109 Mt Meitnerium 266	110 Uun Ununnilium 272								

Detector Families

- Si** - IV semiconductor
- HgCdTe** - II-VI semiconductor
- InGaAs & InSb** - III-V semiconductors

Types of Elements Key:

- Alkali metals
- Alkaline earth metals
- Transition metals
- Lanthanides
- Actinides
- Poor metals
- Semi-metals
- Non-metals
- Noble gases

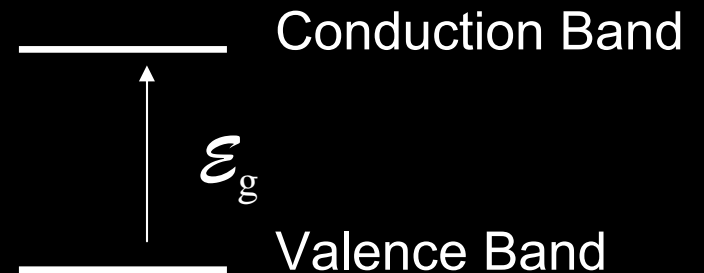
57 La Lanthanum 138.9	58 Ce Cerium 140.1	59 Pr Praseodymium 140.9	60 Nd Neodymium 145.0	61 Pm Promethium 145.0	62 Sm Samarium 150.4	63 Eu Europium 152.0	64 Gd Gadolinium 157.3	65 Tb Terbium 158.9	66 Dy Dysprosium 162.5	67 Ho Holmium 164.9	68 Er Erbium 167.3	69 Tm Thulium 168.9	70 Yb Ytterbium 173.0	71 Lu Lutetium 175.0
89 Ac Actinium 189.0	90 Th Thorium 232.0	91 Pa Protactinium 231.0	92 U Uranium 238.0	93 Np Neptunium 237.0	94 Pu Plutonium 242.0	95 Am Americium 243.0	96 Cm Curium 247.0	97 Bk Berkelium 247.0	98 Cf Californium 251.0	99 Es Einsteinium 254.0	100 Fm Fermium 253.0	101 Md Mendelevium 258.0	102 No Nobelium 254.0	103 Lr Lawrencium 260.0

Photon Detection

For an electron to be excited from the conduction band to the valence band

$$h\nu > \mathcal{E}_g$$

h = Planck constant ($6.63 \cdot 10^{-34}$ Joule•sec)
 ν = frequency of light (cycles/sec) = λ/c
 \mathcal{E}_g = energy gap of material (electron-volts)



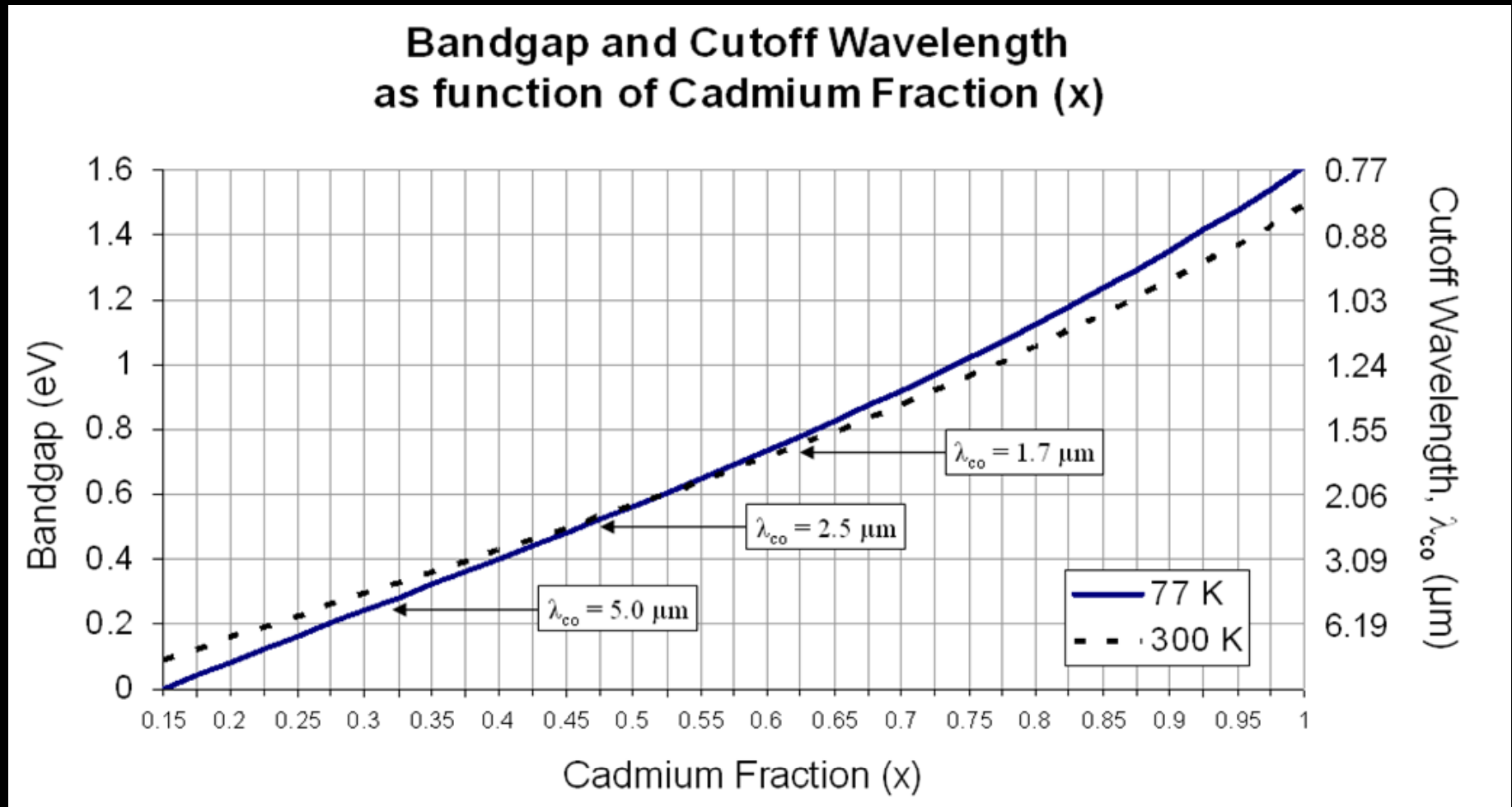
$$\lambda_c = 1.238 / \mathcal{E}_g \text{ (eV)}$$

Material Name	Symbol	\mathcal{E}_g (eV)	λ_c (μm)
Silicon	Si	1.12	1.1
Indium-Gallium-Arsenide	InGaAs	0.73 – 0.48	1.68* – 2.6
Mer-Cad-Tel	HgCdTe	1.00 – 0.07	1.24 – 18
Indium Antimonide	InSb	0.23	5.5
Arsenic doped Silicon	Si:As	0.05	25

*Lattice matched InGaAs ($\text{In}_{0.53}\text{Ga}_{0.47}\text{As}$)

Tunable Wavelength: Valuable property of HgCdTe

$\text{Hg}_{1-x}\text{Cd}_x\text{Te}$ Modify ratio of Mercury and Cadmium to “tune” the bandgap energy



$$E_g = -0.302 + 1.93x - 0.81x^2 + 0.832x^3 + 5.35 \times 10^{-4} T(1 - 2x)$$

G. L. Hansen, J. L. Schmidt, T. N. Casselman, J. Appl. Phys. 53(10), 1982, p. 7099

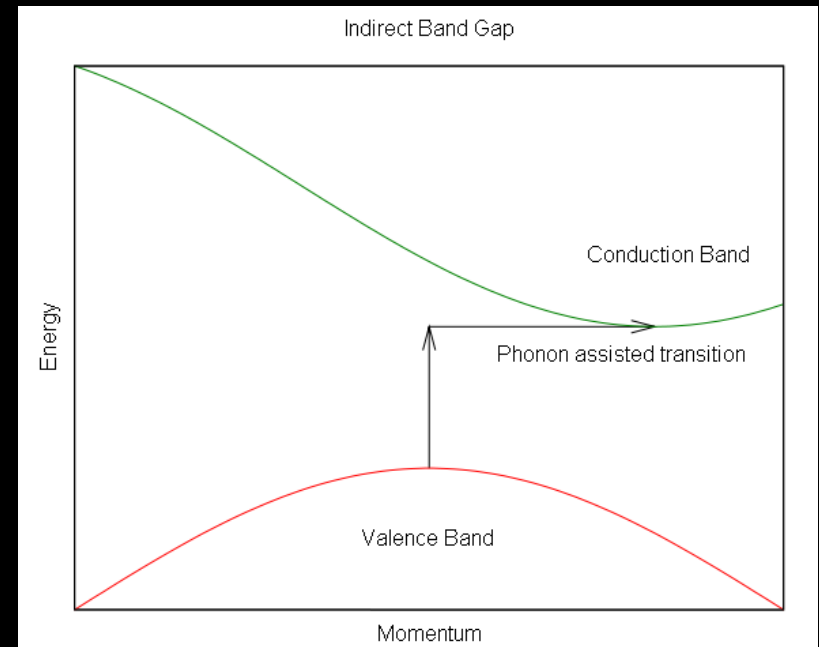
Absorption Depth

The depth of detector material that absorbs 63.2% of the radiation
 $1/e$ of the energy is absorbed

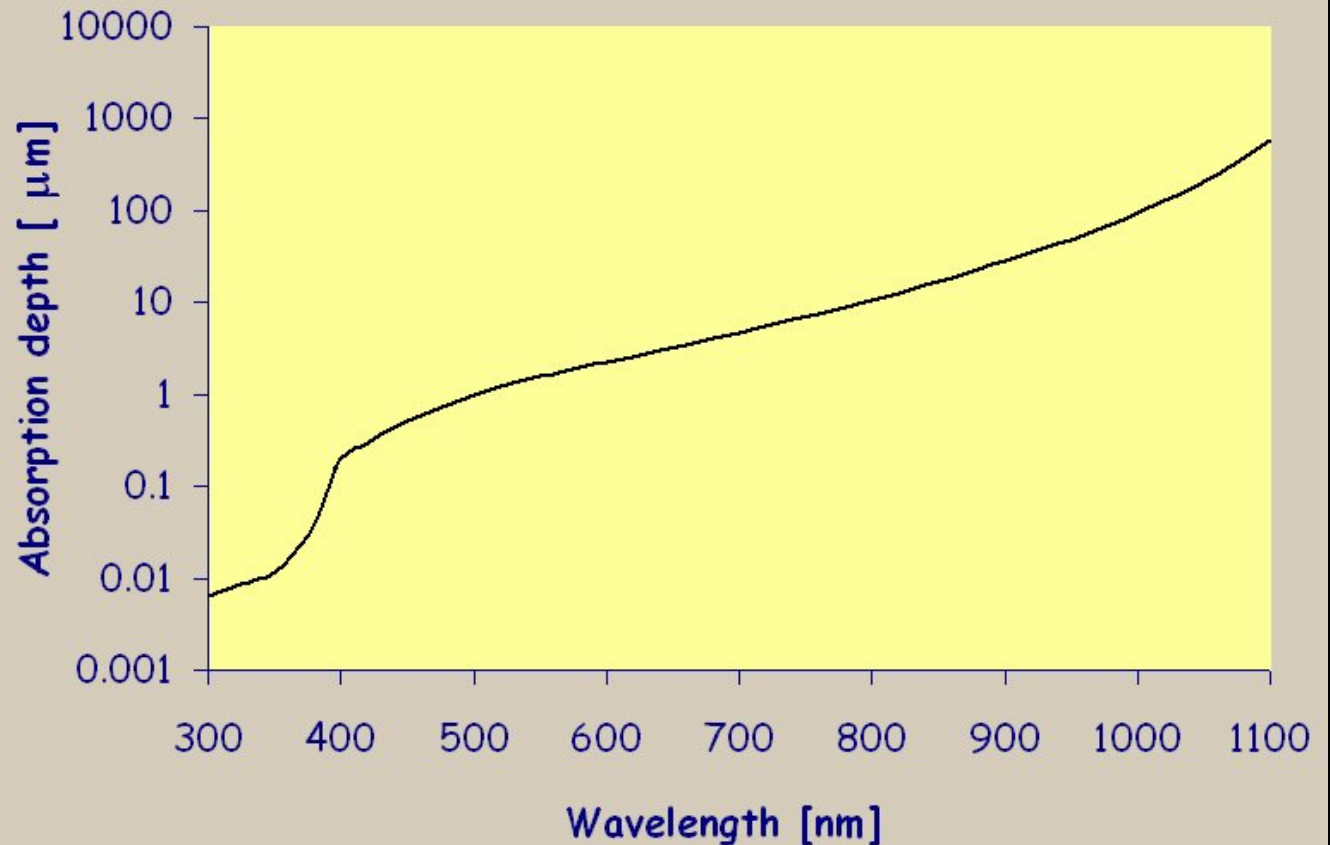
1	absorption depth(s)	63.2% of light absorbed
2		86.5%
3		95.0%
4		98.2%

For high QE, thickness of detector material should be ≥ 3 absorption depths

Silicon is an indirect bandgap material and is a poor absorber of light as the photon energy approaches the bandgap energy. For an indirect bandgap material, both the laws of conservation of energy and momentum must be observed. To excite an electron from the valence band to the conduction band, silicon must simultaneously absorb a photon and a phonon that compensates for the missing momentum vector.



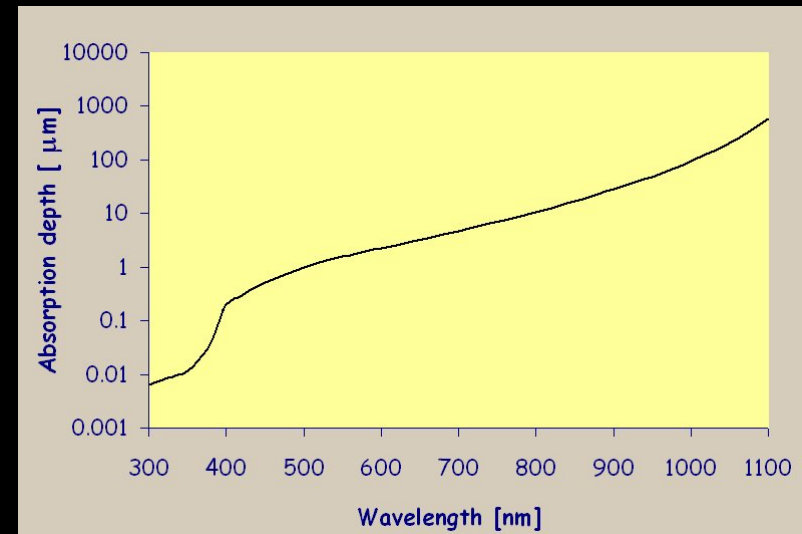
Absorption Depth of Silicon



- For high QE in the near infrared, need very thick (up to 300 microns) silicon detector layer.
- For high QE in the ultraviolet, need to be able to capture photocharge created within 10 nm of the surface where light enters the detector.
- In addition, the index of refraction of silicon varies over wavelength – a challenge for anti-reflection coatings.

UV / Blue CCD Quantum Efficiency

- Need very thin backside passivation layer
- Technologies
 - Boron implant and laser anneal
 - E2V, MIT/LL
 - MBE
 - JPL, MIT/LL
 - Chemisorption coating that produces positive charge
 - University of Arizona (Lesser)
Licensed by Fairchild



Effect of anneal process on QE

BORON DOPANT CONCENTRATION PROFILES

10^{23} silicon atoms per cm^3

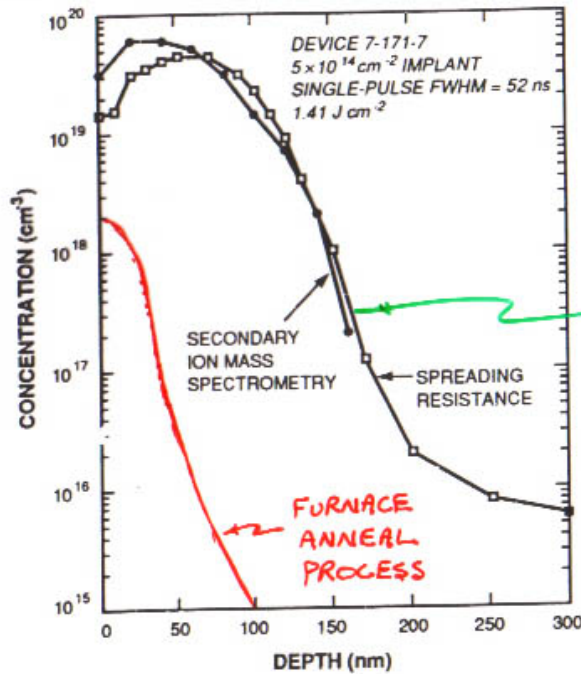
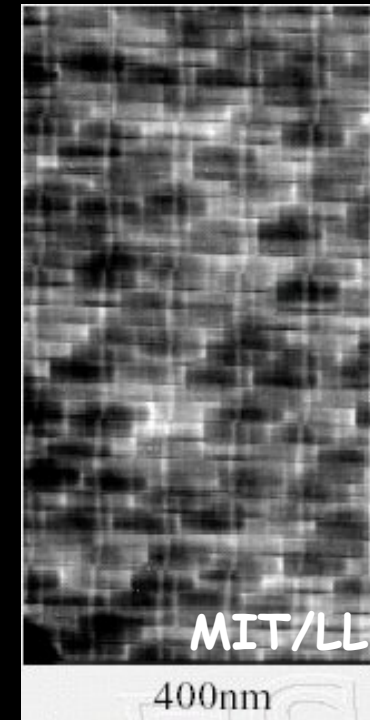
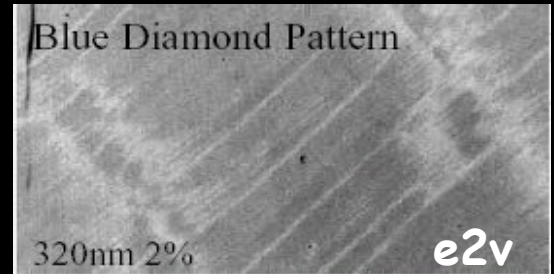
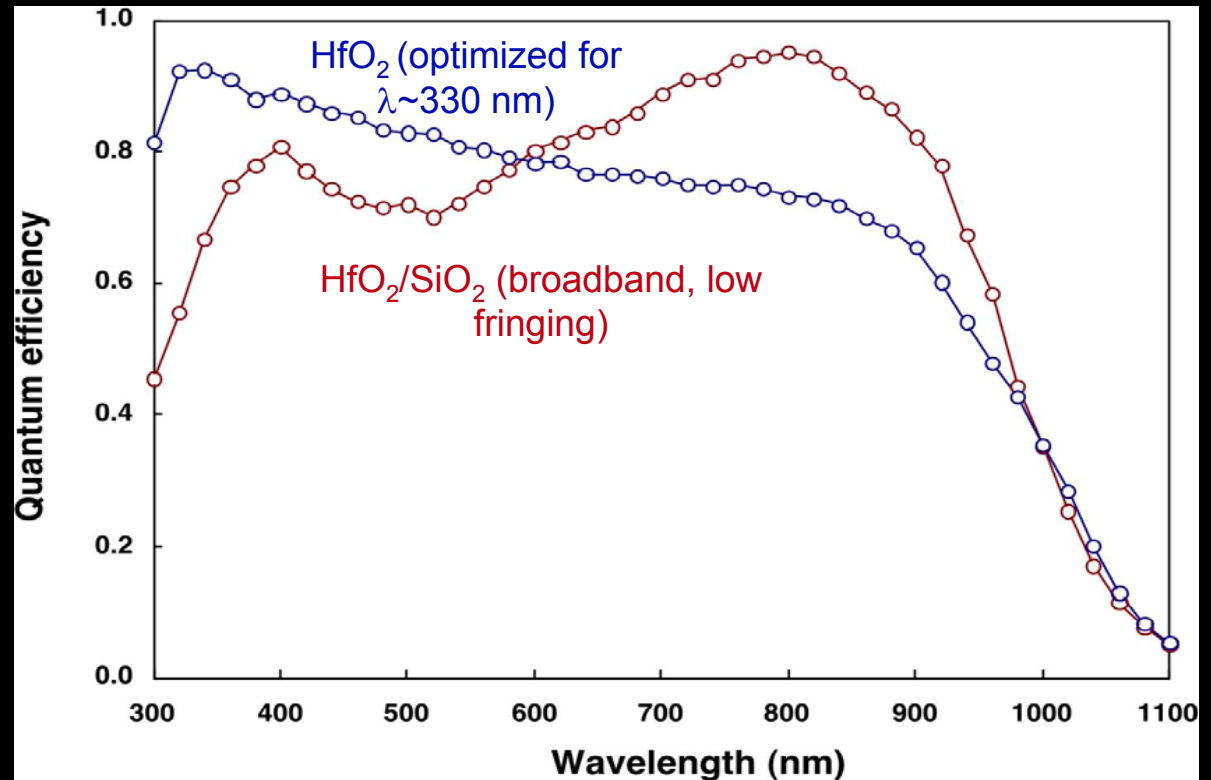
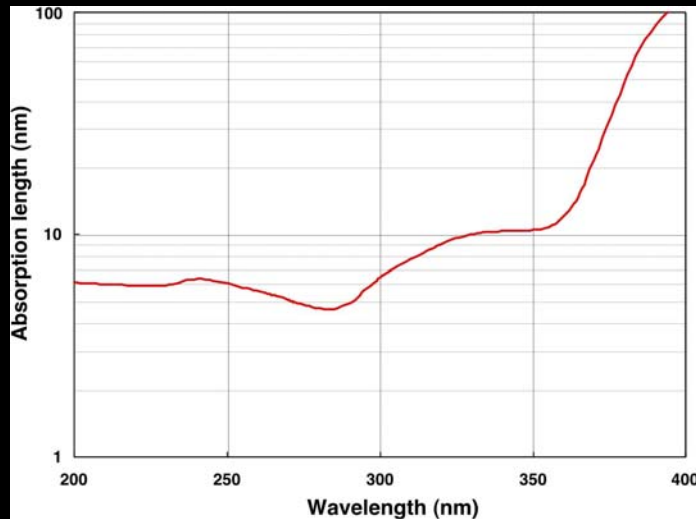


Figure 9. Plot of the active dopant (boron) vs. depth measured using both spreading resistance and secondary ion mass spectrometry (SIMS) methods. The boron was implanted and then activated by a pulsed laser anneal.

MIT/LL DATA



Quantum Efficiency of AR-coated MBE Devices



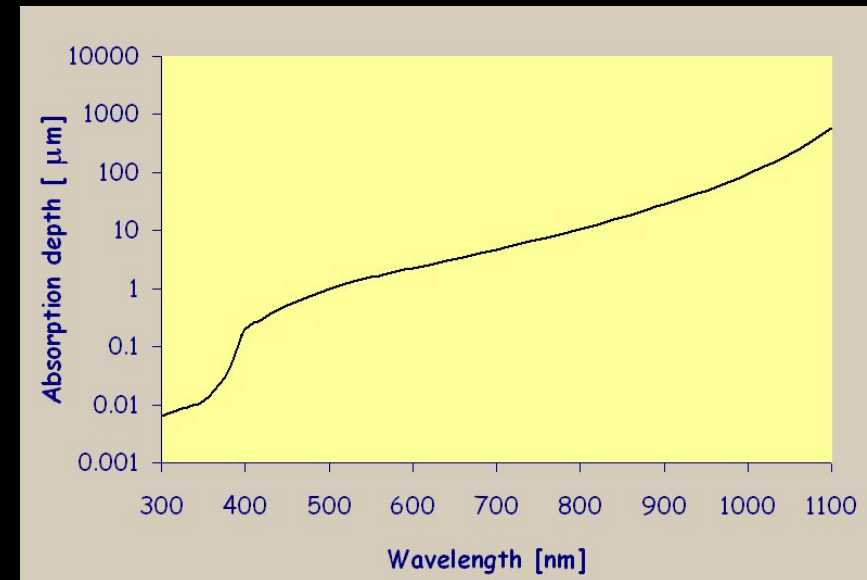
- UV (<400 nm) is challenging
 - Shallow penetration depth of radiation (<10 nm at $\lambda=200-350$ nm)
 - Requires extremely thin, doped surface layer

MBE processed
Device thickness = 45 μ m, T = 20 $^{\circ}$ C

Barry Burke, MIT/LL

NIR Silicon CCD Quantum Efficiency

- Optical absorption depth
 - 800 nm 11 μm
 - 900 nm 29 μm
 - 1000 nm 94 μm
- N-channel CCD (collect electrons)
 - Standard CCDs 10-15 μm thick
 - Thick high-resistivity 40-50 μm thick
 - MIT/LL, e2v
- P-channel CCD (collect holes)
 - Very thick 200-300 μm thick
 - LBNL

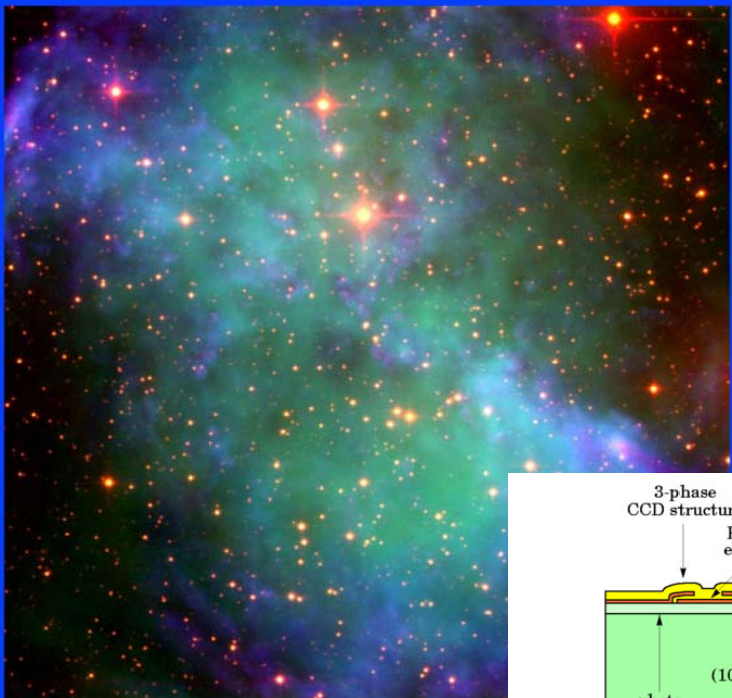


Near-IR Imaging enabled by very thick silicon sensors

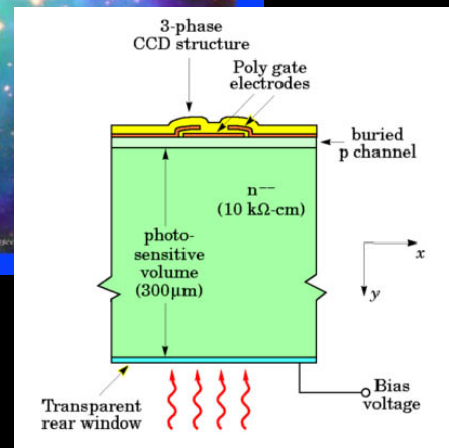
NATIONAL OPTICAL ASTRONOMY OBSERVATORY
Cerro Tololo • Kitt Peak • U.S. Gemini Program

NATIONAL SOLAR OBSERVATORY
GONG • Kitt Peak • Sacramento Peak

Newsletter 67 September 2001




Operated by the Association of Universities for Research in Astronomy (AURA), Inc., under cooperative agreement with the National Science Foundation



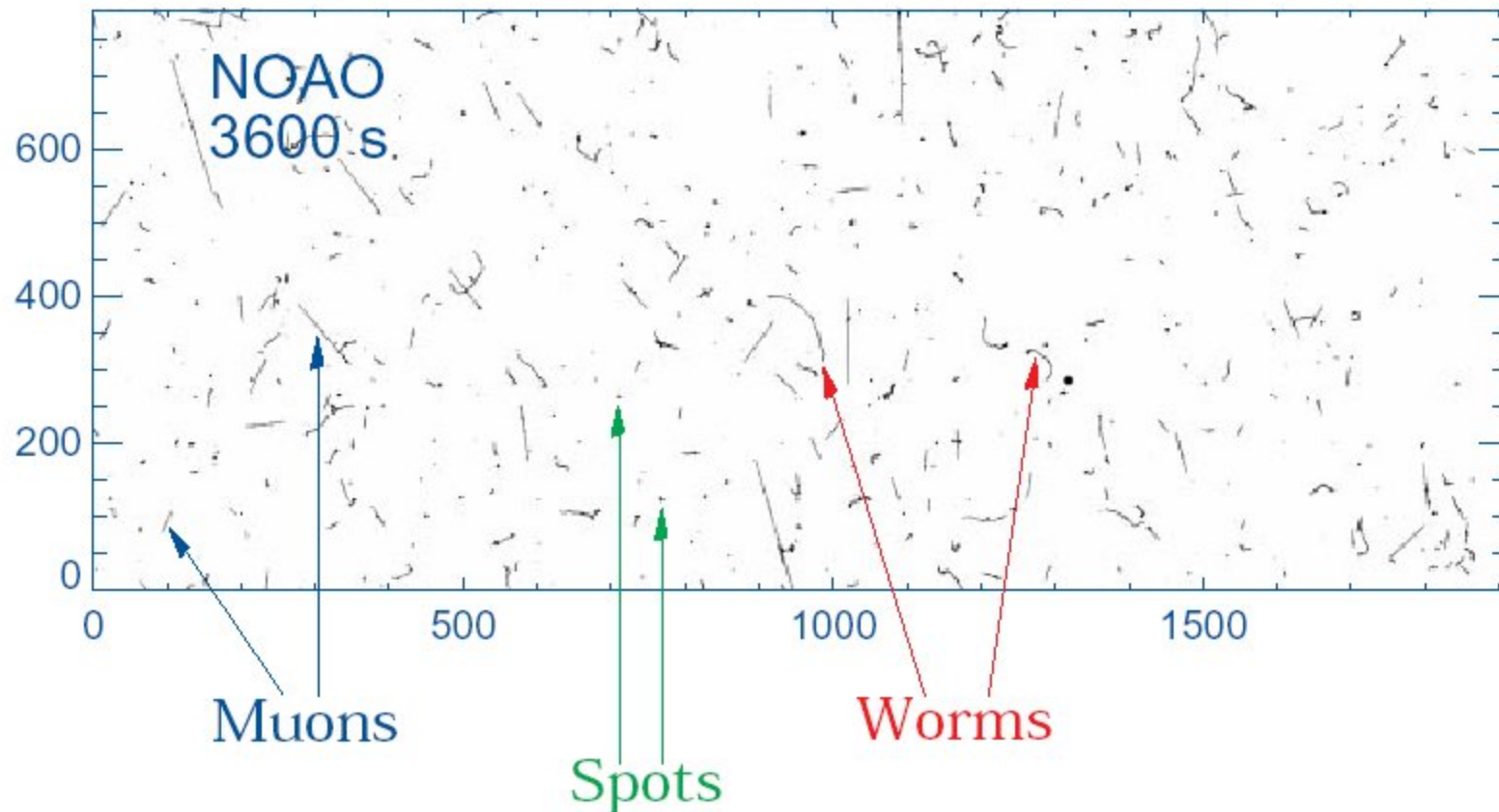

Planetary Nebula NGC 6853 (M 27) - VLT UT1+FORs1

ESO PR Photo 38a/98 (7 October 1998)

© ESO European Southern Observatory

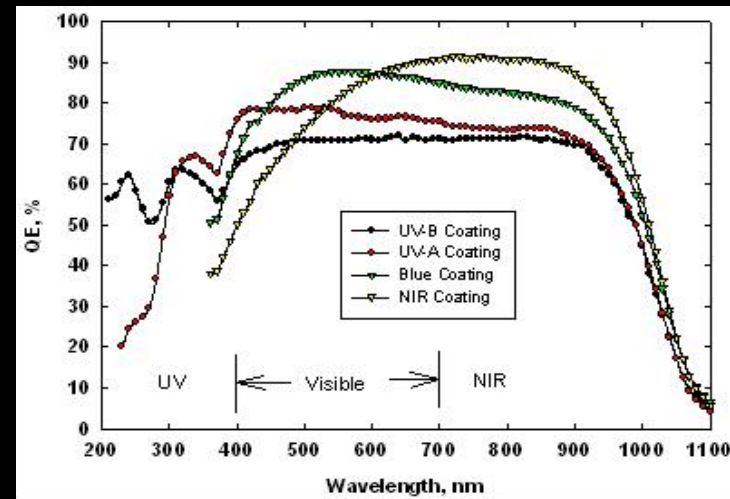
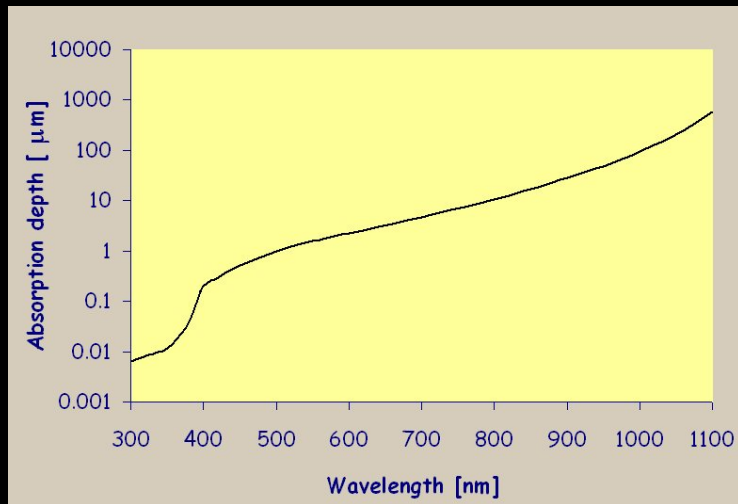


A very thick silicon detector is also a very good sensor of cosmic rays

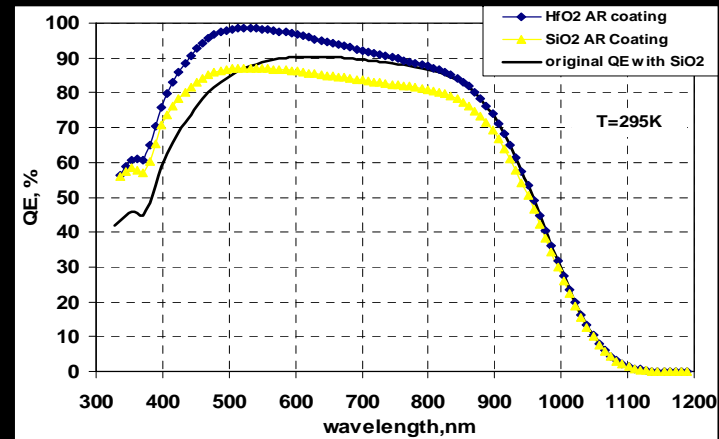
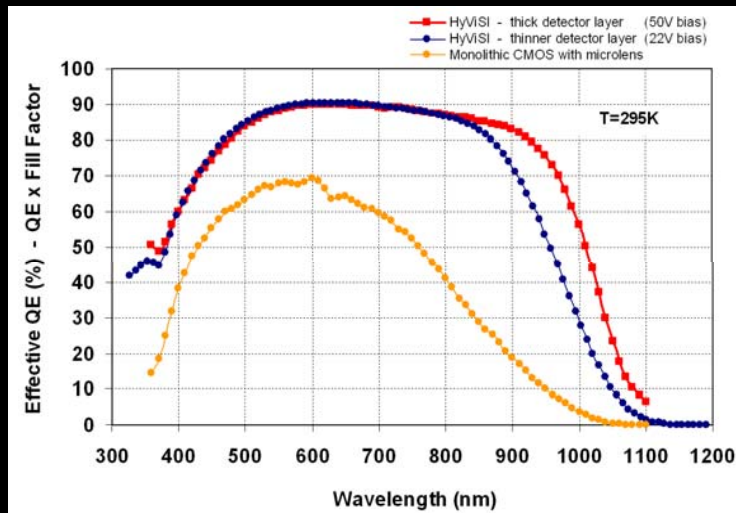


Our 300- μm thick depleted CCD gives us the great advantage (curse?) that we can see the events in new detail

Hybrid Silicon PIN Quantum Efficiency achieves as high QE as CCDs in the NIR



Measured data



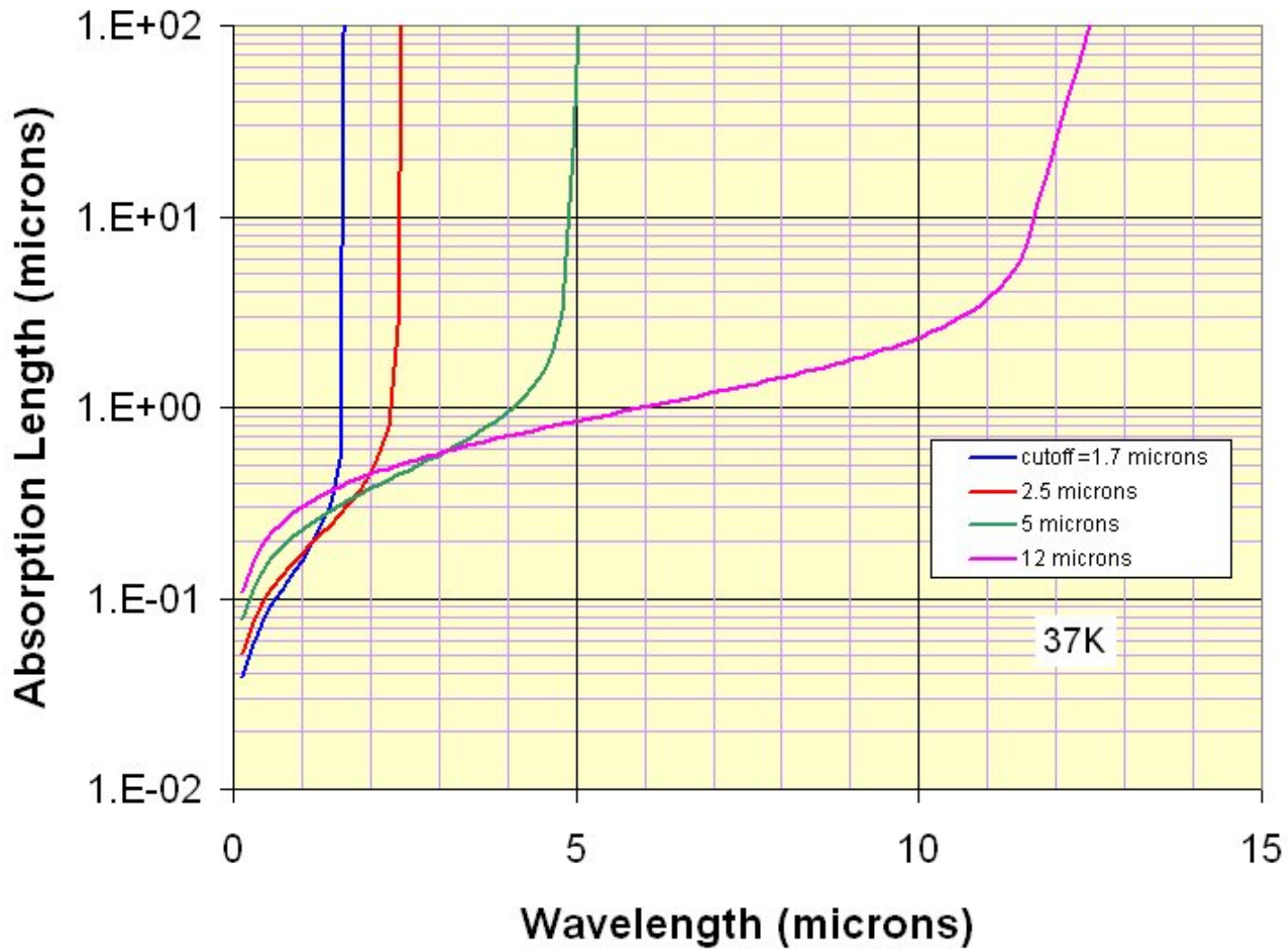
Computed QE curves

Teledyne Imaging Sensors

Absorption Depth of HgCdTe

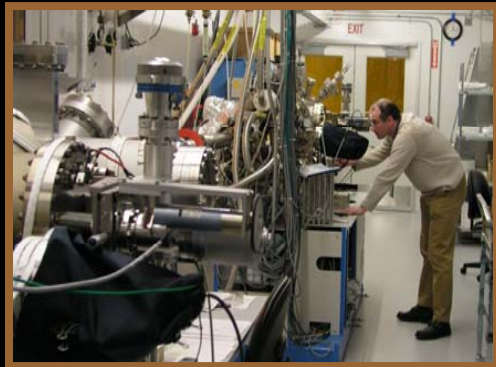
Rule of Thumb

Thickness of HgCdTe layer needs to be about equal to the cutoff wavelength



Two methods for growing HgCdTe

1. Liquid Phase Epitaxy (LPE)
2. Molecular Beam Epitaxy (MBE)
 - Enables very accurate deposition \Rightarrow "bandgap engineering"
 - Teledyne has 4 MBE machines for detector growth



RIBER 10-in MBE 49 System

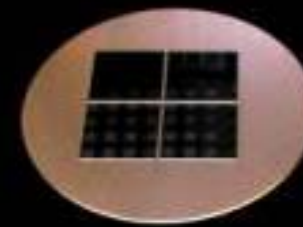


RIBER 3-in MBE Systems



3 inch diameter platen allows growth on one 6x6 cm substrate

More than 7500 MCT wafers grown to date



10 inch diameter platen allows simultaneous growth on four 6x6 cm substrates

Teledyne Imaging Sensors

Quantum Yield: one photoelectron for every detected photon

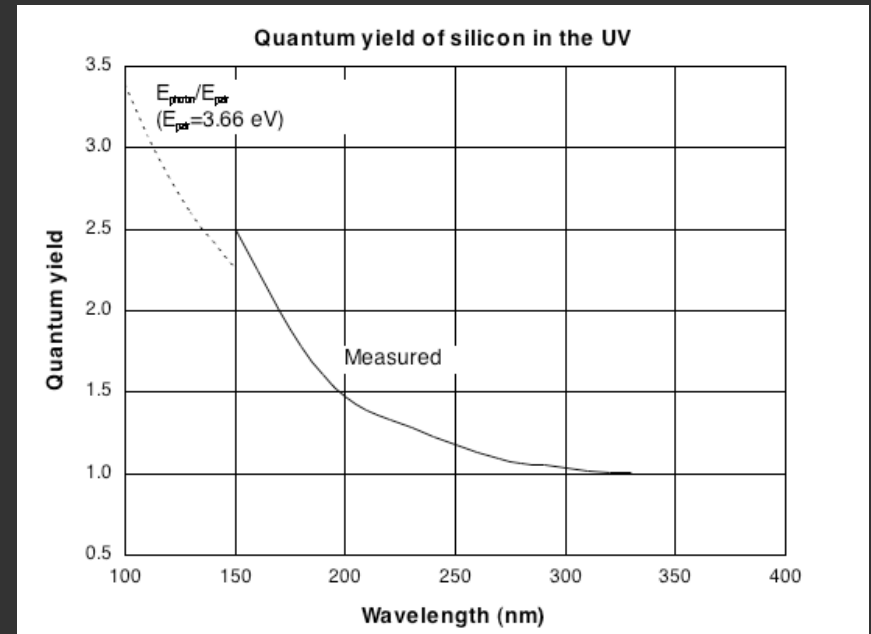
...for most wavelengths of interest to ground-based astronomy

Silicon

For wavelengths that are 30% to 100% of the cutoff wavelength, there will be a single electron-hole pair created for every detected photon.

For shorter wavelengths (higher energies), there is an increasing probability of producing multiple electron-hole pairs.

For silicon, this effect commences at ~30% of the cutoff wavelength ($\lambda < 330$ nm).



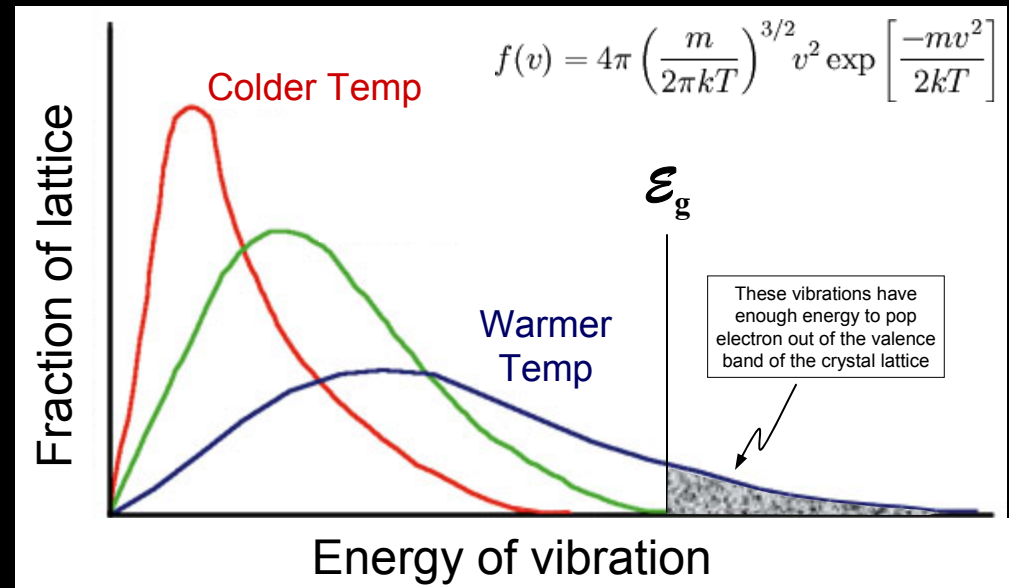
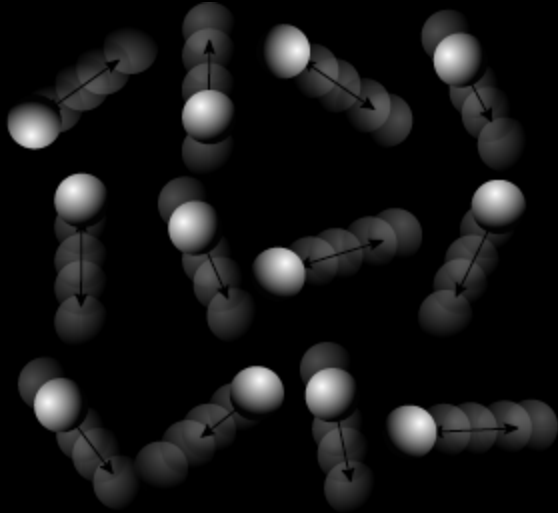
Data from Barry Burke, MIT Lincoln Laboratory

HgCdTe

- Limited data from HgCdTe detectors shows that quantum yield is not significant at 800 nm for a 5400 nm cutoff detector (11% of cutoff wavelength).
- The quantum yield of HgCdTe is still being investigated.

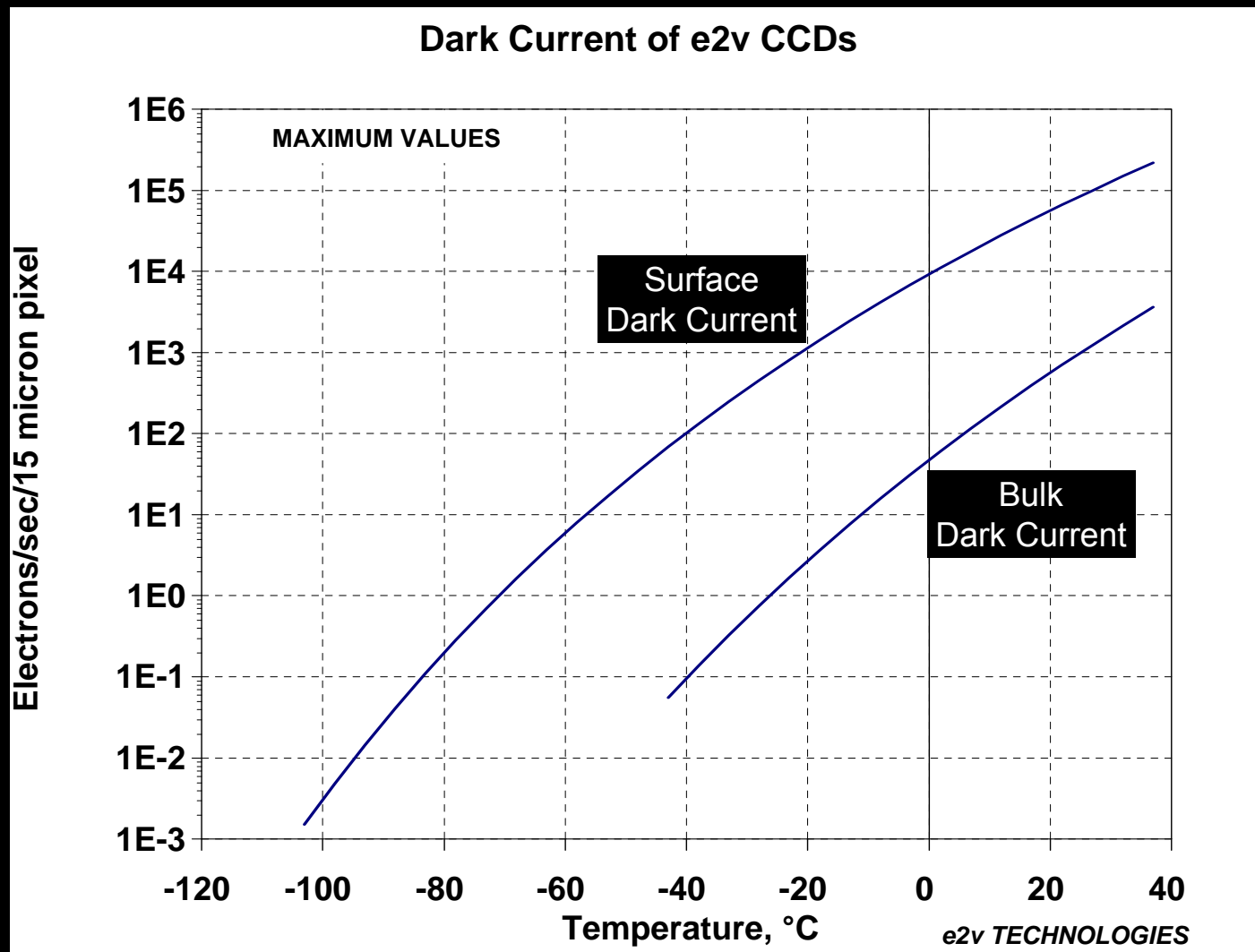
Dark Current

Undesirable byproduct of light detecting materials



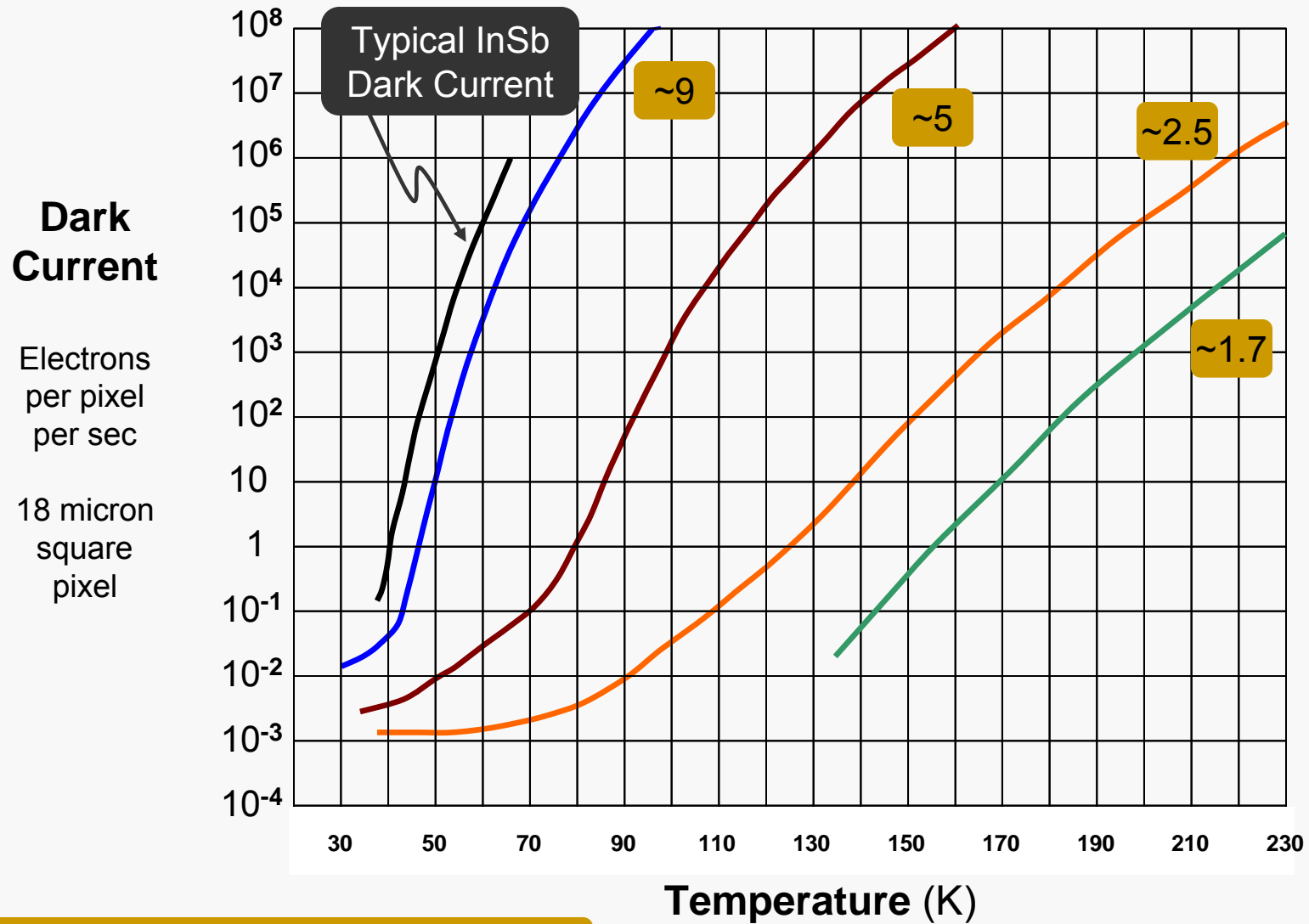
- The vibration of particles (includes crystal lattice phonons, electrons and holes) has energies described by the Maxwell-Boltzmann distribution. Above absolute zero, some vibration energies may be larger than the bandgap energy, and will cause electron transitions from valence to conduction band.
- Need to cool detectors to limit the flow of electrons due to temperature, i.e. the **dark current** that exists in the absence of light.
- The smaller the bandgap, the colder the required temperature to limit dark current below other noise sources (e.g. readout noise)

Dark Current of Silicon-based Detectors



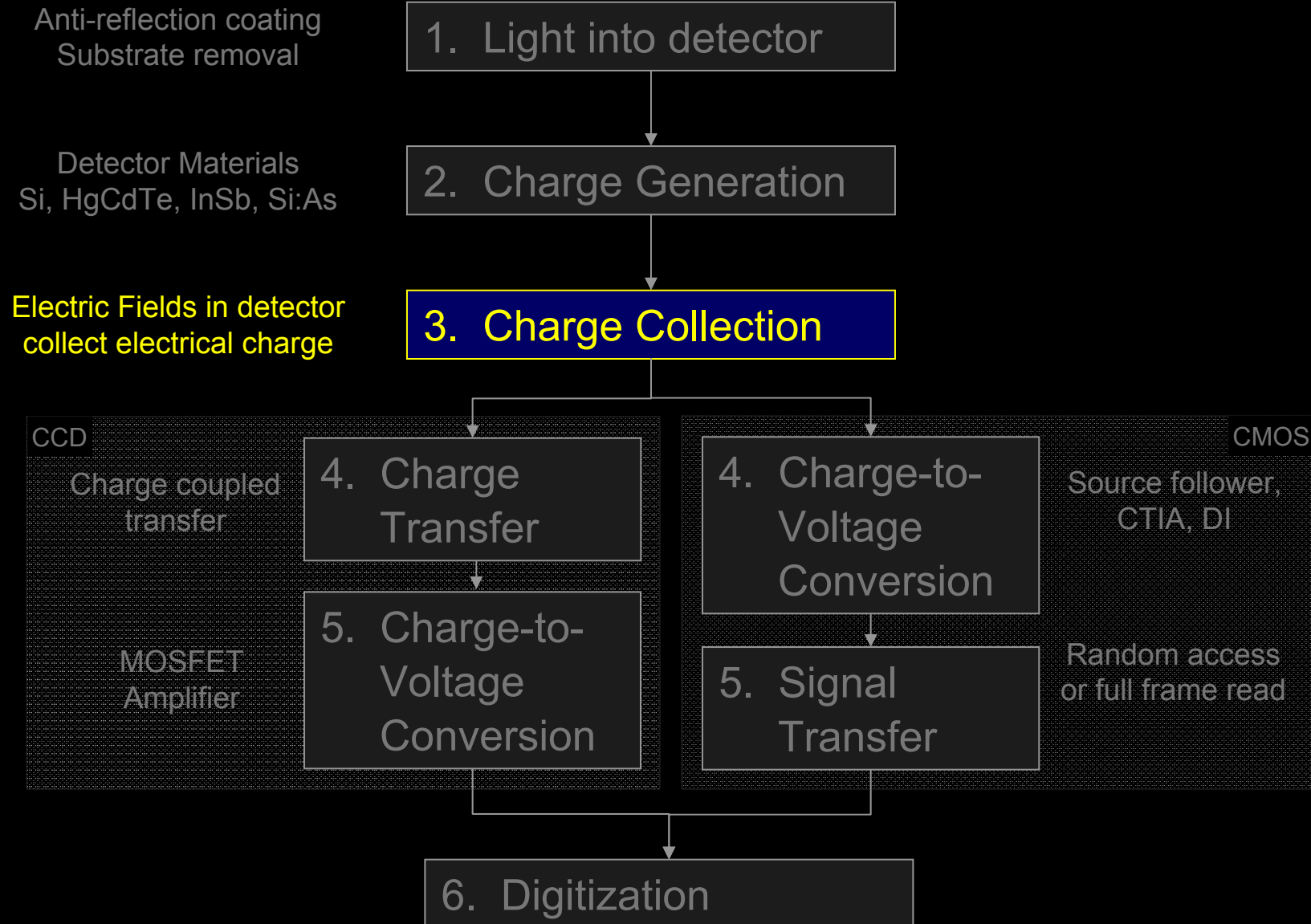
In silicon, dark current usually dominated by surface defects

Dark Current of HgCdTe Detectors



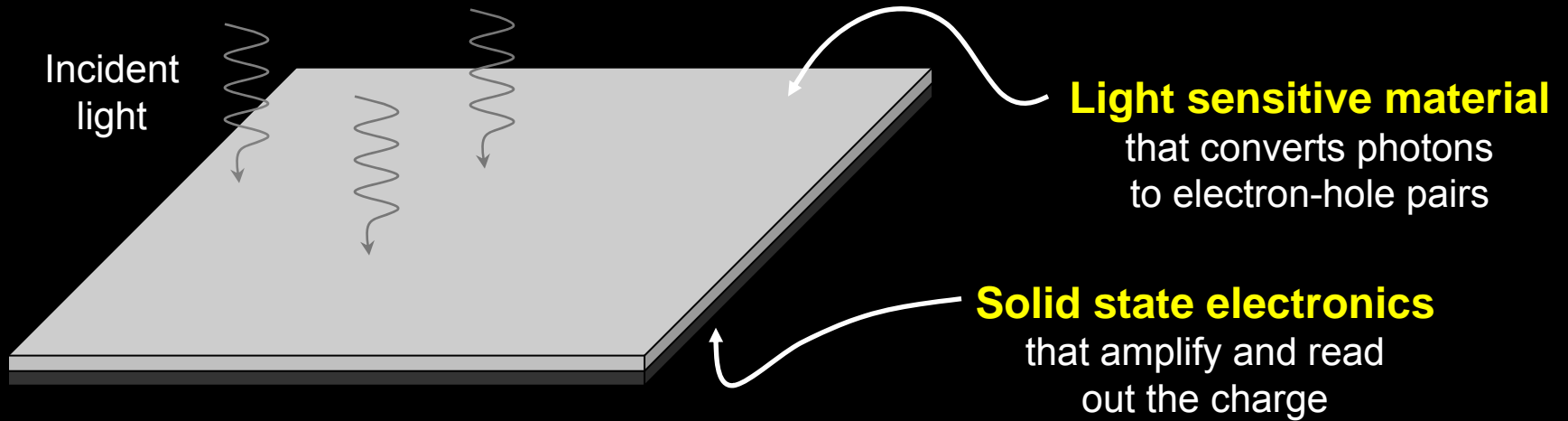
HgCdTe cutoff wavelength (microns)

6 steps of optical / IR photon detection

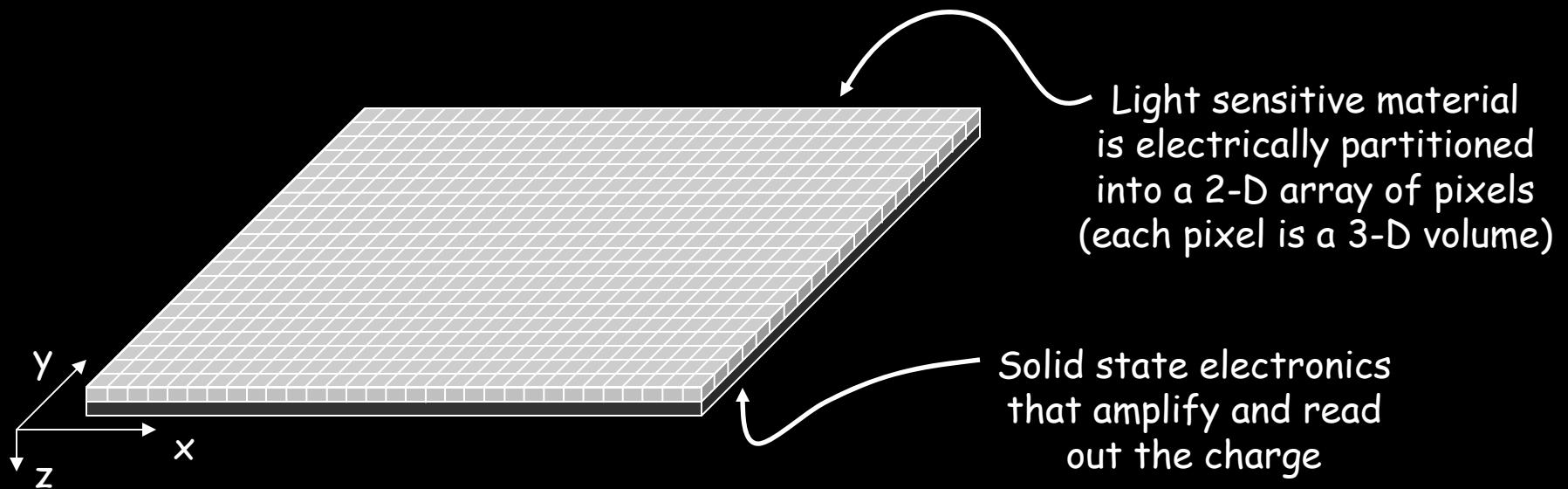


Two main parts of an imaging detector

Detector material & Solid state electronics



3. Charge Collection



- Intensity image is generated by collecting photocharge generated in 3-D volume into 2-D array of pixels.
- Optical and IR focal plane arrays both collect charges via electric fields.
- In the z-direction, optical and IR use a p-n junction to “sweep” charge toward pixel collection nodes.

Periodic Table

Number of electrons in outer shell

3

4

5

2

He

Helium
4.0

5

B

Boron
10.8

6

C

Carbon
12.0

7

N

Nitrogen
14.0

8

O

Oxygen
16.0

9

F

Fluorine
19.0

10

Ne

Neon
20.2

13

Al

Aluminum
27.0

14

Si

Silicon
28.1

15

P

Phosphorus
31.0

16

S

Sulfur
32.1

17

Cl

Chlorine
35.5

18

Ar

Argon
40.0

	26	27	28	29	30	31	32	33	34	35	36
	Fe	Co	Ni	Cu	Zn	Ga	Ge	As	Se	Br	Kr
	Iron 55.9	Cobalt 58.9	Nickel 58.7	Copper 63.5	Zinc 65.4	Gallium 69.7	Germanium 72.6	Arsenic 74.9	Selenium 79.0	Bromine 79.9	Krypton 83.8
	44	45	46	47	48	49	50	51	52	53	54
	Ru	Rh	Pd	Ag	Cd	In	Sn	Sb	Te	I	Xe
	Ruthenium 101.0	Rhodium 102.9	Palladium 106.4	Silver 107.9	Cadmium 112.4	Indium 114.8	Tin 118.7	Antimony 121.8	Tellurium 127.6	Iodine 126.9	Xenon 131.3
	76	77	78	79	80	81	82	83	84	85	86
	Os	Ir	Pt	Au	Hg	Tl	Pb	Bi	Po	At	Rn
	Osmium 190.2	Iridium 192.2	Platinum 195.1	Gold 197.0	Mercury 200.6	Thallium 204.4	Lead 207.2	Bismuth 209.0	Polonium 210.0	Astatine 210.0	Radon 222.0
	108	109	110								
	Hs	Mt	Uun								
	Hassium 265	Meitnerium 266	Ununnilium 272								

Types of Elements Key:



Alkali metals

Periodic Table

Number of electrons in outer shell

3

4

5

2

He

Helium
4.0

5

B

Boron
10.8

6

C

Carbon
12.0

7

N

Nitrogen
14.0

8

O

Oxygen
16.0

9

F

Fluorine
19.0

10

Ne

Neon
20.2

13

Al

Aluminum
27.0

14

Si

Silicon
28.1

15

P

Phosphorus
31.0

16

S

Sulfur
32.1

17

Cl

Chlorine
35.5

18

Ar

Argon
40.0

	26	27	28	29	30	31	32	33	34	35	36
	Fe	Co	Ni	Cu	Zn	Ga	Ge	As	Se	Br	Kr
	Iron 55.9	Cobalt 58.9	Nickel 58.7	Copper 63.5	Zinc 65.4	Gallium 69.7	Germanium 72.6	Arsenic 74.9	Selenium 79.0	Bromine 79.9	Krypton 83.8
	44	45	46	47	48	49	50	51	52	53	54
	Ru	Rh	Pd	Ag	Cd	In	Sn	Sb	Te	I	Xe
	Ruthenium 101.0	Rhodium 102.9	Palladium 106.4	Silver 107.9	Cadmium 112.4	Indium 114.8	Tin 118.7	Antimony 121.8	Tellurium 127.6	Iodine 126.9	Xenon 131.3
	76	77	78	79	80	81	82	83	84	85	86
	Os	Ir	Pt	Au	Hg	Tl	Pb	Bi	Po	At	Rn
	Osmium 190.2	Iridium 192.2	Platinum 195.1	Gold 197.0	Mercury 200.6	Thallium 204.4	Lead 207.2	Bismuth 209.0	Polonium 210.0	Astatine 210.0	Radon 222.0
	108	109	110								
	Hs	Mt	Uun								
	Hassium 265	Meitnerium 266	Ununnilium 272								

Types of Elements Key:



Alkali metals

Periodic Table

Number of electrons in outer shell

3

4

5

2

He

Helium
4.0

5

B

Boron
10.8

6

C

Carbon
12.0

7

N

Nitrogen
14.0

8

O

Oxygen
16.0

9

F

Fluorine
19.0

10

Ne

Neon
20.2

13

Al

Aluminum
27.0

14

Si

Silicon
28.1

15

P

Phosphorus
31.0

16

S

Sulfur
32.1

17

Cl

Chlorine
35.5

18

Ar

Argon
40.0

	26	27	28	29	30	31	32	33	34	35	36
	Fe	Co	Ni	Cu	Zn	Ga	Ge	As	Se	Br	Kr
	Iron 55.9	Cobalt 58.9	Nickel 58.7	Copper 63.5	Zinc 65.4	Gallium 69.7	Germanium 72.6	Arsenic 74.9	Selenium 79.0	Bromine 79.9	Krypton 83.8
	44	45	46	47	48	49	50	51	52	53	54
	Ru	Rh	Pd	Ag	Cd	In	Sn	Sb	Te	I	Xe
	Ruthenium 101.0	Rhodium 102.9	Palladium 106.4	Silver 107.9	Cadmium 112.4	Indium 114.8	Tin 118.7	Antimony 121.8	Tellurium 127.6	Iodine 126.9	Xenon 131.3
	76	77	78	79	80	81	82	83	84	85	86
	Os	Ir	Pt	Au	Hg	Tl	Pb	Bi	Po	At	Rn
	Osmium 190.2	Iridium 192.2	Platinum 195.1	Gold 197.0	Mercury 200.6	Thallium 204.4	Lead 207.2	Bismuth 209.0	Polonium 210.0	Astatine 210.0	Radon 222.0
	108	109	110								
	Hs	Mt	Uun								
	Hassium 265	Meitnerium 266	Ununnilium 272								

Types of Elements Key:

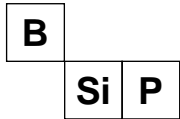


Alkali metals

Photovoltaic Detector Potential Well

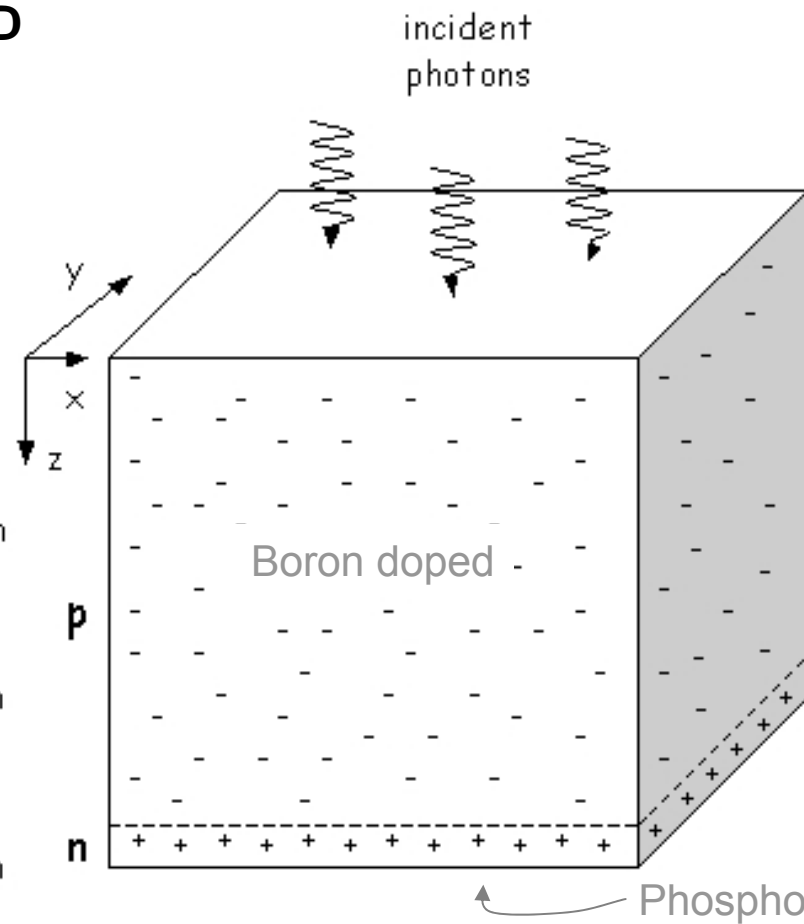
n-channel CCD

3 4 5

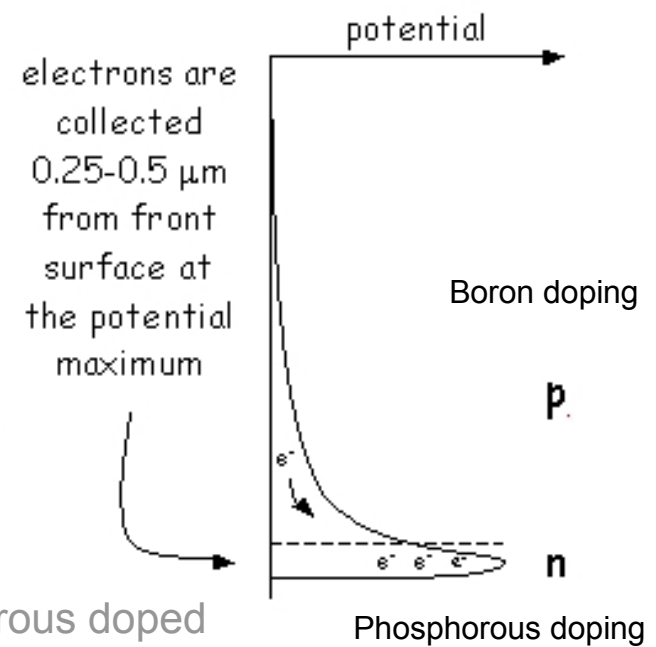


distance
from back
surface

5 μm
10 μm
15 μm



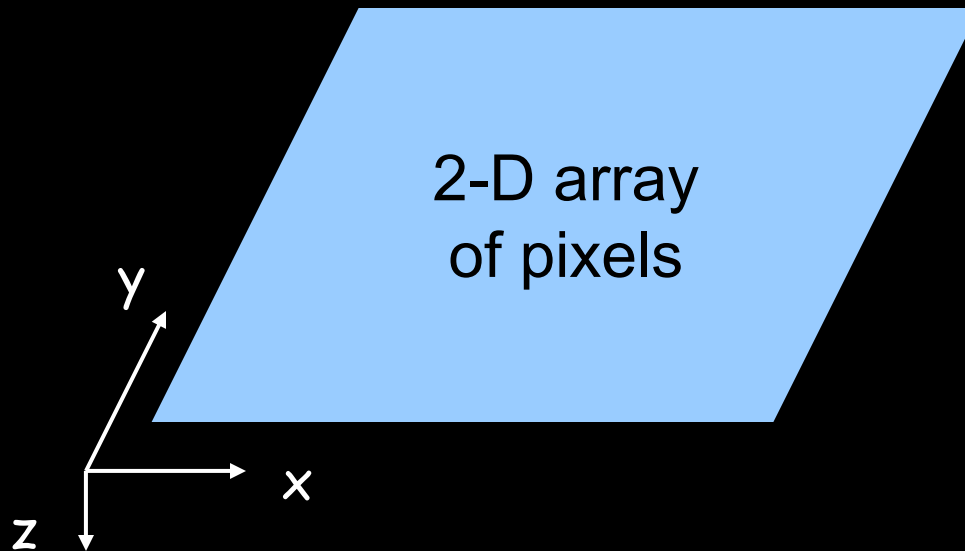
Nota bene !
Can collect either
electrons or holes



Silicon, HgCdTe and InSb are photovoltaic detectors. All use a pn-junction to generate E-field in the z-direction of each pixel. This electric field separates the electron-hole pairs generated by a photon.

Charge Collection

- CCD and CMOS focal plane arrays are different for charge collection in the x and y dimensions.
- CMOS – collect charge at each pixel and have amplifiers and readout multiplexer
- CCD – collect charge in array of pixels. At end of frame, move charge to edge of array where one (or more) amplifier (s) read out the pixels.



6 steps of optical / IR

Anti-reflection coating
Substrate removal

Detector Materials
Si, HgCdTe, InSb, Si:As

Electric Fields in detector
collect electrical charge

CCD

Charge coupled
transfer

MOSFET
Amplifier

CMOS

Source follower,
CTIA, DI

Random access
or full frame read

1. Light into d

2. Charge Ge

3. Charge Collection

4. Charge
Transfer

5. Charge-to-
Voltage
Conversion

4. Charge-to-
Voltage
Conversion

5. Signal
Transfer

6. Digitization

Charge collection in the x-y plane is where CCD and CMOS diverge.

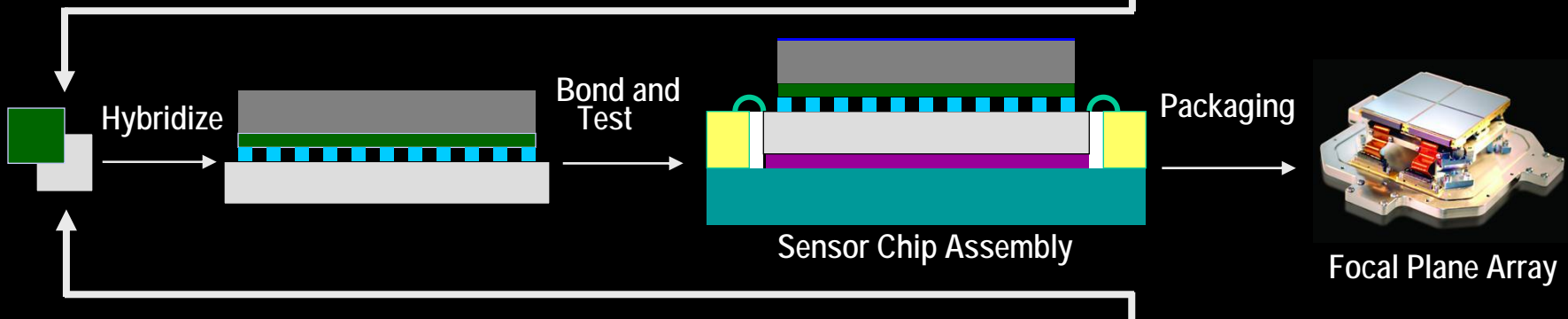
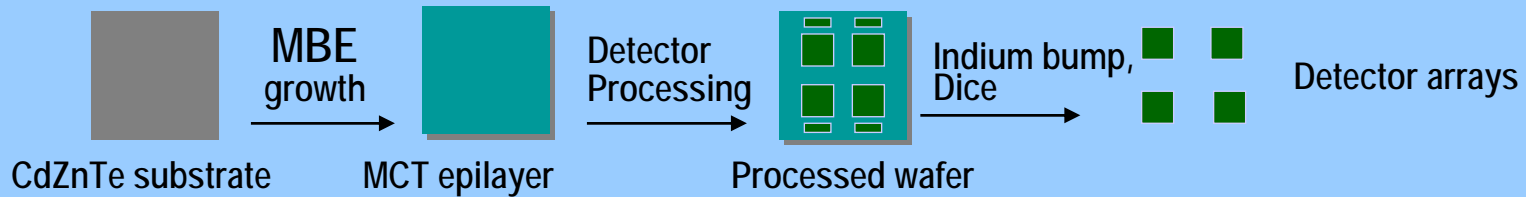
Concentrate now on CMOS:

- Charge collection in x-y plane
- Charge-to-voltage conversion
- Signal transfer

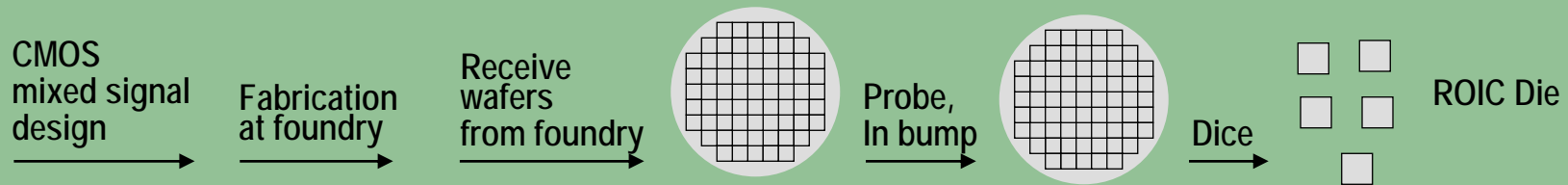
Start with IR array fabrication.

HgCdTe IR FPA Manufacturing Process

Detector Fabrication

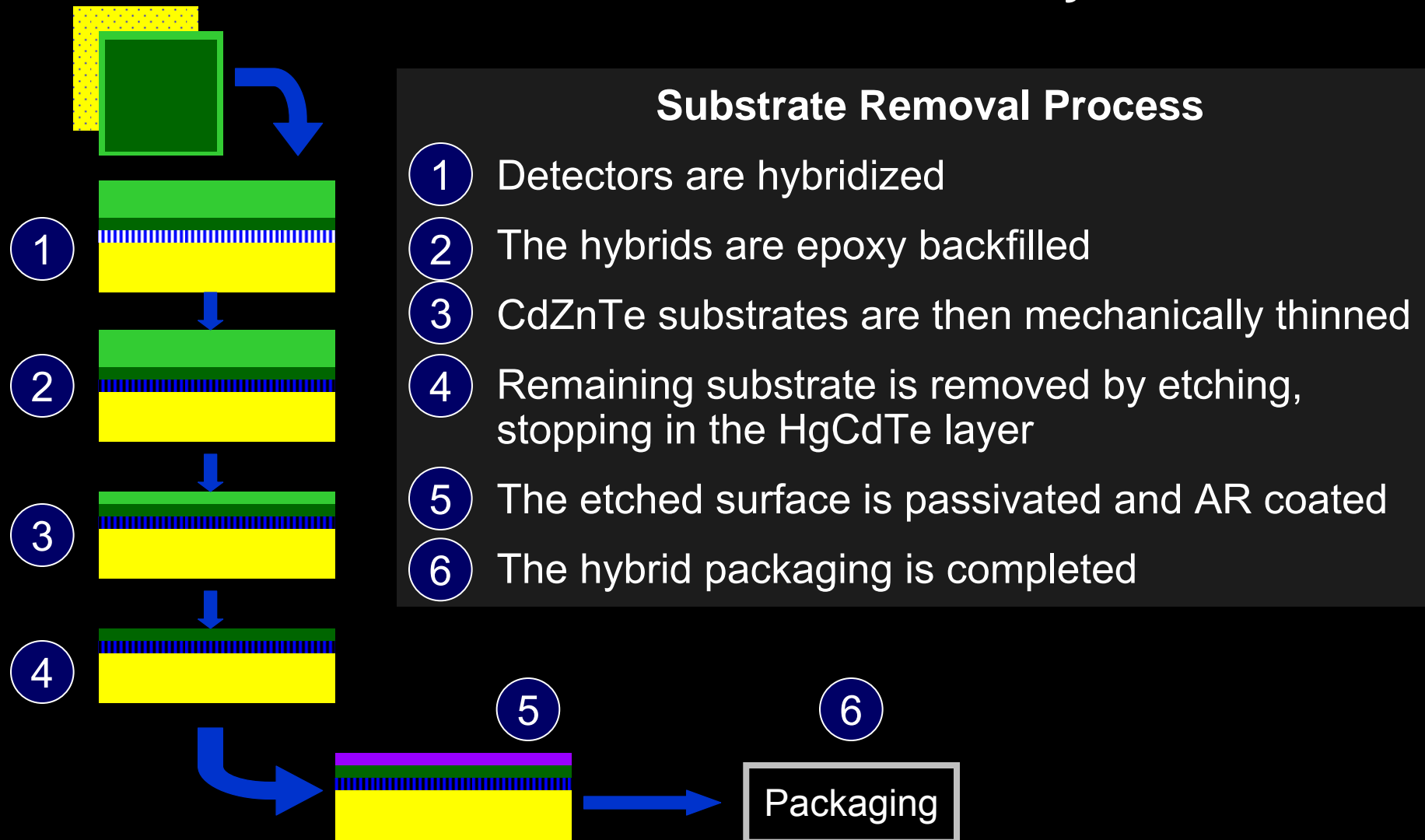


Multiplexer Design and Fabrication

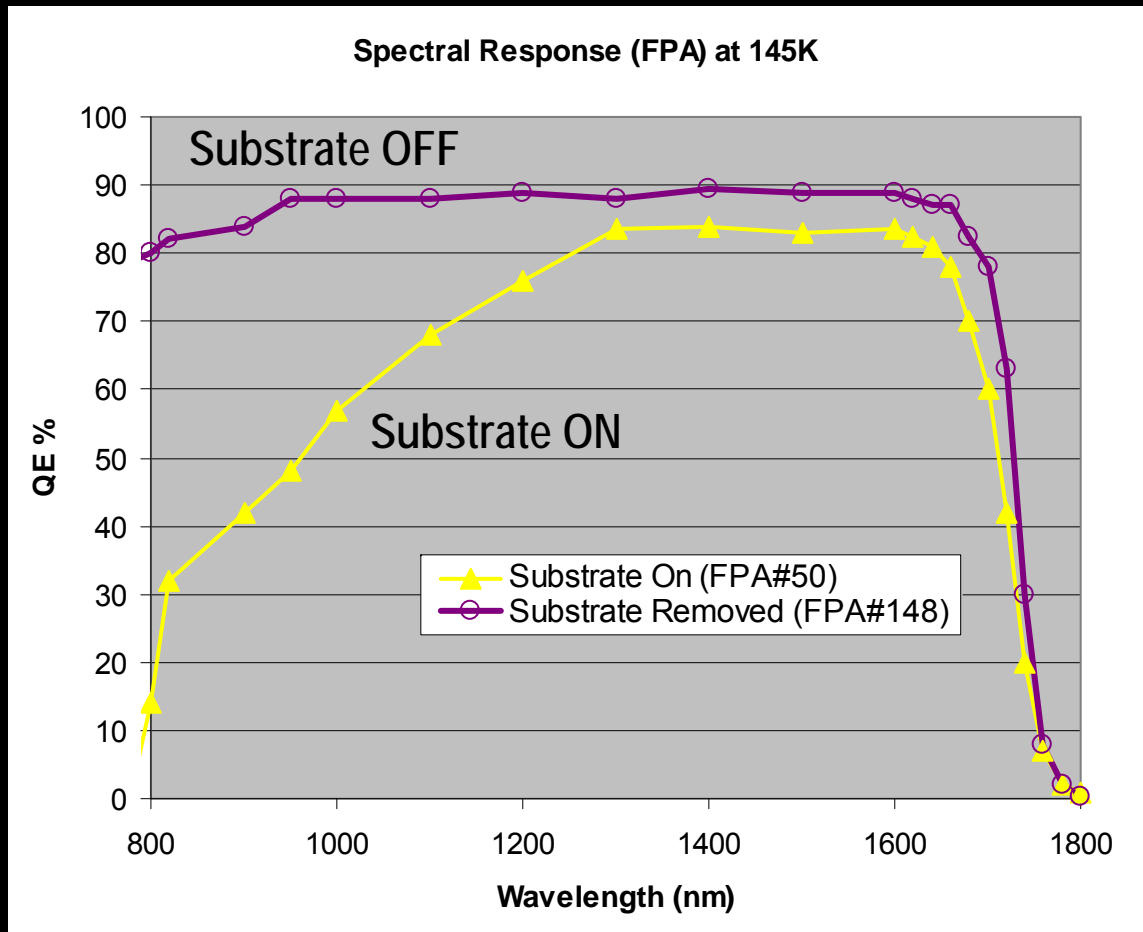


Substrate Removal of HgCdTe

The new standard in astronomy



QE Improvement With Substrate Removal



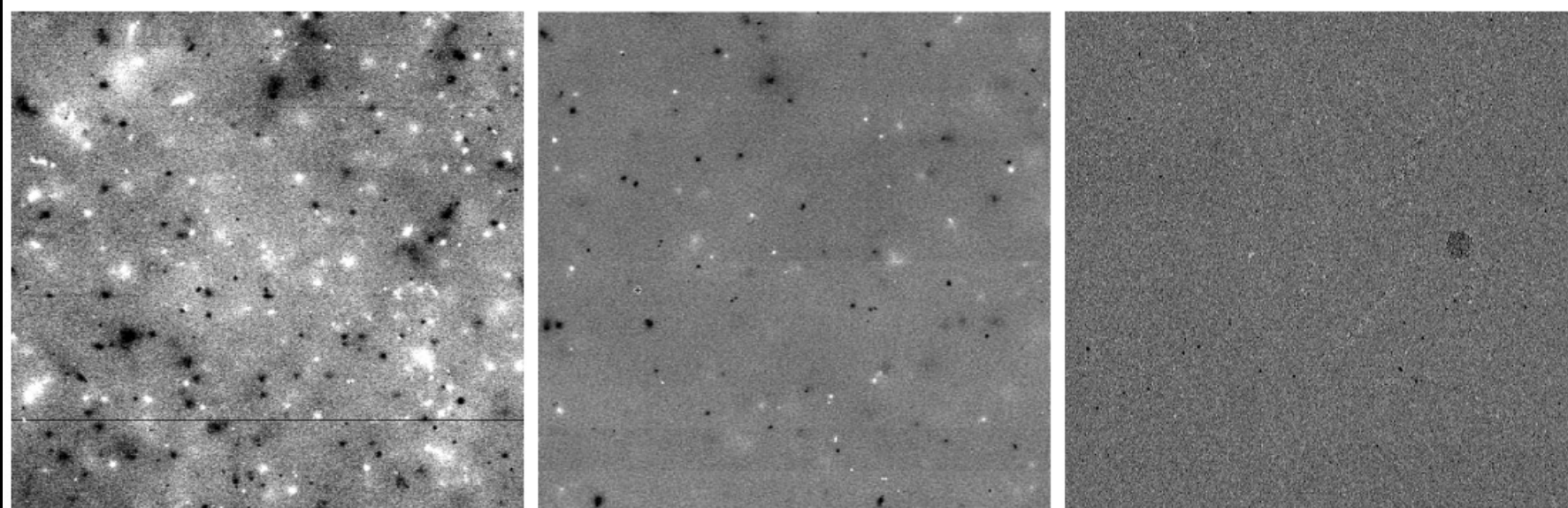
Quantum efficiency improves across the IR band after substrate removal, particularly at short wavelengths, and HgCdTe is sensitive to visible light.



FPA QE measured by NASA Goddard Detector Characterization Laboratory (no IPCC)

Cosmic Rays and Substrate Removal

- Cosmic ray events produce clouds of detected signal due to particle-induced flashes of infrared light in the CdZnTe substrate; removal of the substrate eliminates the effect



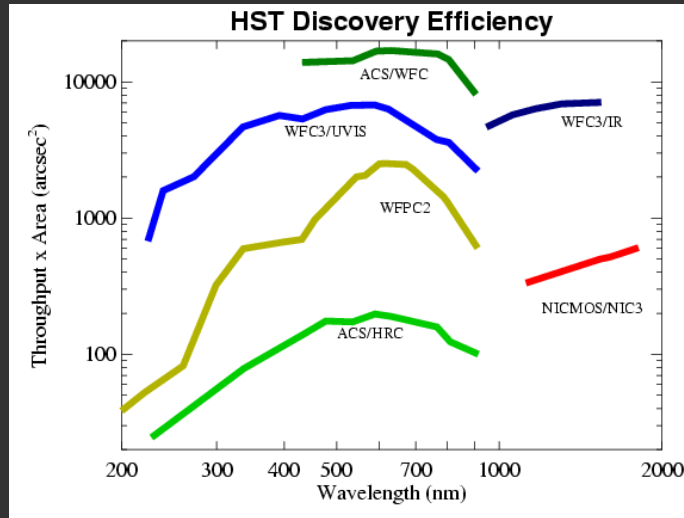
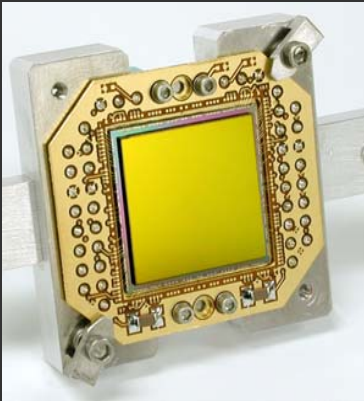
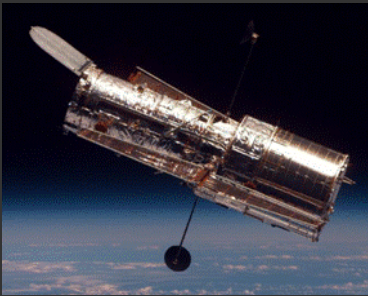
2.5um cutoff, substrate **on**

1.7um cutoff, substrate **on**

1.7um cutoff, substrate **off**

*Roger Smith (Caltech) SPIE 5-25-2006

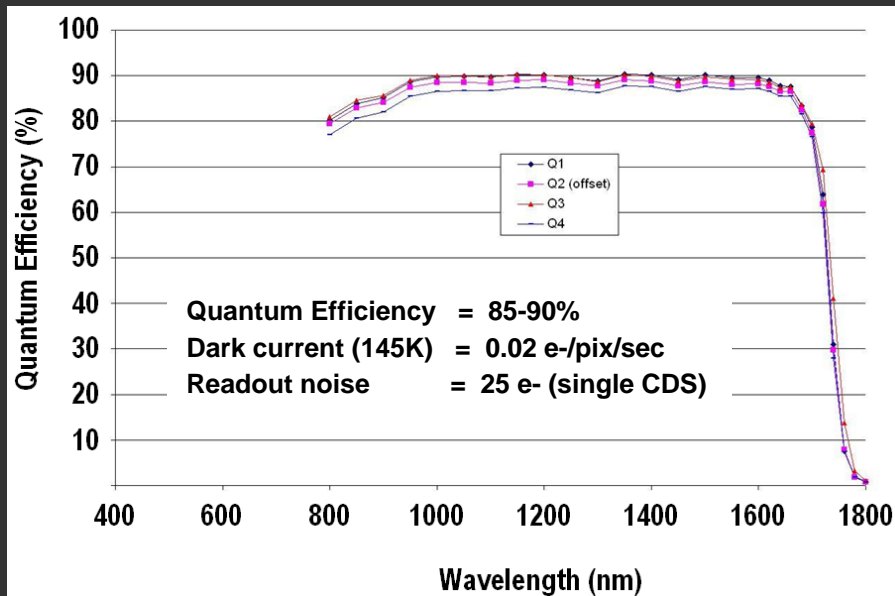
Hubble Space Telescope Wide Field Camera 3



Stellar Jet in the Carina Nebula
Hubble Space Telescope • WFC3/UVIS/IR

NASA, ESA, and the Hubble SM4 ERO Team

STScI-PRC09-25b

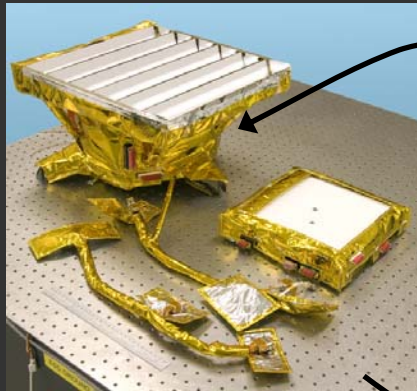


- 1024×1024 pixels, 18.5 micron pitch
- Substrate-removed 1.7 μm HgCdTe arrays
- Nearly 30x increase in HST discovery efficiency

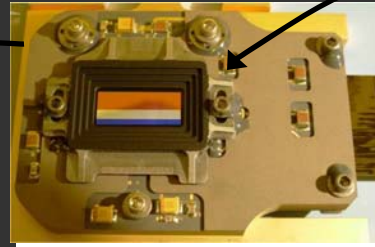
Moon Mineralogy Mapper Discovers Water on the Moon

Moon water findings are a game-changer

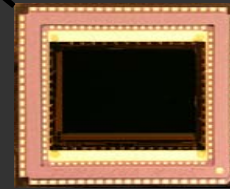
Discovery calls into question 40 years of assumptions about lunar surface



Instrument at JPL before shipment to India



Focal Plane Assembly



Sensor Chip Assembly

Teledyne Infrared FPA

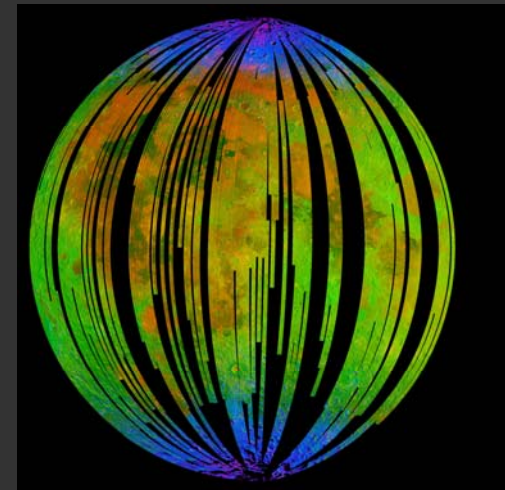
- 640 x 480 pixels (27 μm pitch)
- Substrate-removed HgCdTe (0.4 to 3.0 μm)
- 650,000 e- full well, <100 e- noise
- 100 Hz frame rate (integrate while read)
- < 70 mW power dissipation
- Package includes order sorting filter
- Total FPA mass: 58 grams

By Andrea Thompson

SPACE

updated 12:38 p.m. PT, Thurs., Sept. 24, 2009

The discovery of widespread but small amounts of water on the surface of the moon, announced Wednesday, stands as one of the most surprising findings in planetary science.



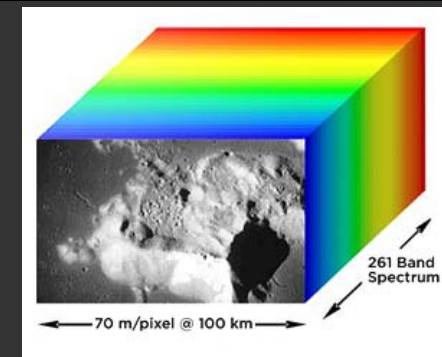
Completion of Chandrayaan-1 spacecraft integration
Moon Mineralogy Mapper is white square at end of arrow



Chandrayaan-1 in the
Polar Satellite Launch Vehicle

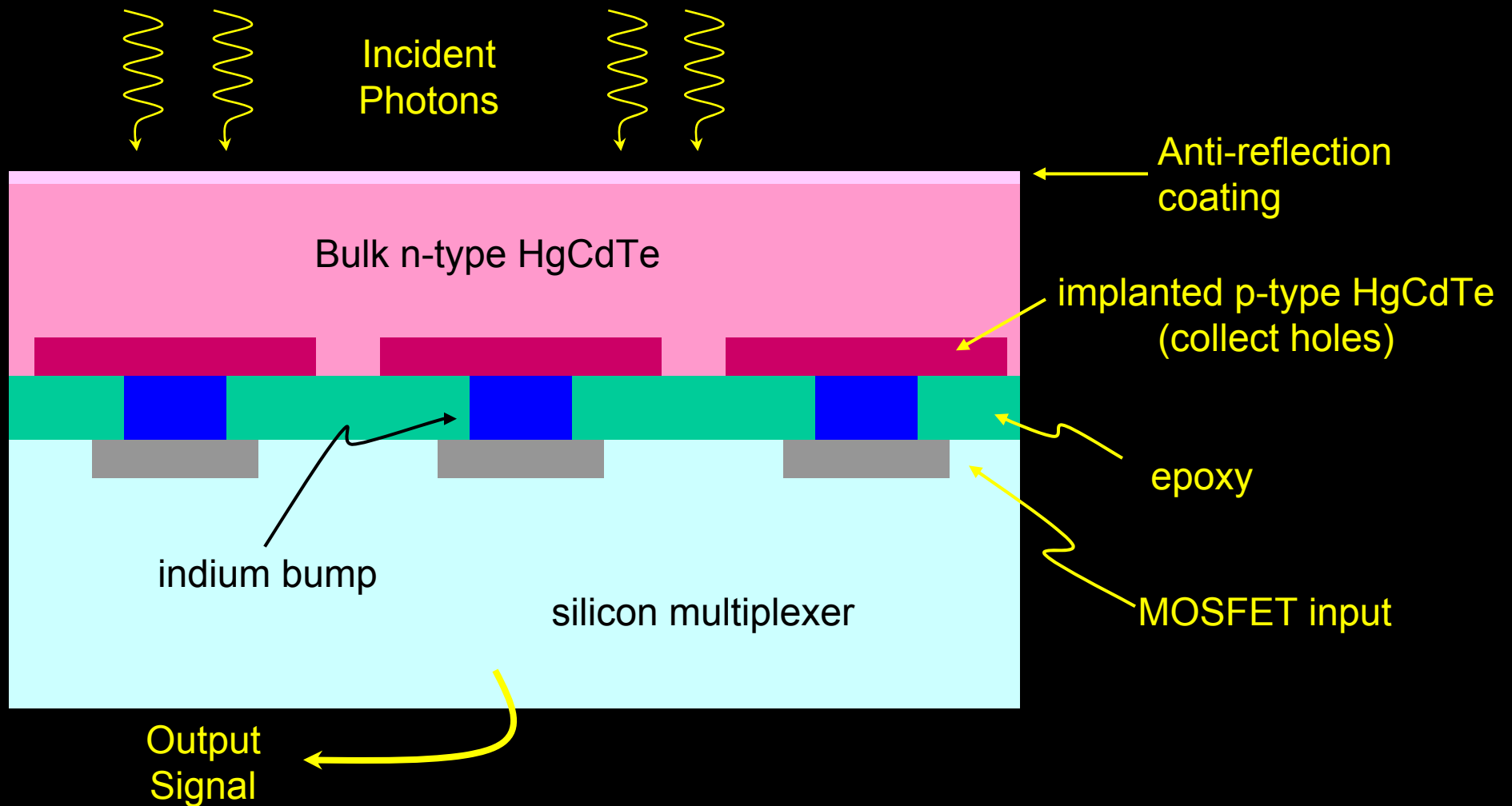


Launch from Satish
Dhawan Space Centre

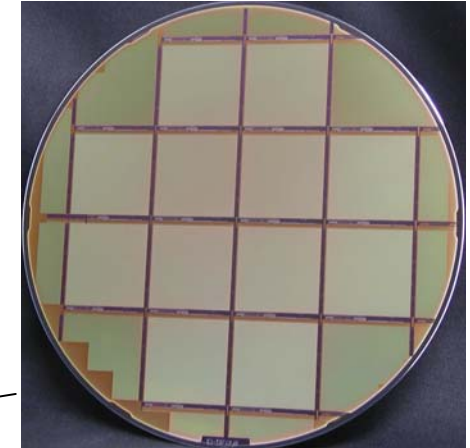
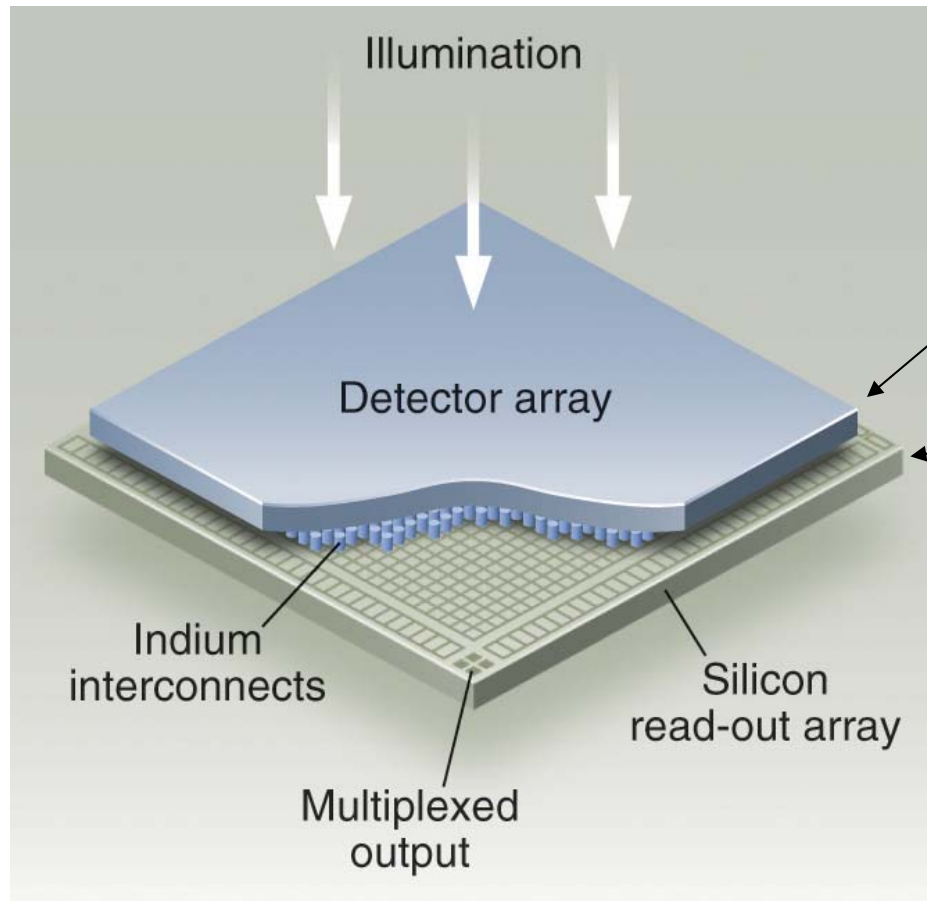


Moon Mineralogy Mapper resolves visible and infrared to 10 nm spectral resolution, 70 m spatial resolution
100 km altitude lunar orbit

HgCdTe hybrid FPA cross-section (substrate removed)



Hybrid CMOS Infrared Imaging Sensors

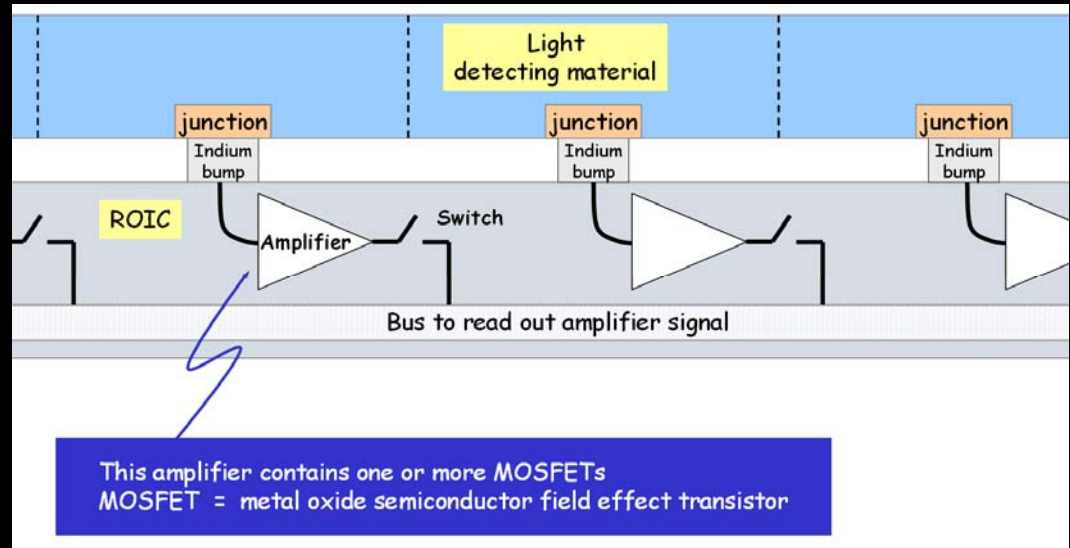
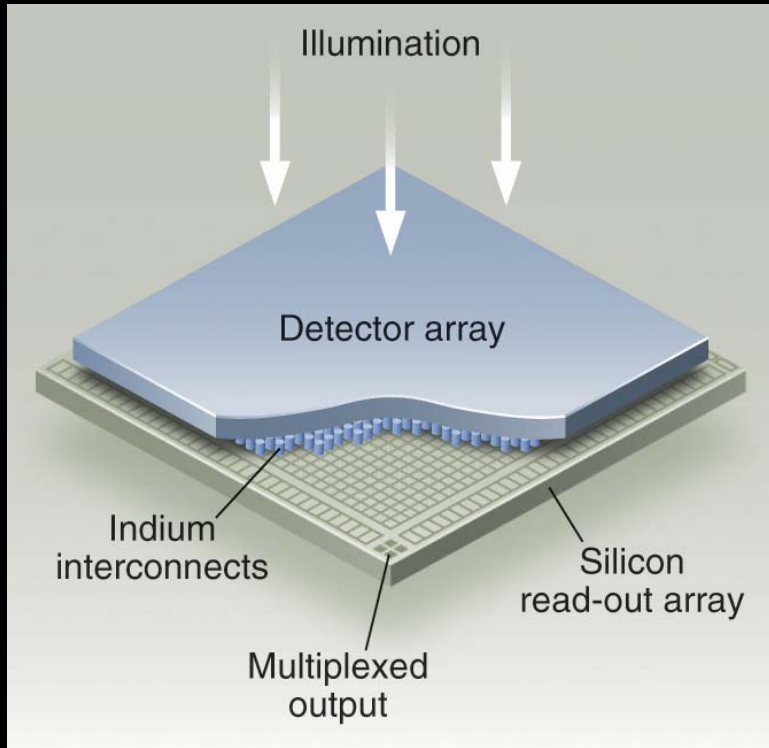


Large, high performance IR arrays

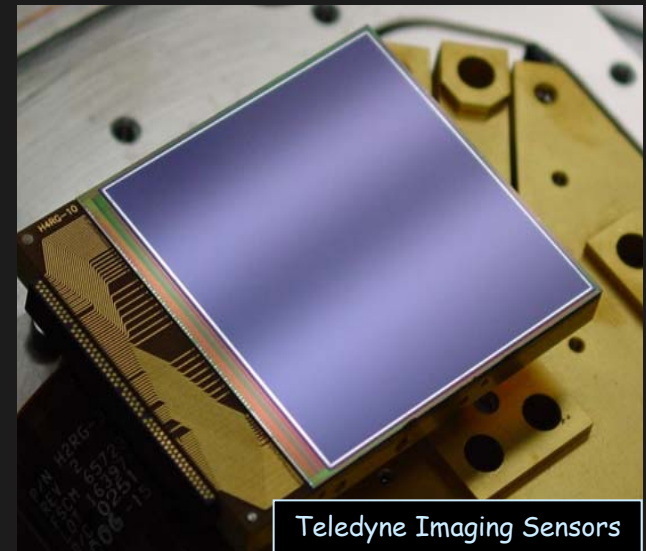
Three Key Technologies

1. Growth and processing of the HgCdTe detector layer
2. Design and fabrication of the CMOS readout integrated circuit (ROIC)
3. Hybridization of the detector layer to the CMOS ROIC

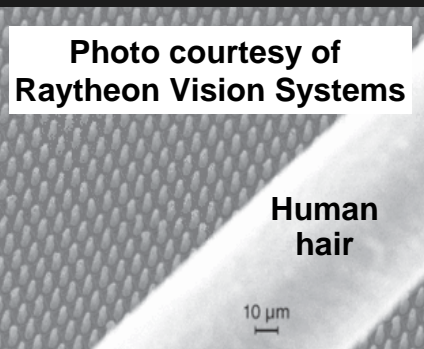
Hybrid Imager Architecture



H4RG-10
4096x4096 pixels
10 micron pixel pitch
HyViSI silicon PIN



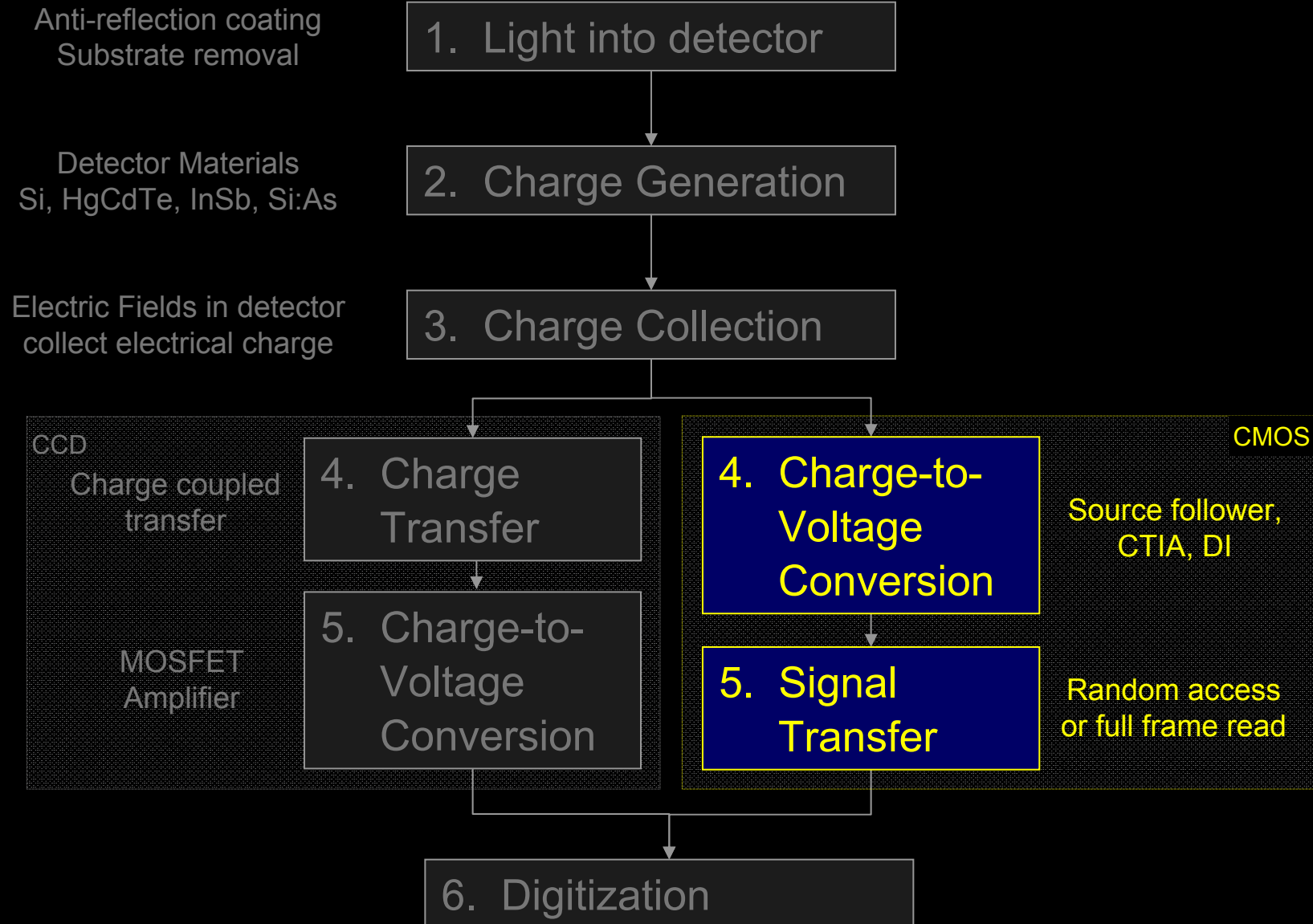
Teledyne Imaging Sensors



Mature interconnect technique:

- Over 16,000,000 indium bumps per Sensor Chip Assembly (SCA) demonstrated
- >99.9% interconnect yield

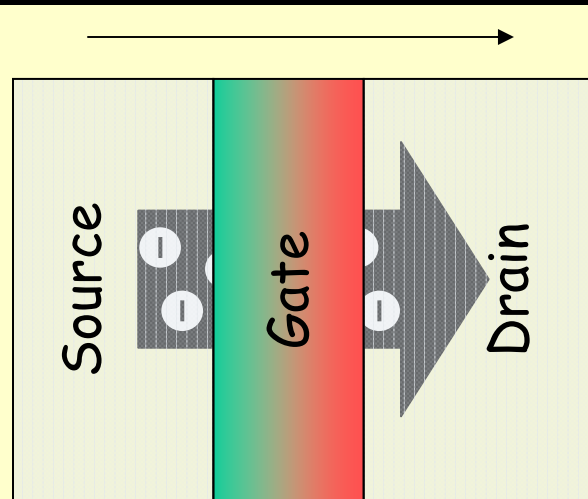
6 steps of optical / IR photon detection



MOSFET Principles

MOSFET = metal oxide semiconductor field effect transistor

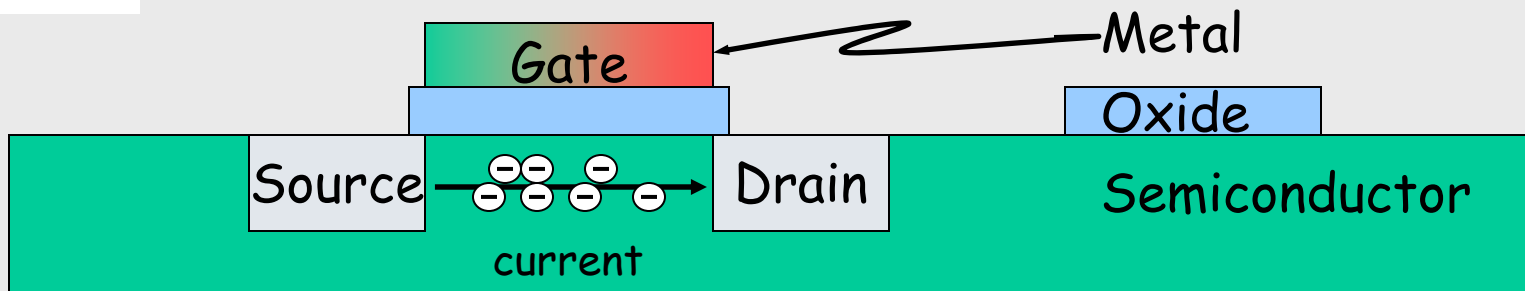
Top view



Turn on the MOSFET and current flows from source to drain

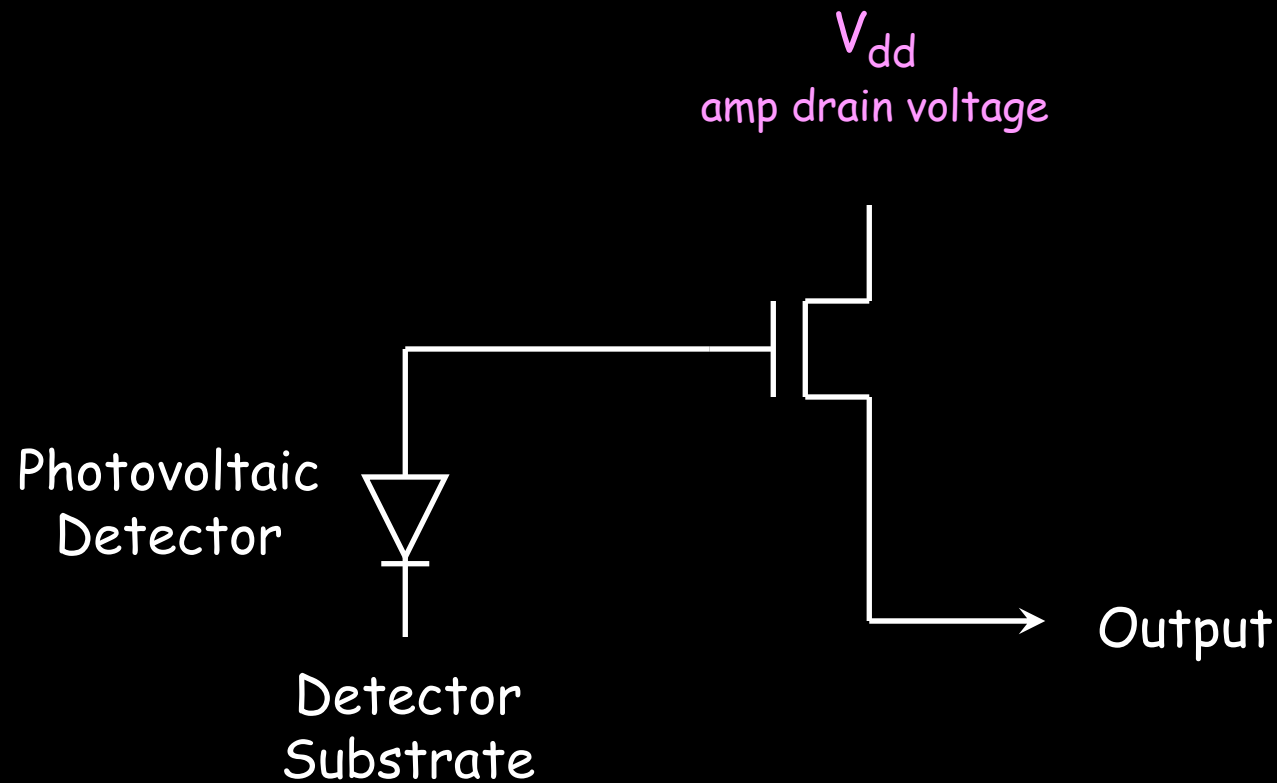
Add charge to gate & the current flow changes since the effect of the field of the charge will reduce the current

Side view

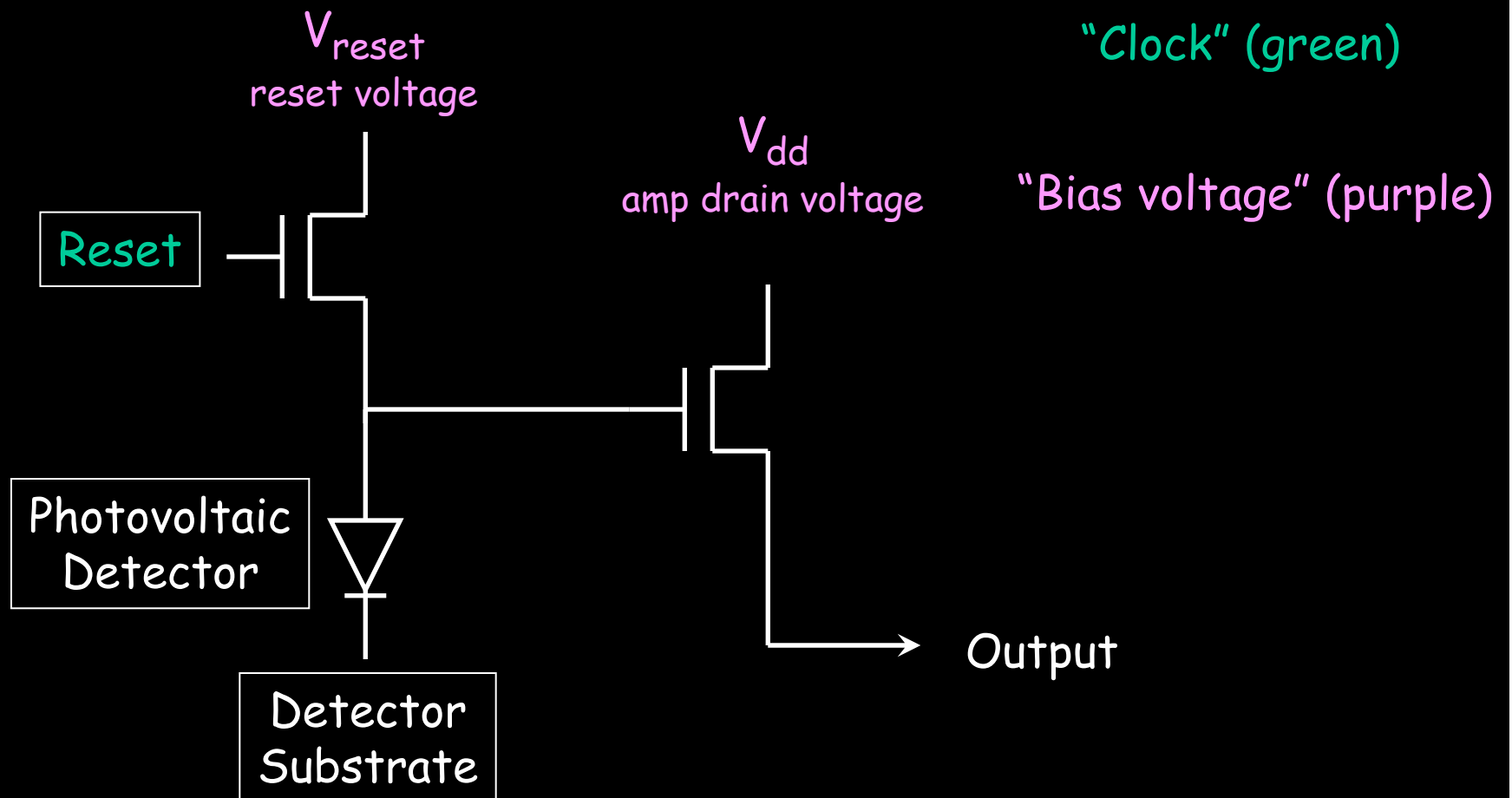


Fluctuations in current flow produce “readout noise”
Fluctuations in reset level on gate produces “reset noise”

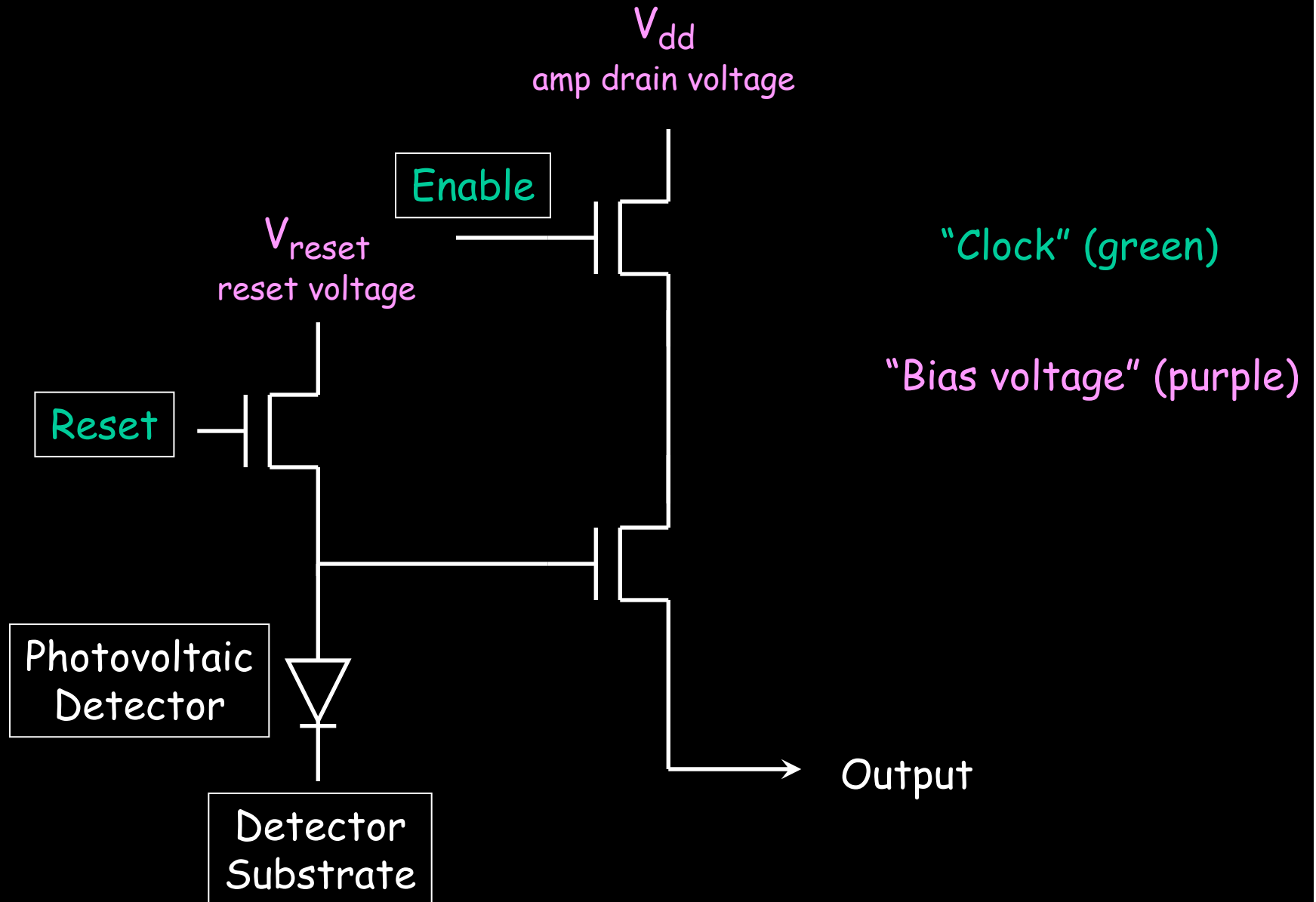
IR multiplexer pixel architecture



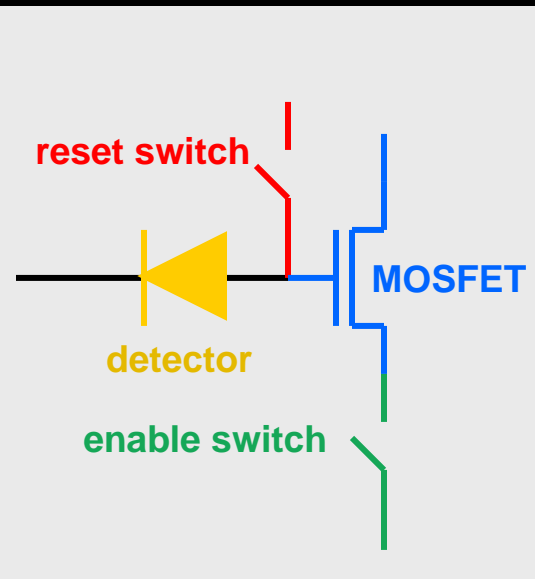
IR multiplexer pixel architecture



IR multiplexer pixel architecture

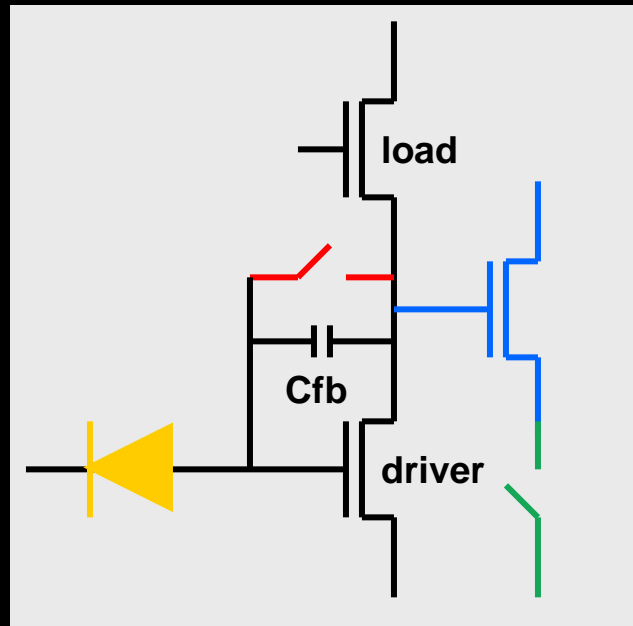


CMOS Pixel Amplifier Types



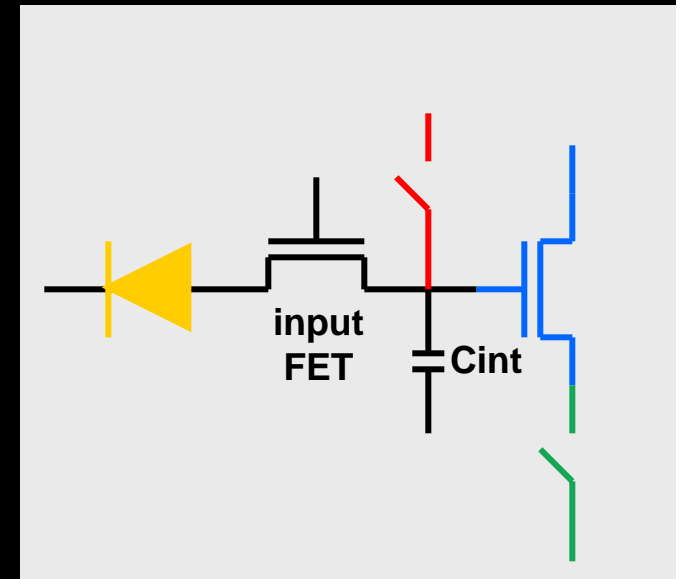
Source follower
per Detector (SFD)

- Integration on detector node
- Low power & compact
(3 FETs / pixel)
- Ideal for small pixels and low flux
- Poor performance for high flux



Capacitive TransImpedance
Amplifier (CTIA)

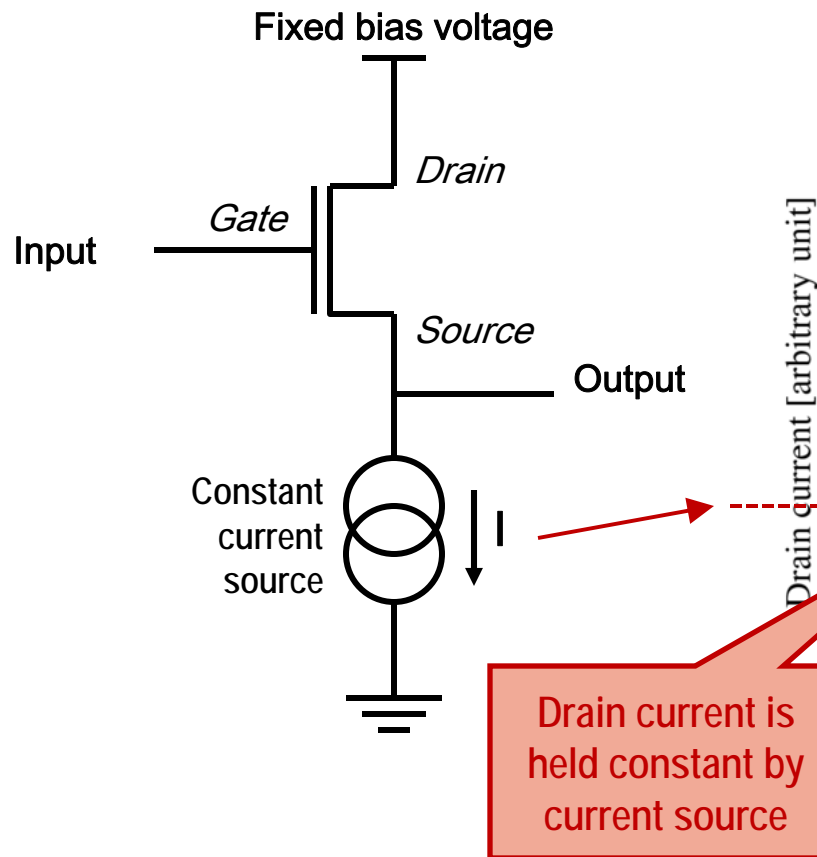
- Versatile circuit suitable for all backgrounds and detectors
- High linearity
- High power, higher noise and larger circuit than SFD for low flux
- Difficult for high flux due to the need for a large capacitor and high operating current



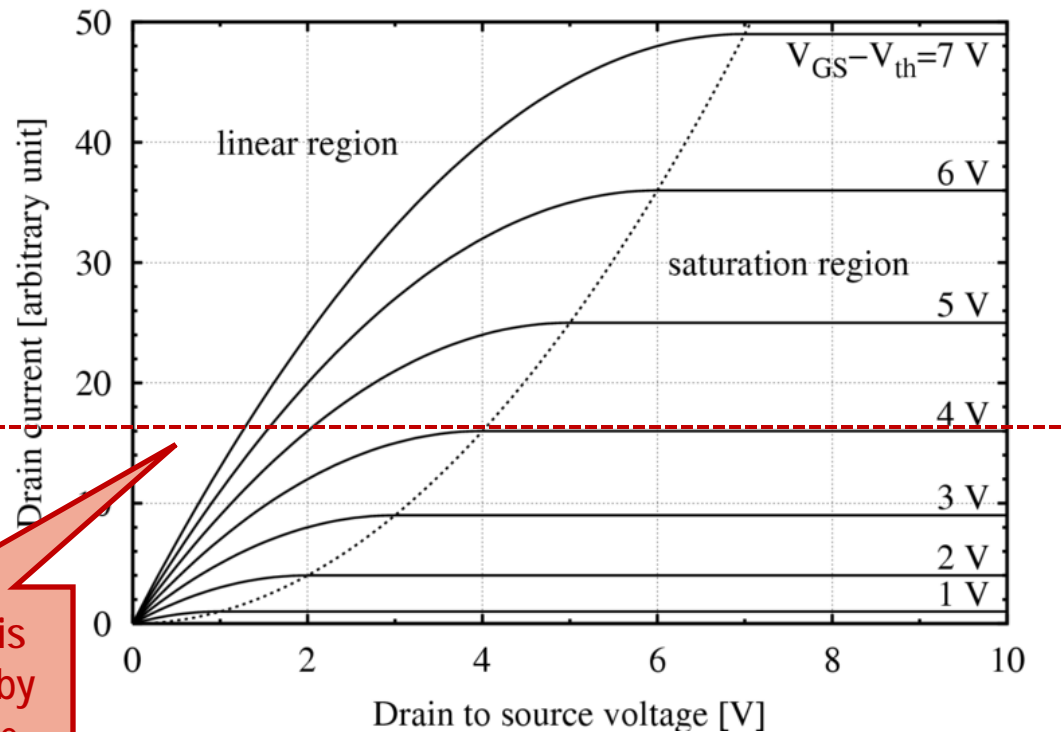
Direct Injection
(DI)

- Extremely small circuit
- Large integration density in pixel
- High well capacity for high flux applications
- Ultra low power
- Poor injection efficiency for low flux applications

Source Follower Operation



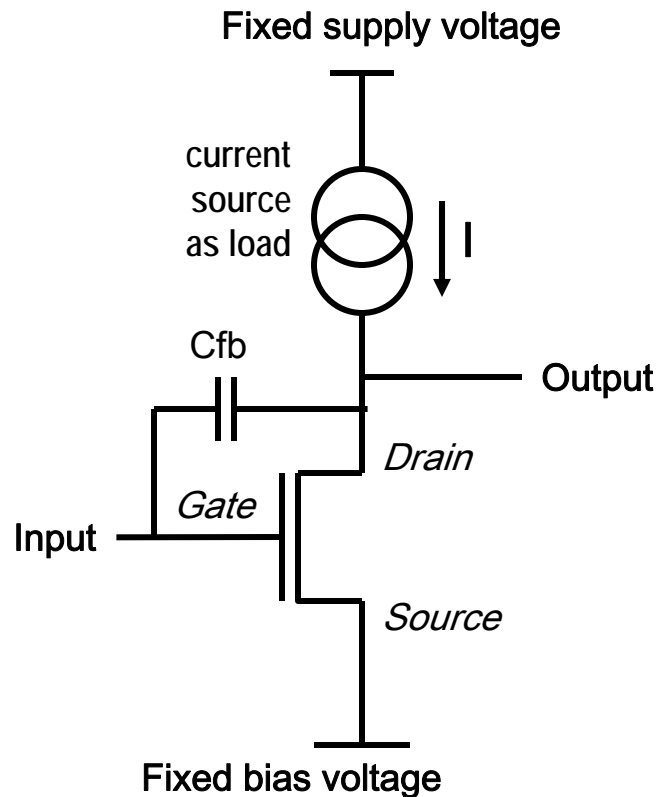
Characteristic Transistor Curves (NFET)



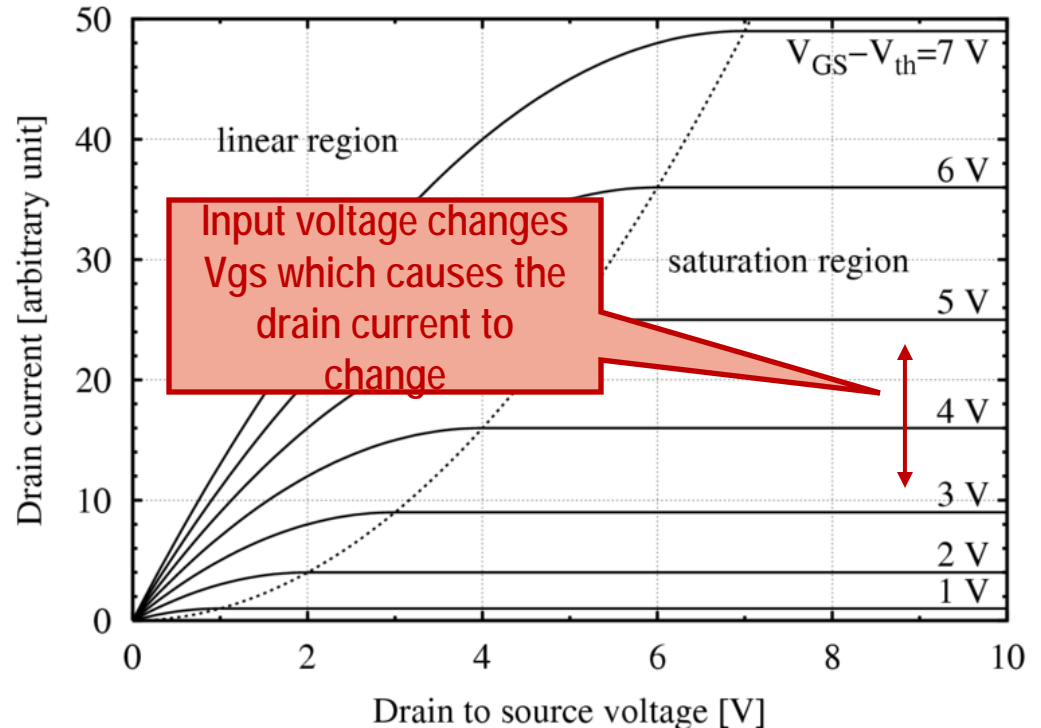
If the drain current is constant, the gate-source voltage (V_{gs}) is constant as long as the transistor operates in saturation:

=> If V_g moves, V_s will follow to keep V_{gs} constant

Capacitive Trans-Impedance Amplifier Operation



Characteristic Transistor Curves (NFET)



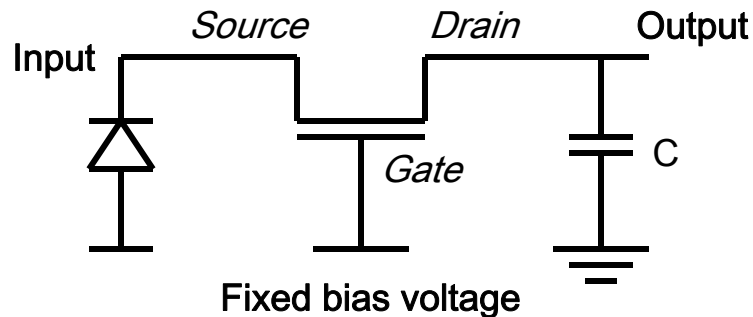
Inverting amplifier:

When the input increases, the drain current increases => The output node is pulled down by the transistor
 When the input decreases, the drain current decreases => The output node is pulled up by the current source

Capacitive feedback:

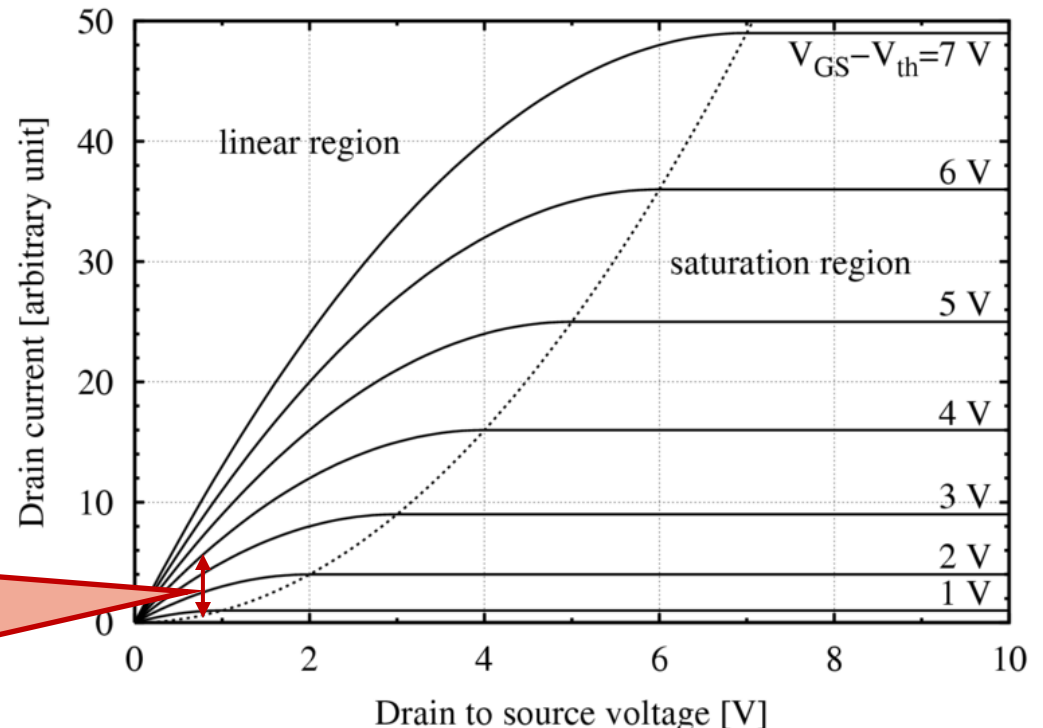
negative feedback that counteracts the initial input voltage change
 => charge at the input is converted to a voltage at the output, the input voltage is held constant by the feedback.

Direct Injection Operation



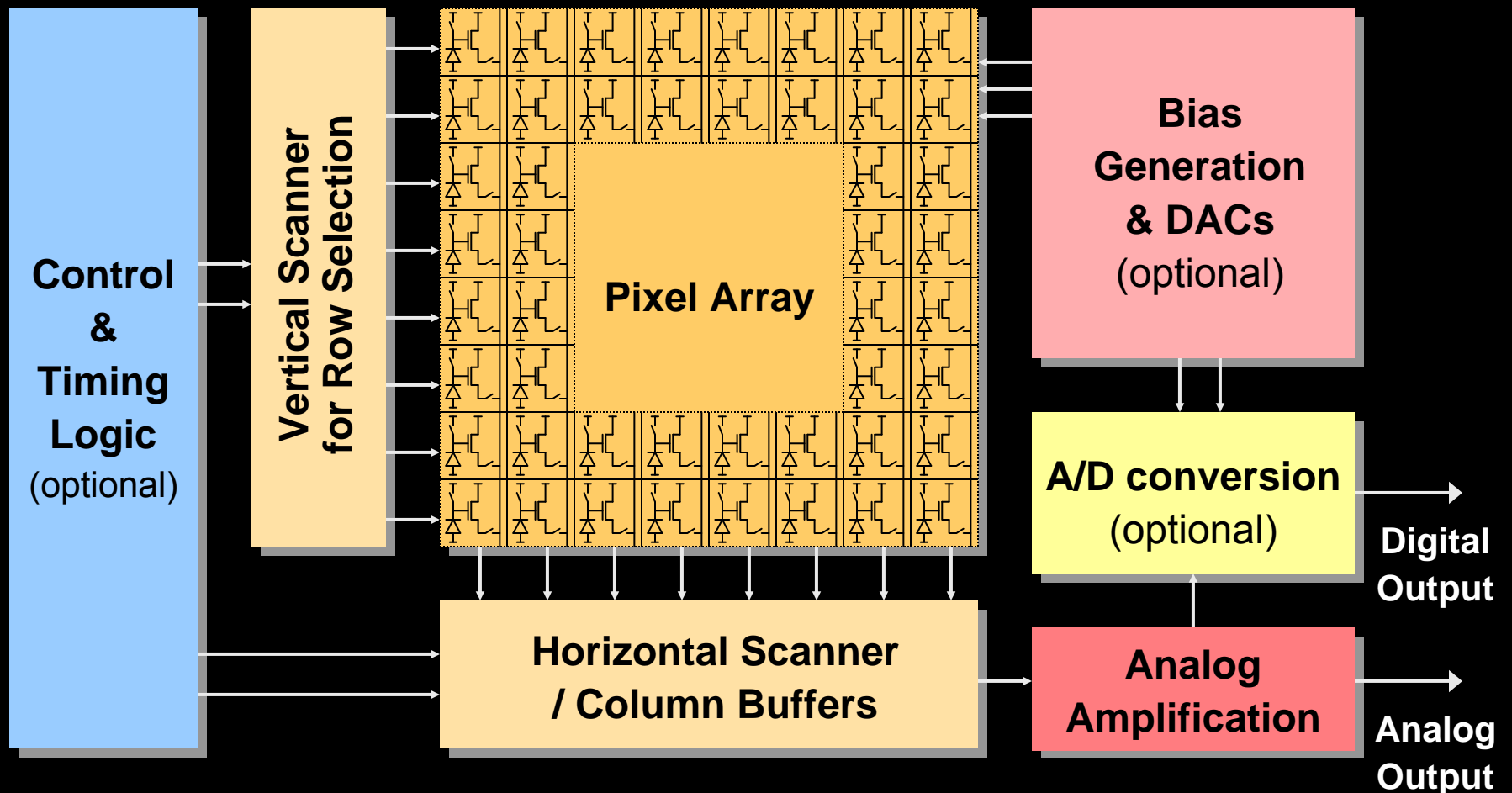
Decrease of input voltage (source) increases V_{GS} which increases the drain current.
Usually operates in subthreshold region (small currents)

Characteristic Transistor Curves (NFET)



- DI transistor does not work as amplifier, works more like a passgate
 - Whenever the detector diode generates photo charges, its voltage decreases (due to built-in capacitance)
 - This will increase V_{GS} which in turn will allow an increased drain current through the transistor
 - This current moves the collected charges from the photodiode into the integration capacitor C
 - Removing charges from the detector increases its voltage again, causing the drain current to decrease

General Architecture of CMOS-Based Image Sensors

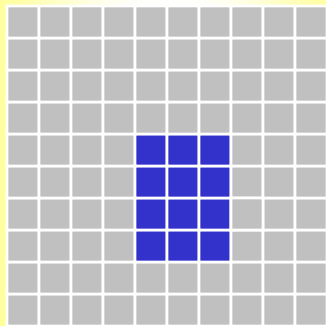


Special Scanning Techniques Supported by CMOS

- Different scanning methods are available to reduce the number of pixels being read:
 - Allows for higher frame rate or lower pixel rate (reduction in noise)
 - Can reduce power consumption due to reduced data

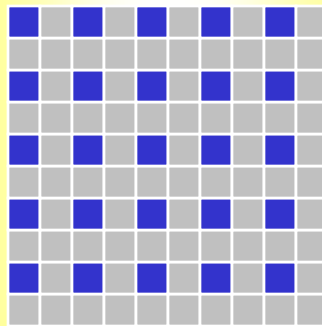
Windowing

- Reading of one or multiple rectangular subwindows
- Used to achieve higher frame rates (e.g. AO, guiding)



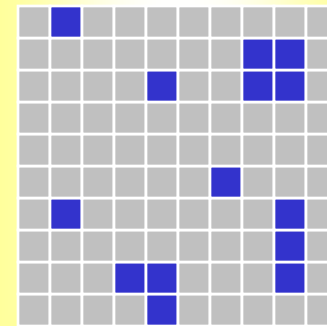
Subsampling

- Skipping of certain pixels/rows when reading the array
- Used to obtain higher frame rates on full-field images



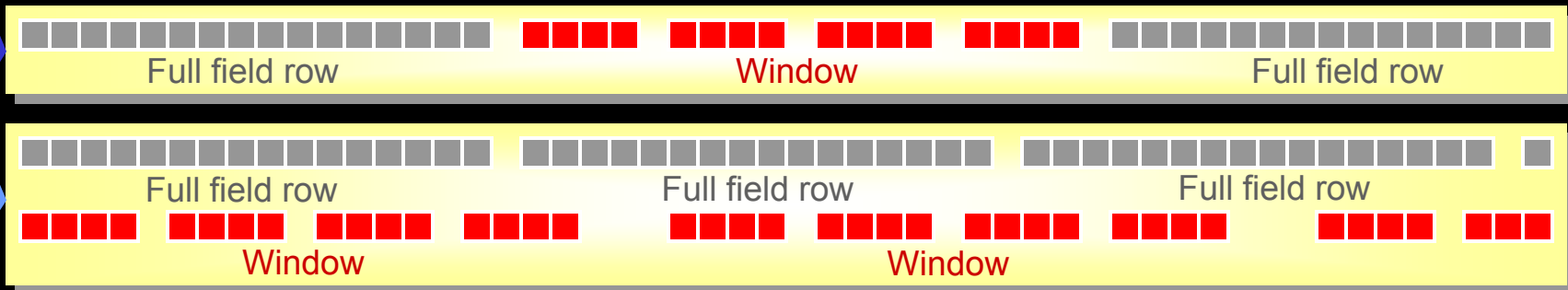
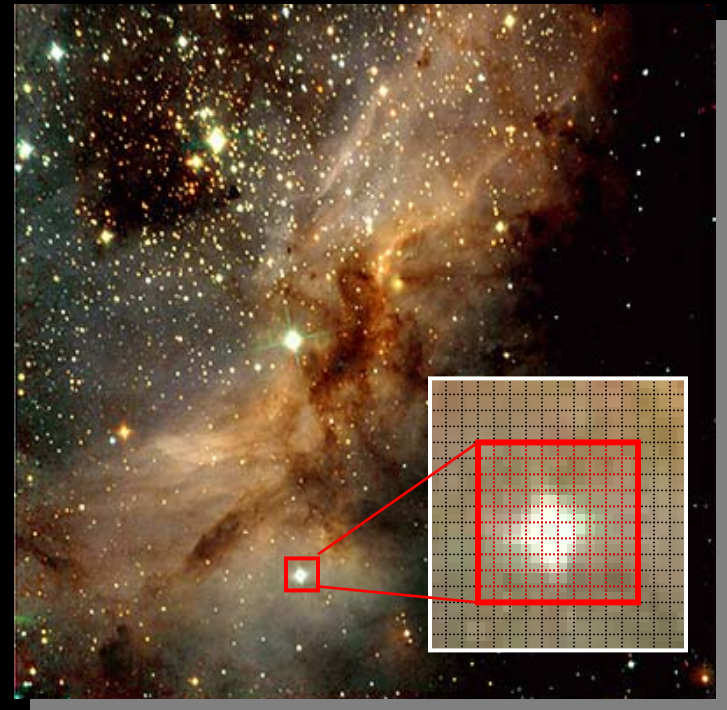
Random Read

- Random access (read or reset) of certain pixels
- Selective reset of saturated pixels
- Fast reads of selected pixels



Astronomy Application: Guiding

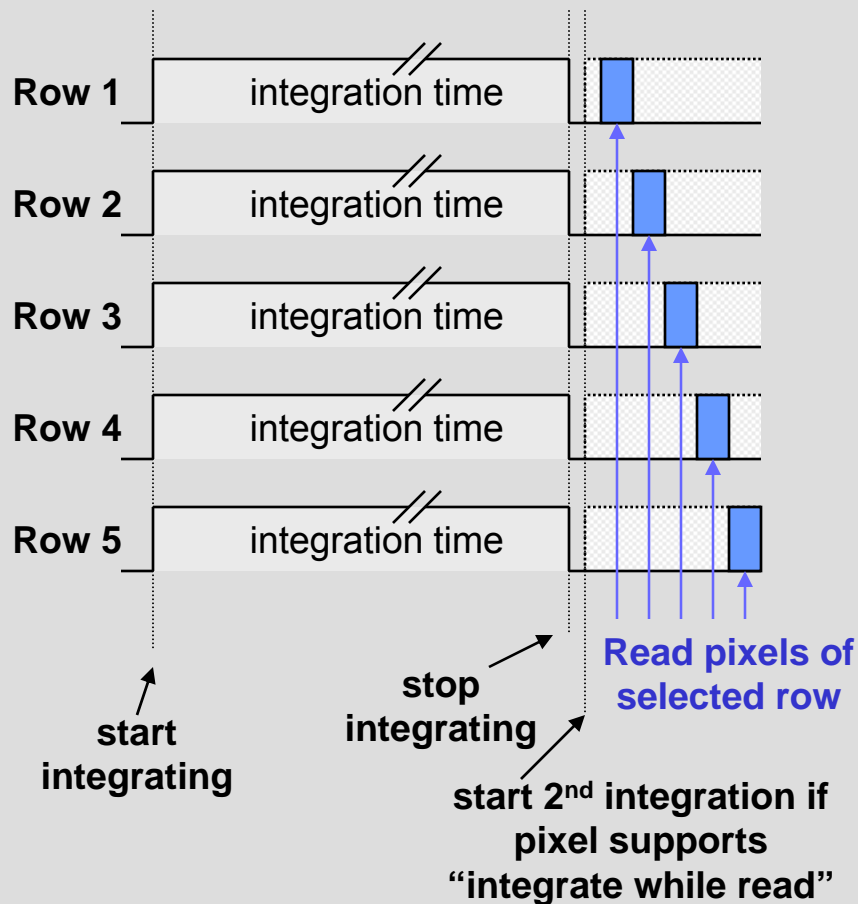
- Special windowing can be used to perform full-field science integration in parallel with fast window reads.
 - ⇒ Simultaneous guide operation and science data capture within the same detector.
- Two methods possible:
 - Interleaved reading of full-field and window
 - No scanning restrictions or crosstalk issues
 - Overhead reduces full-field frame rate
 - Parallel reading of full-field and window
 - Requires additional output channel
 - Parallel read may cause crosstalk or conflict
 - No overhead ⇒ maintains maximum full-field frame rate



Electronic Shutter: Snapshot vs. Rolling Shutter

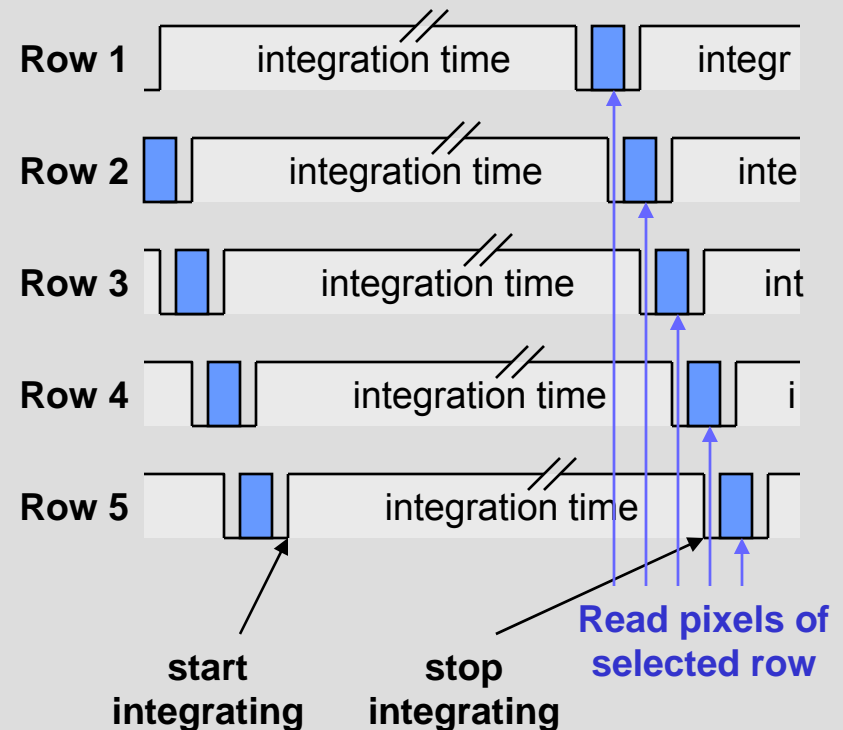
• Snapshot Shutter

- All rows are integrating at the same time.
- Typically more transistors per pixel and higher noise.



• Rolling Shutter (Ripple Read)

- Each row starts and stops integrating at a different time (progressively).
- Typically less transistors per pixel and lower noise.



CMOS-Based Detector Systems

- Three possible CMOS Detector Electronics Configurations

Single Chip

- All electronics integrated in sensor chip
- Small, low system power
- Not always desirable (high design effort, glow)

Detector Array

Includes ADC, bias & clock generation

Digital data

Acquisition System

Discrete Electronics

- Assembly of discrete chips and boards
- Large, higher power
- Reusable, modular, only PCB design required

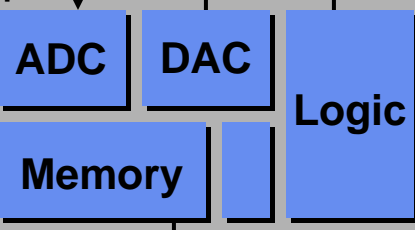
Detector Array

Requires ext. ADC, bias and/or clock generation

Analog output

Bias

Clocks



Digital data

Acquisition System

Dual Chip

- All electronics integrated in a single companion chip
- Small, low system power
- Can be placed next to detector => low noise

Detector Array

Requires ext. ADC, bias and/or clock generation

Analog output

Bias

Clocks

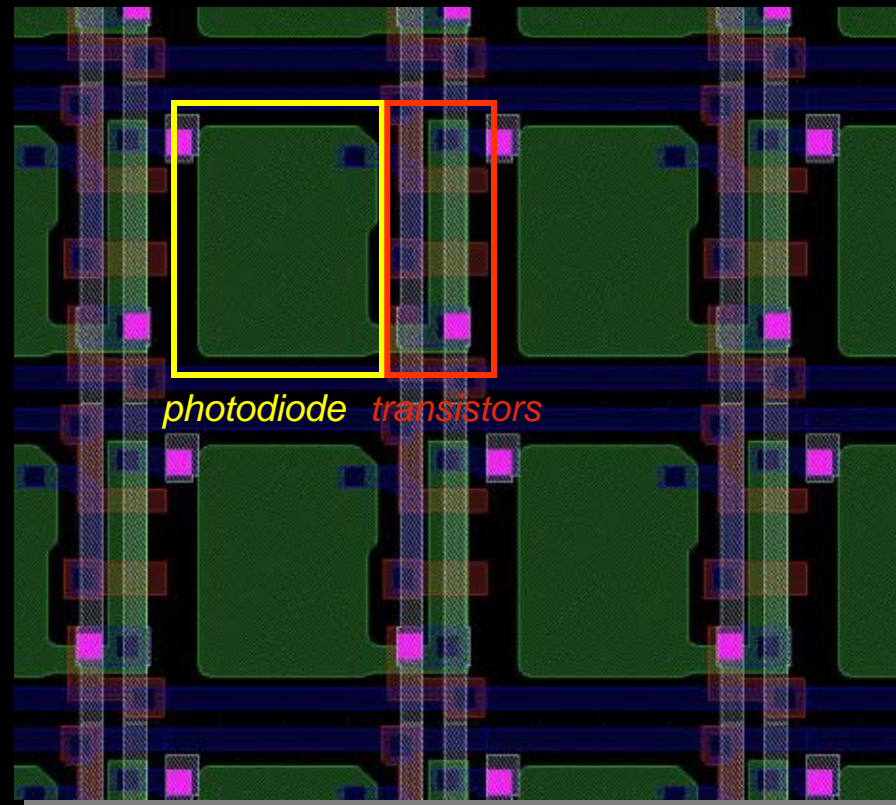
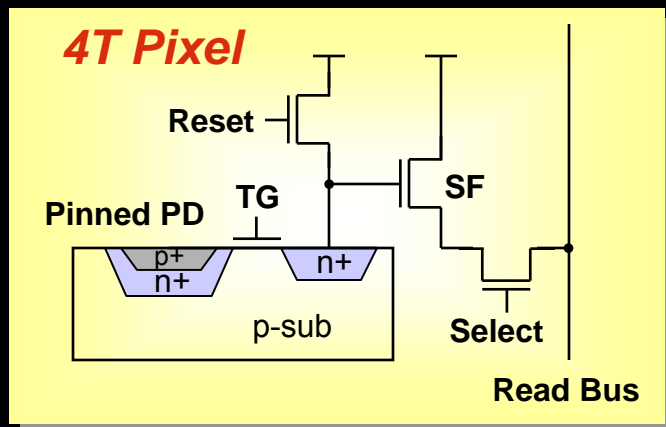
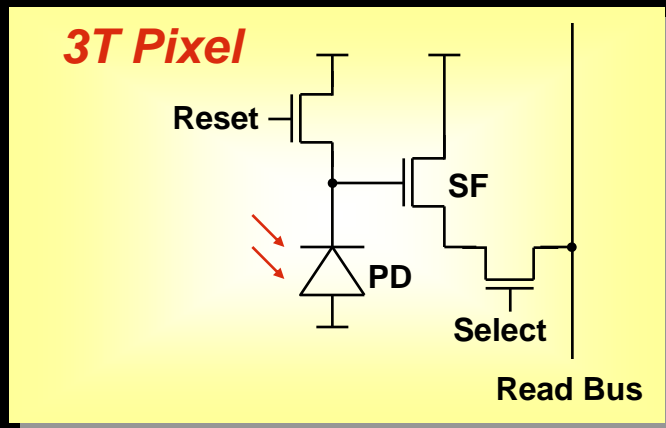
ASIC

Digital data

Acquisition System

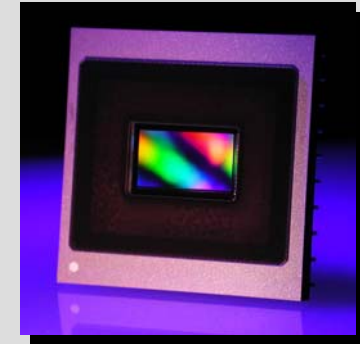
Monolithic CMOS

- A monolithic CMOS image sensor combines the photodiode and the readout circuitry in one piece of silicon
 - Photodiode and transistors share the area => less than 100% fill factor
 - Small pixels and large arrays can be produced at low cost => consumer applications (digital cameras, cell phones, etc.)



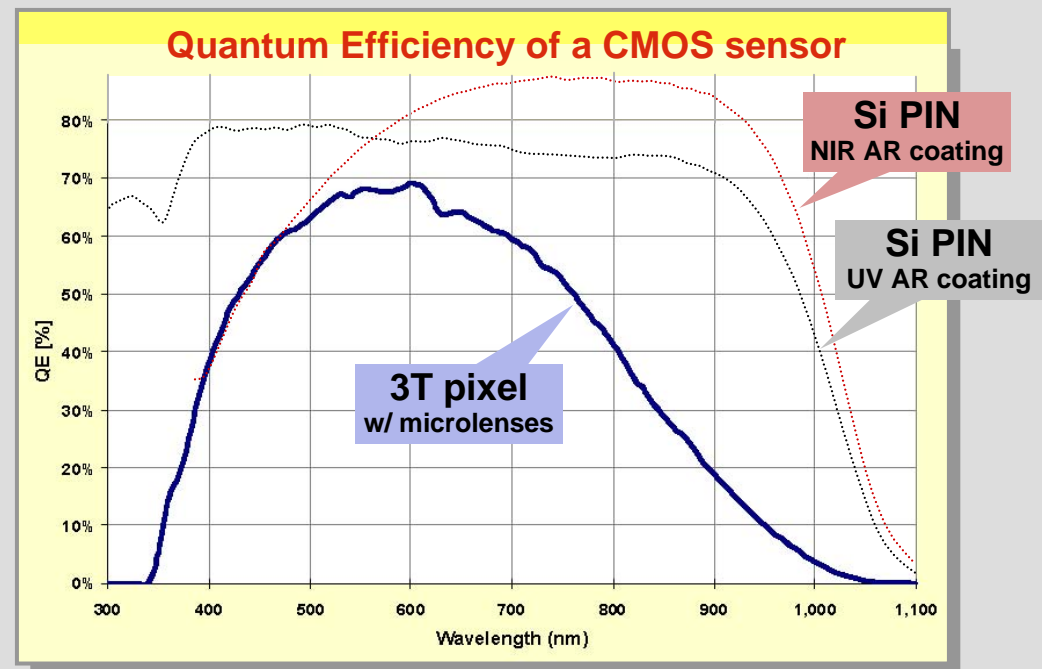
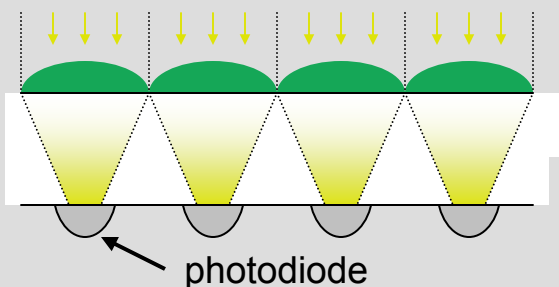
Complete Imaging Systems-on-a-Chip

- Monolithic CMOS technology has enabled highly integrated, complete imaging systems-on-a-chip:
 - Single chip cameras for video and digital still photography
 - Performance has significantly improved over last decade and is better or comparable to CCDs for many applications.
 - Especially suited for high frame rate sensors (> Gigapixel/s) or other special features (windowing, high dynamic range, etc.)
- However, monolithic CMOS is still limited with respect to quantum efficiency:
 - Photodiode is relatively shallow => low red response
 - Metal and dielectric layers on top of the diode absorb or reflect light => low overall QE
 - **Backside illumination possible, but requires modification of CMOS process**

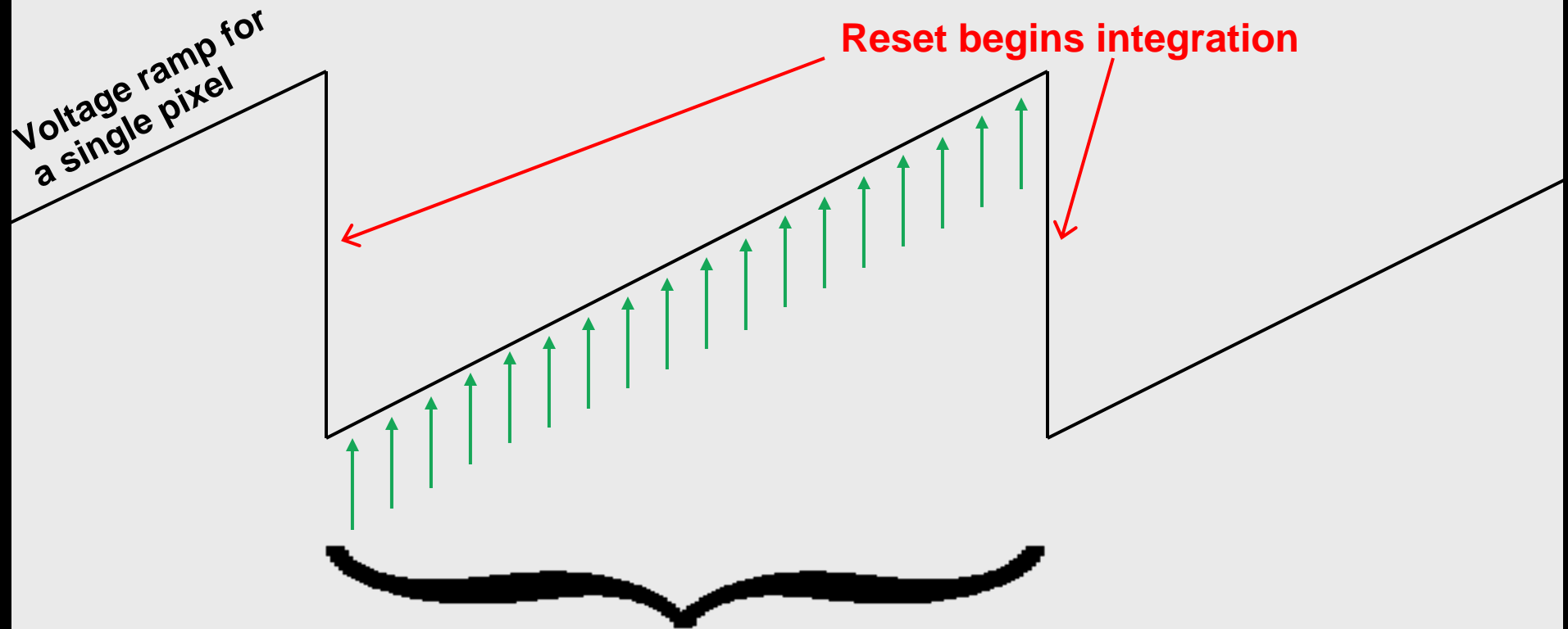


2 Mpixel HDTV CMOS Sensor

- Microlenses increase fill factor:



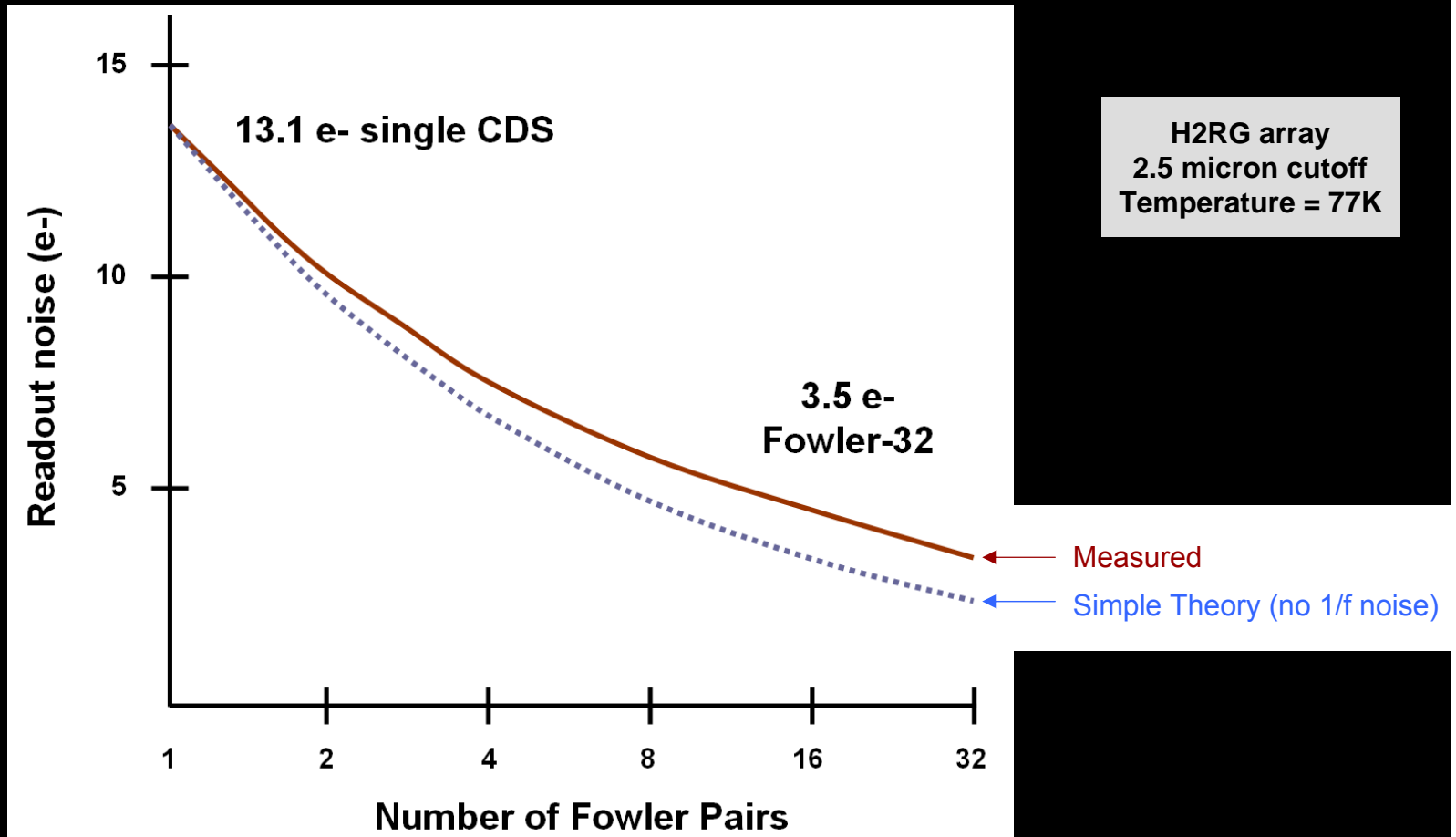
CMOS SCA Sampling Techniques



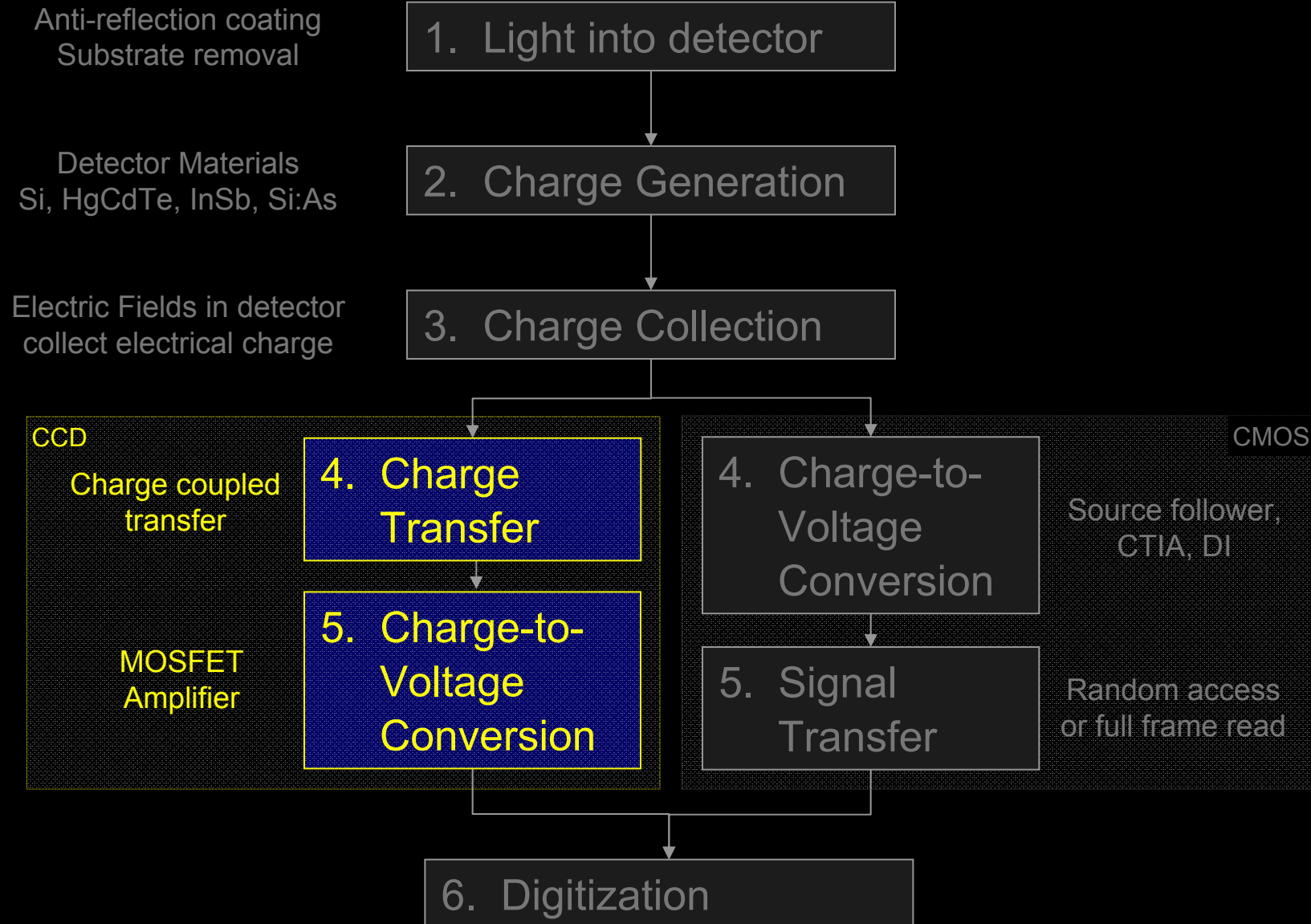
- **Periodic sampling of detector signal possible during a long integration**
- **Two general methods of white noise reduction by multiple sampling**
 - Fowler sampling: average 1st N samples and last N samples; then subtract
 - Sample up the ramp (SUTR): fit line (or polynomial) to all samples

Example of Noise vs Number of Fowler Samples

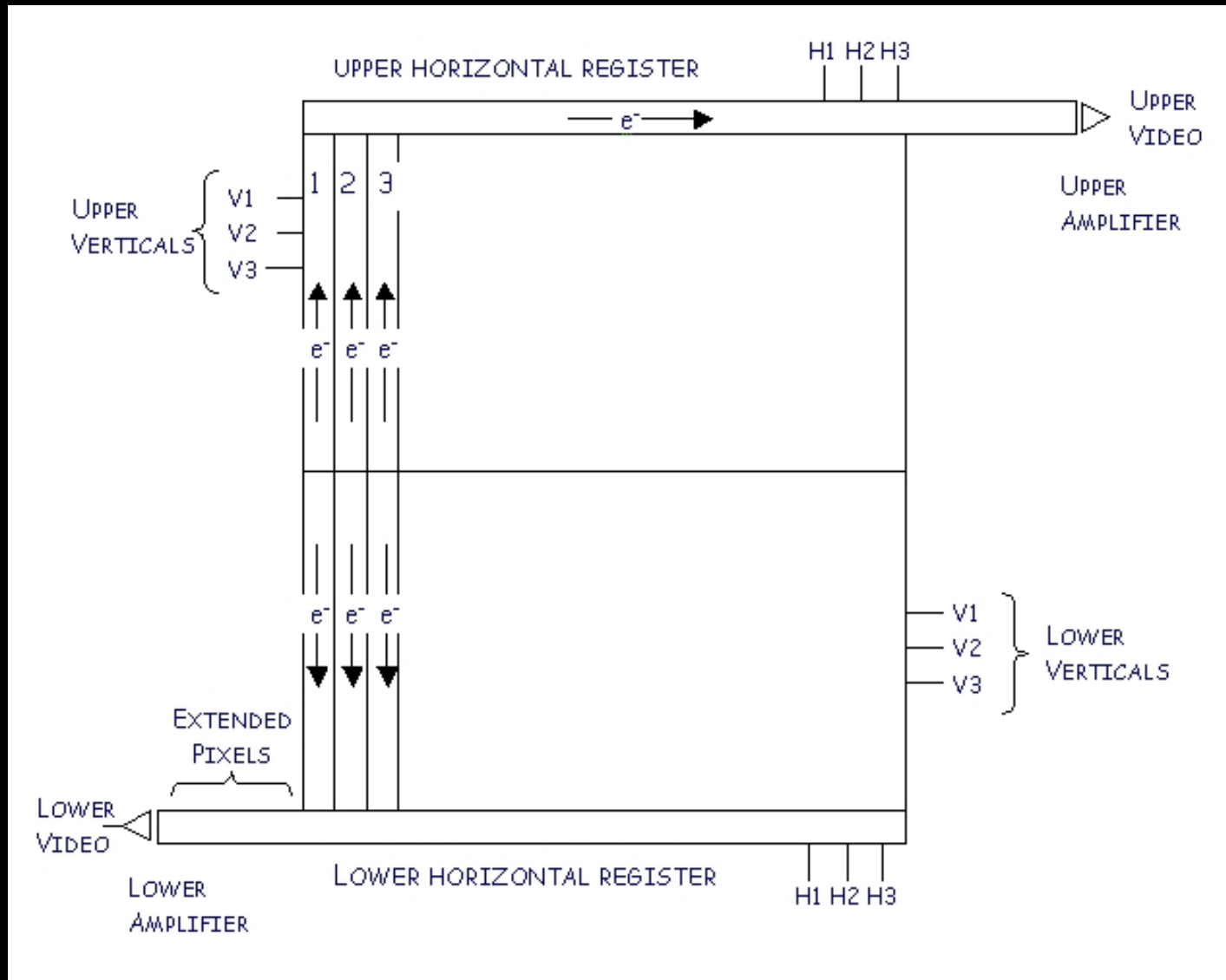
Non-destructive readout enables reduction of noise from multiple samples



6 steps of optical / IR photon detection

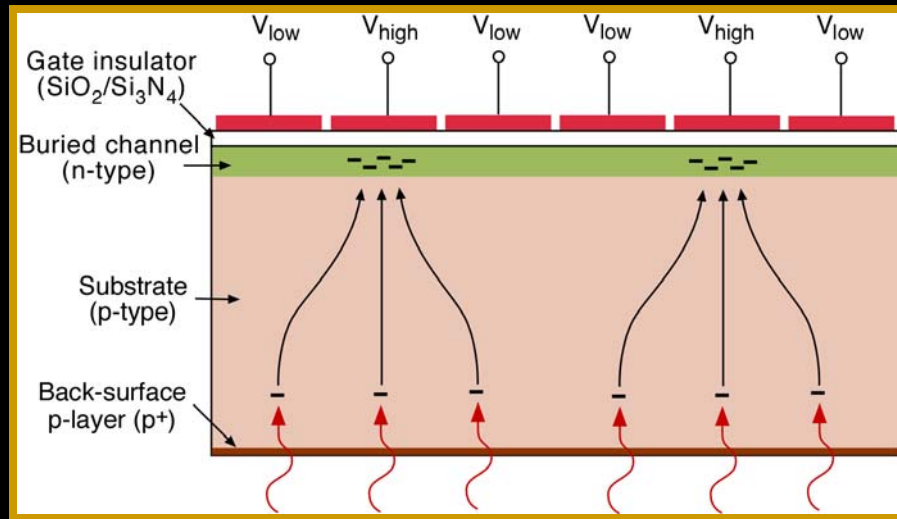


CCD Architecture

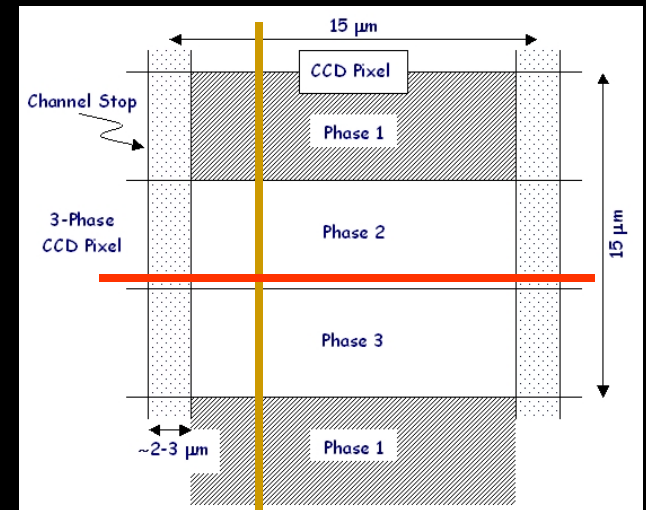
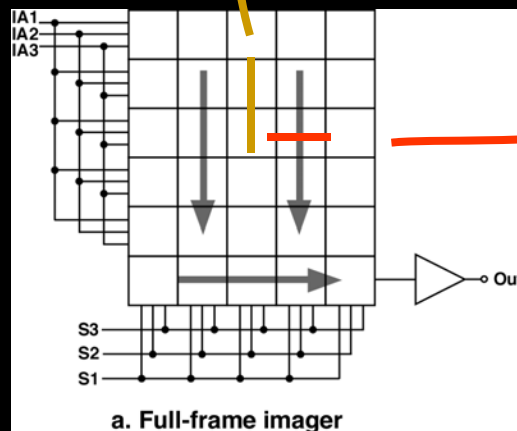
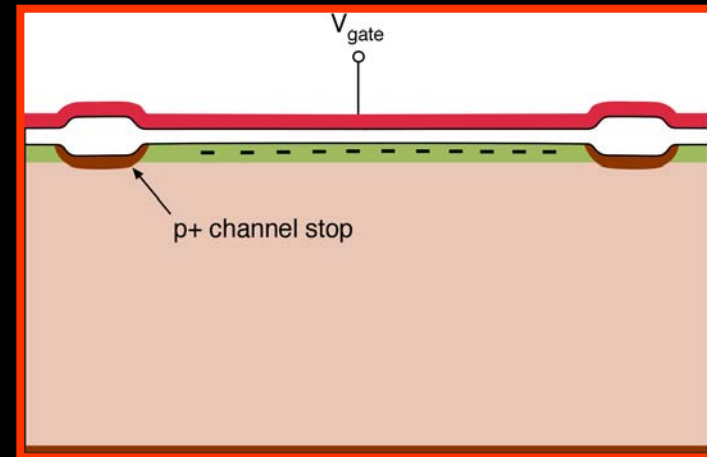


Basic CCD Structure

View along charge-transfer direction

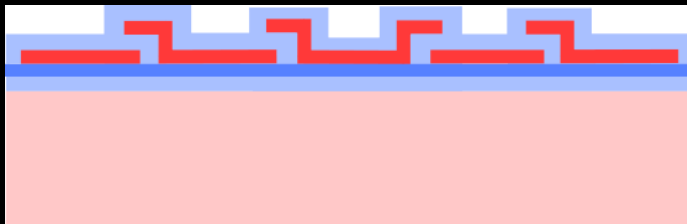
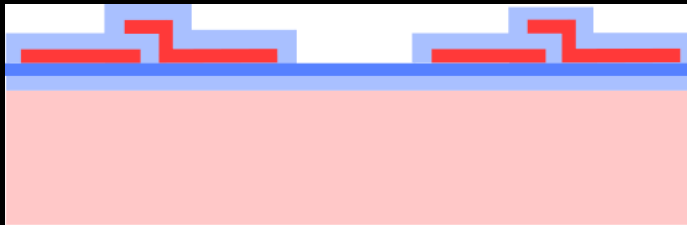
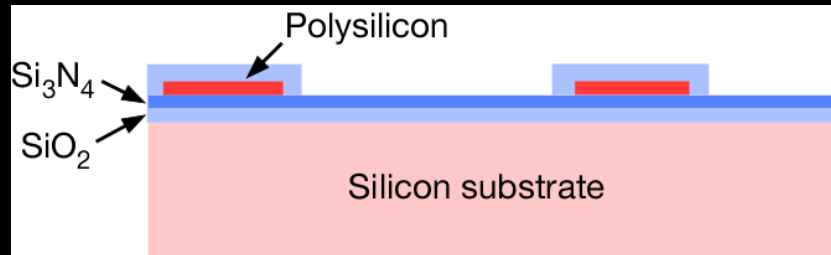


View across CCD channel

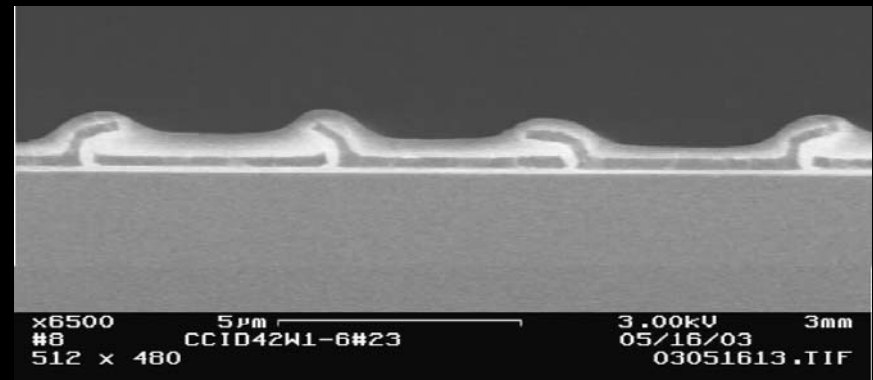
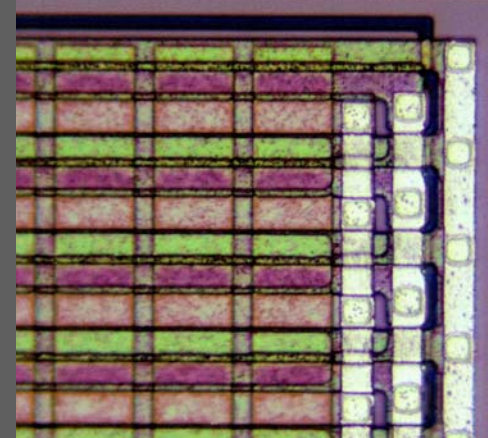


Basic CCD Manufacturing Process

Process: three phase, triple poly

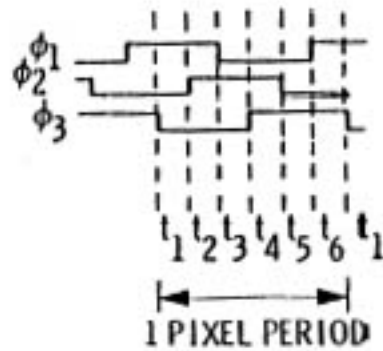


Final product (top view)



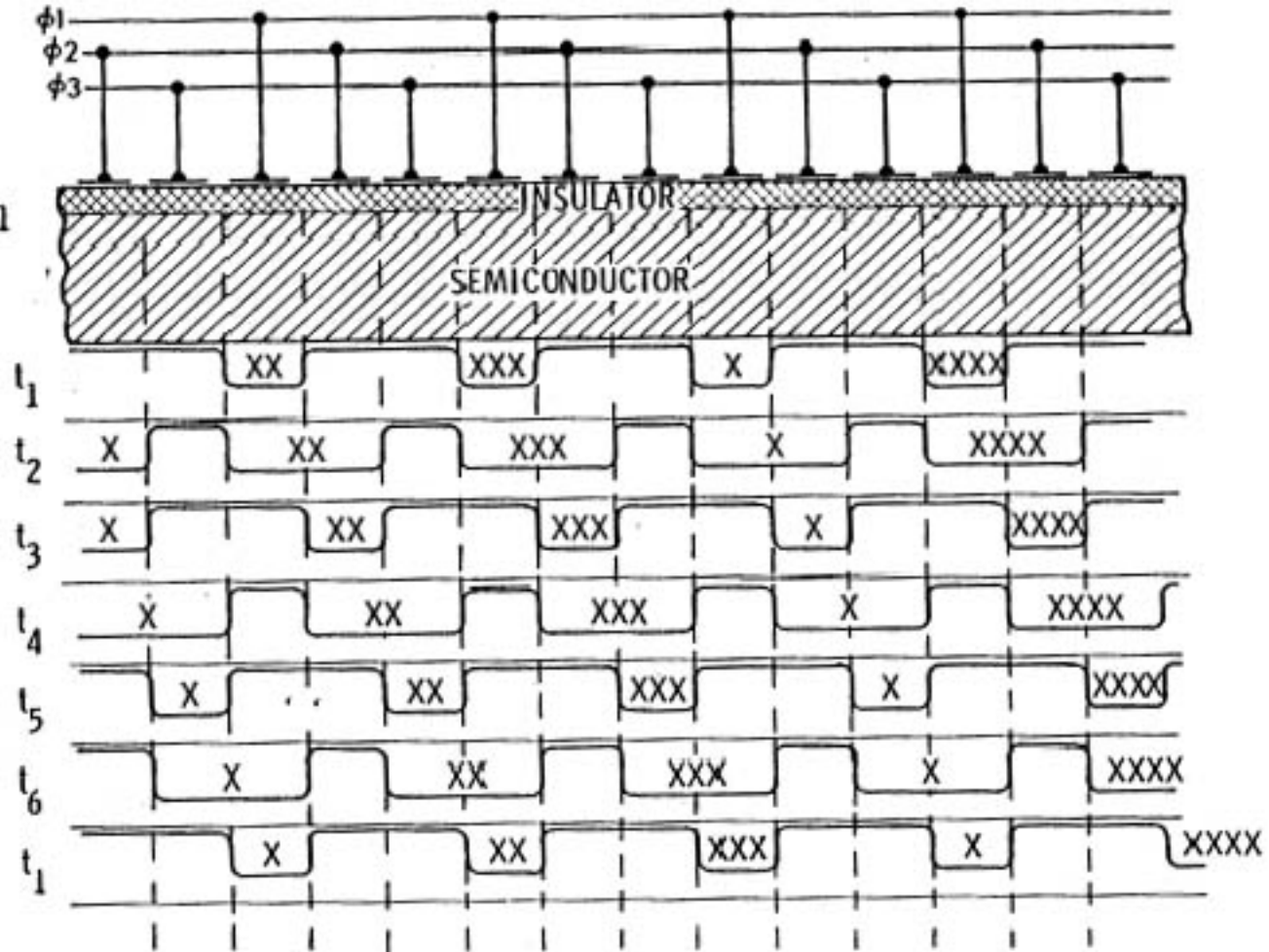
SEM cross section

CCD Timing

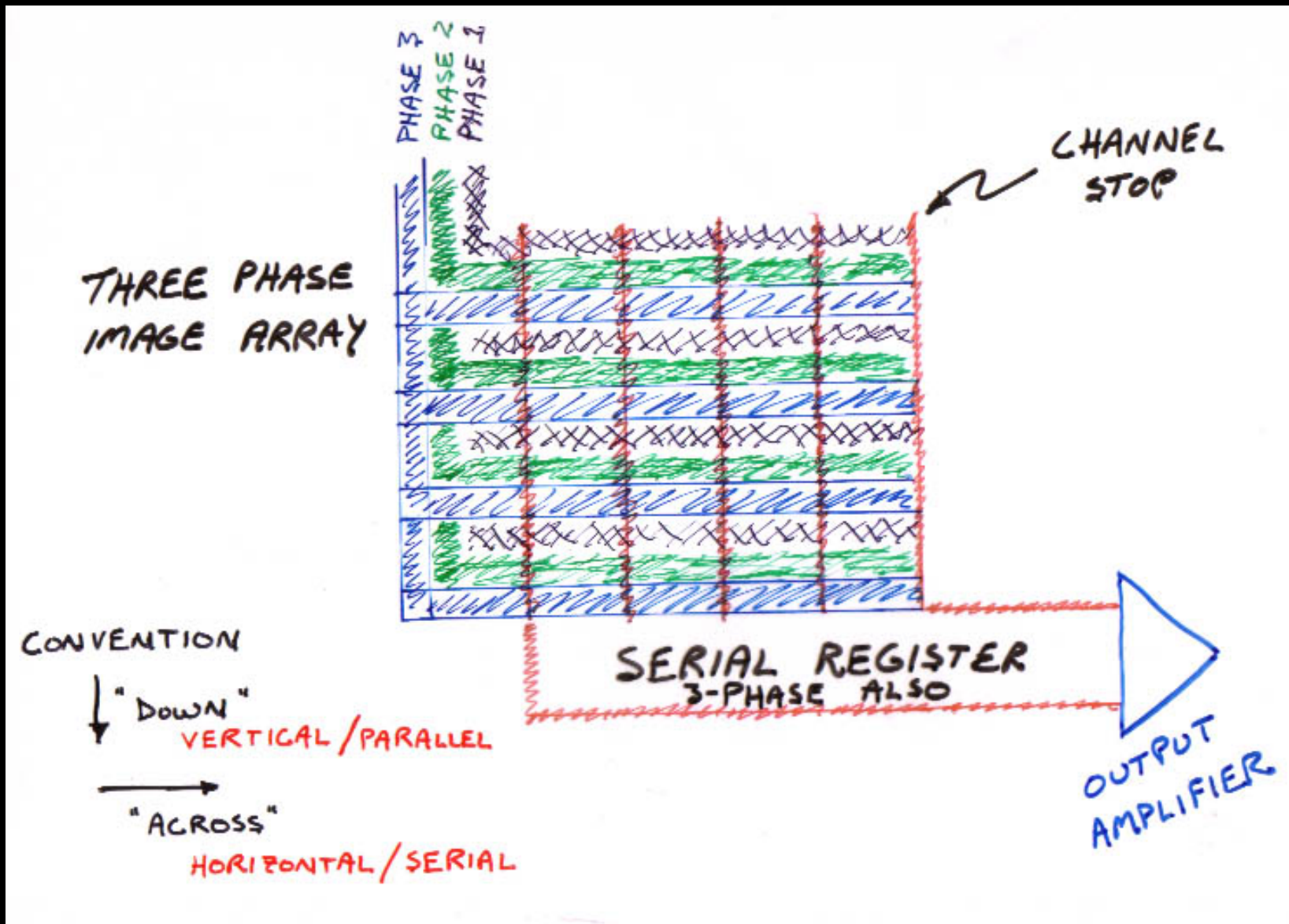


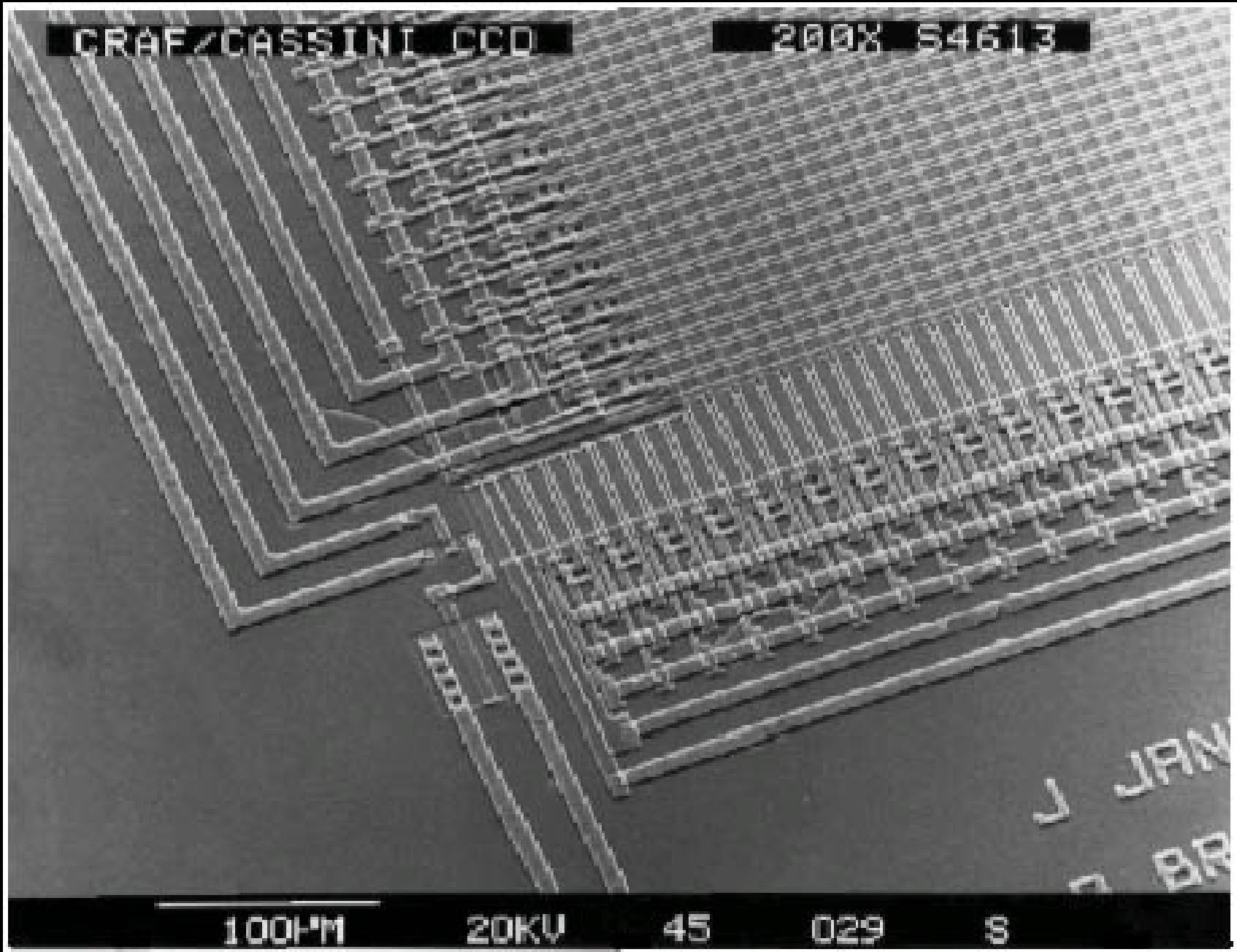
Movement of charge is "coupled"

Charge
Coupled
Device



CCD – 3 Phase Serial Register





CRAF/CASSINI CCD

200X S4613

100 micron diameter human hair

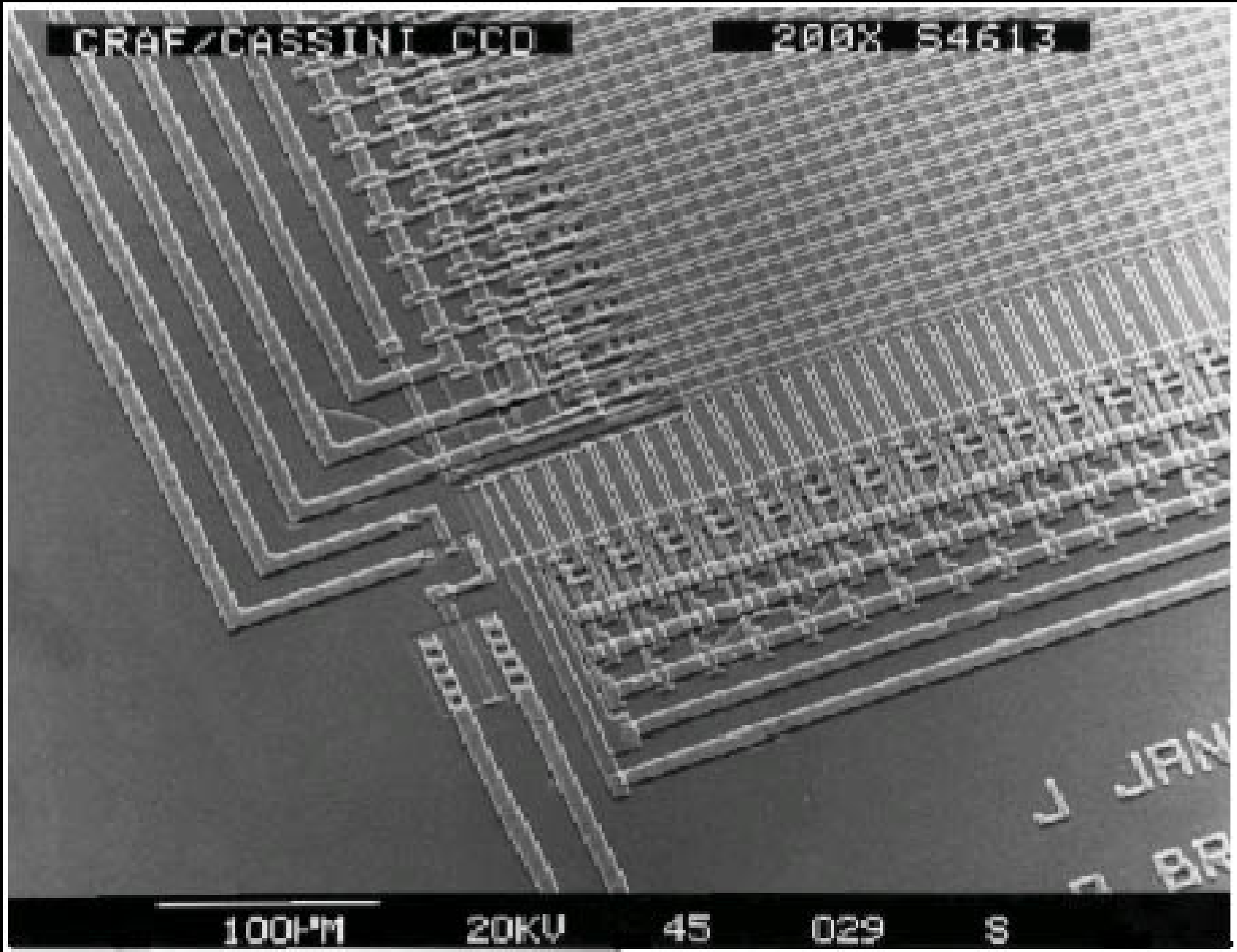
100µm

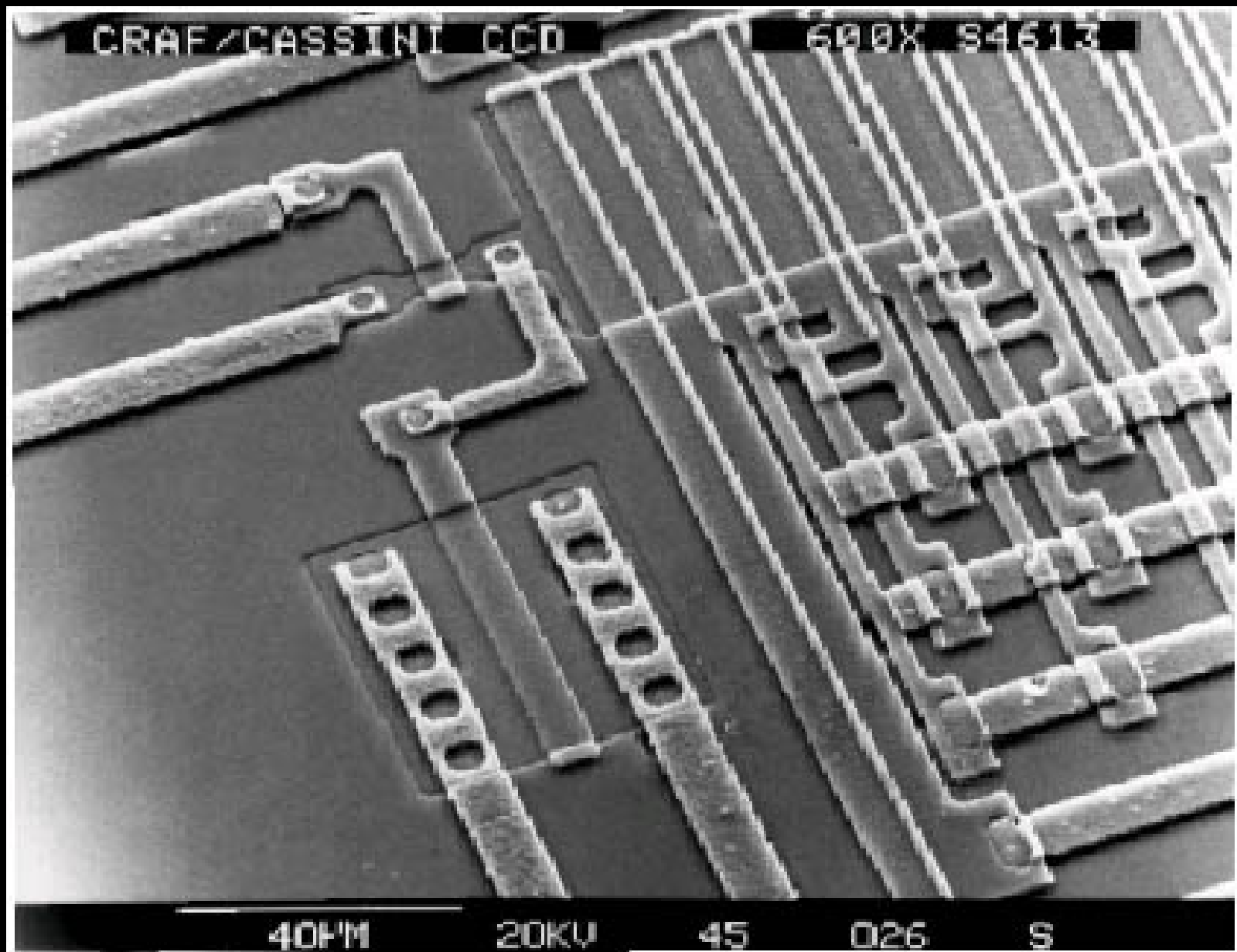
20KV

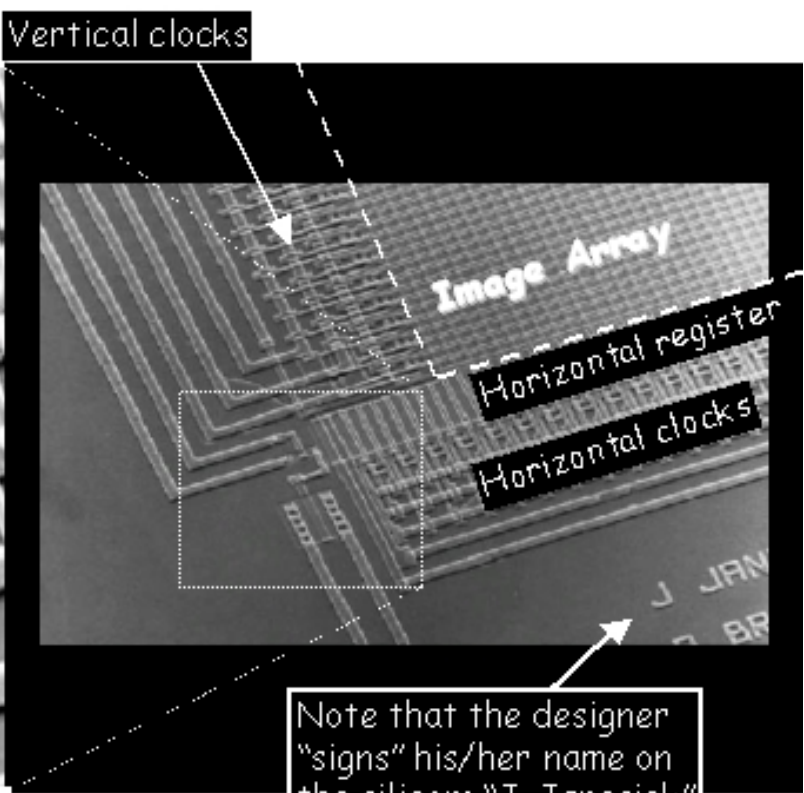
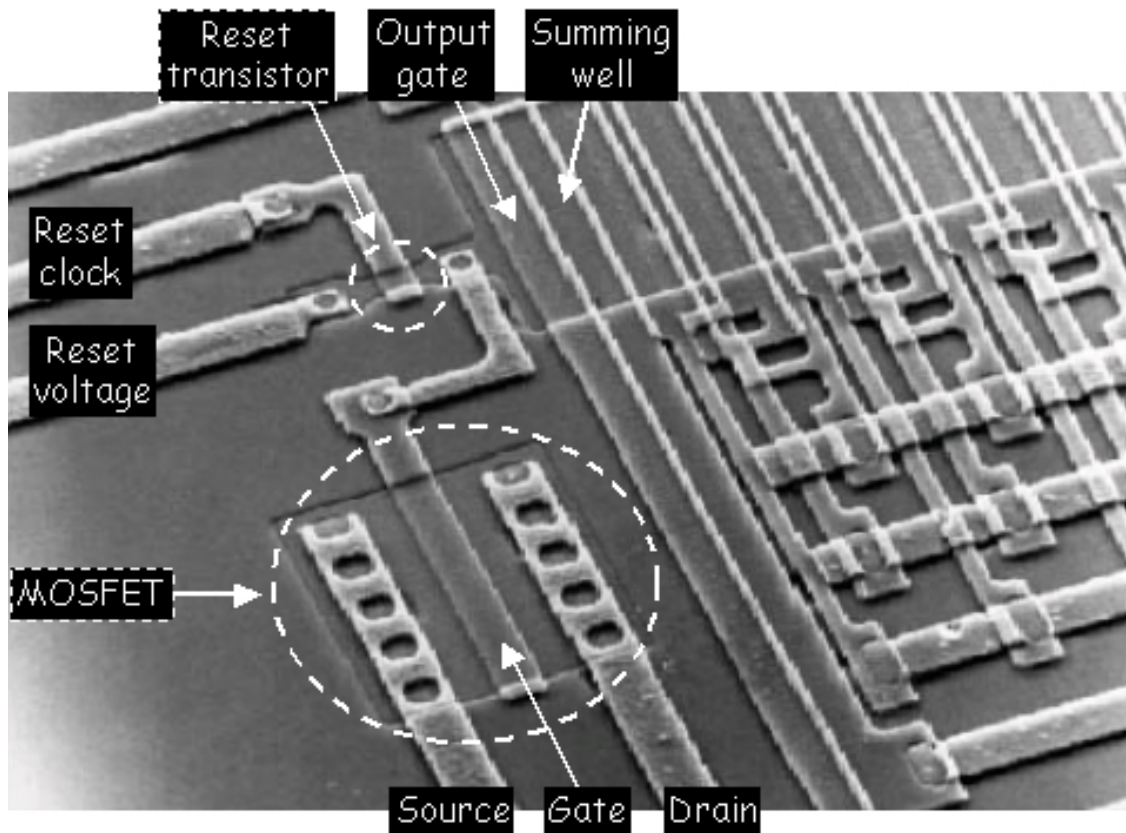
45

029

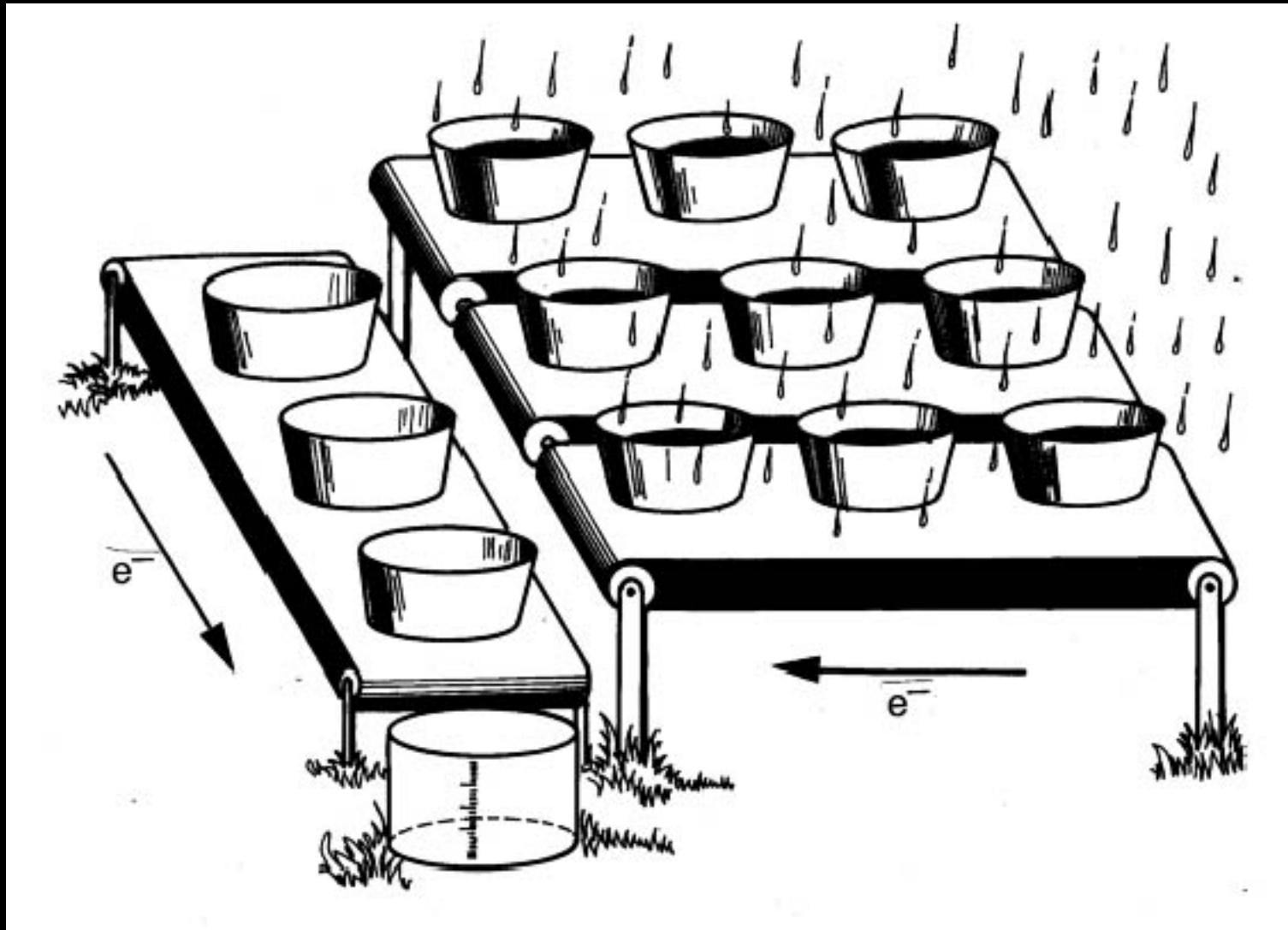
S





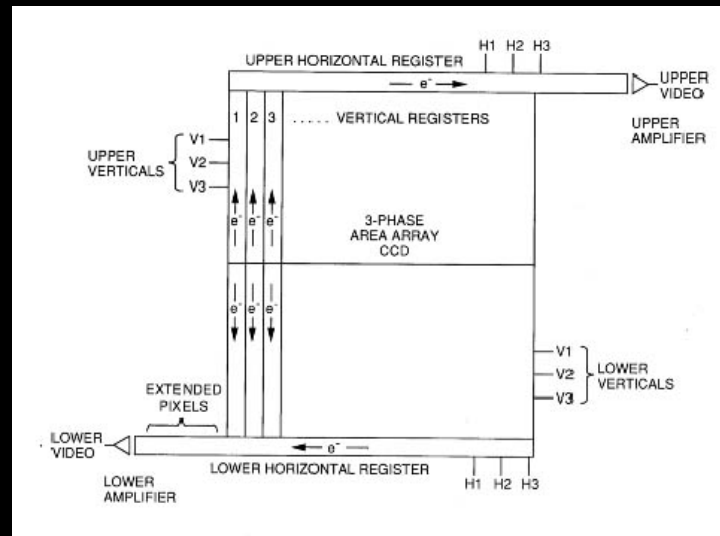


CCD Rain bucket analogy



CCD Charge transfer

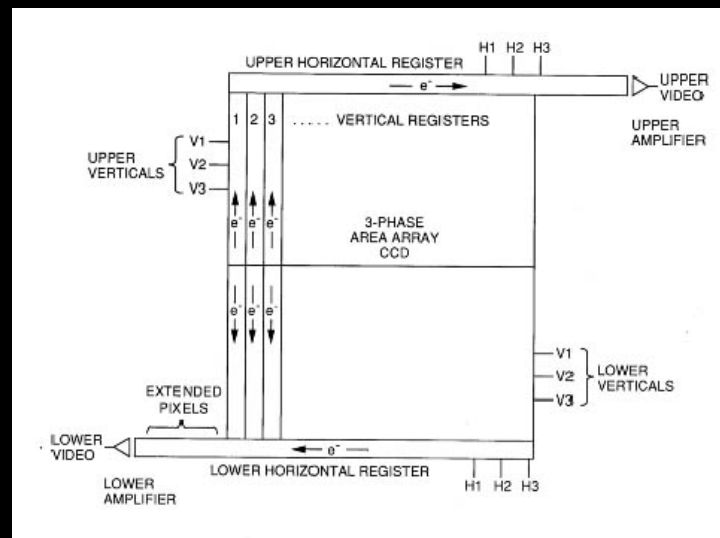
The good, the bad & the ugly



CCD Charge transfer

The good, the bad & the ugly

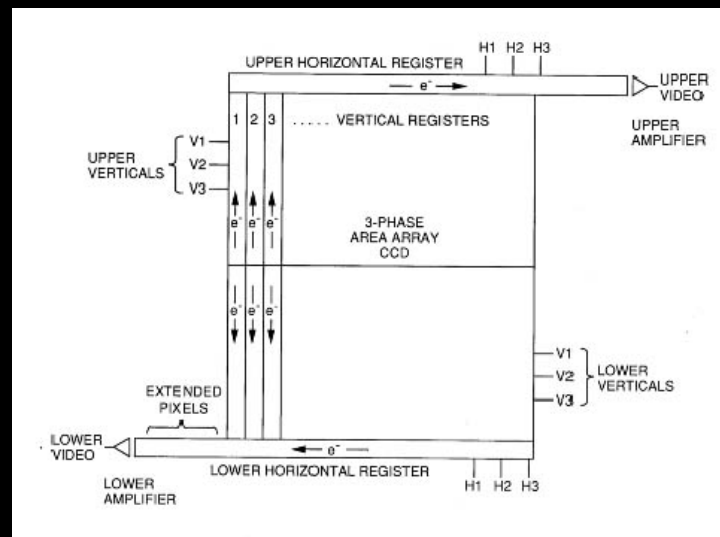
- “Bad & ugly” aspects of charge transfer
 - Takes time (limited max frame rate)
 - Can blur image if no shutter used
 - Can lose / blur charge during move (may limit astrometry accuracy)
 - Can bleed charge from saturated pixel up/down column
 - Can have a blocked column
 - Can have a hot pixel that releases charge into all passing pixels



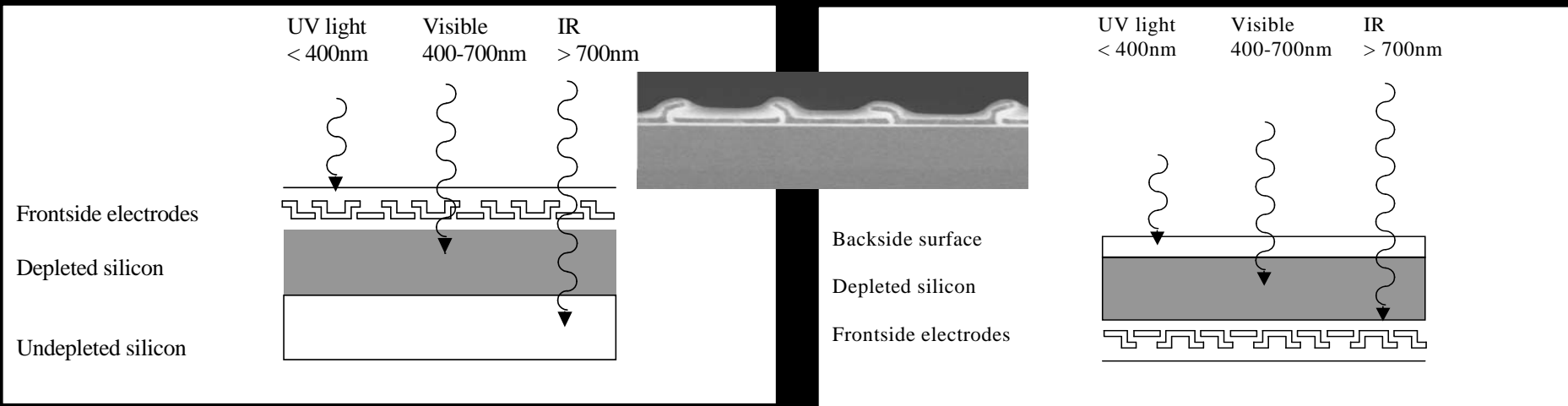
CCD Charge transfer

The good, the bad & the ugly

- “Good” aspects of charge transfer
 - Can bin charge “on-chip” – noiseless process
 - Can charge shift for tip/tilt correction or to eliminate systematic errors
 - “va-et-vient”, “nod-and-shuffle”
 - Can build special purpose designs that integrate different areas (curvature wavefront sensing, Shack-Hartmann laser guide star wavefront sensing)
 - Can do drift scanning
 - No indium bump issues that can cause inoperable pixels
 - **Have space to build a great low noise amplifier !**



Frontside & Backside illuminated CCD



Frontside

Backside

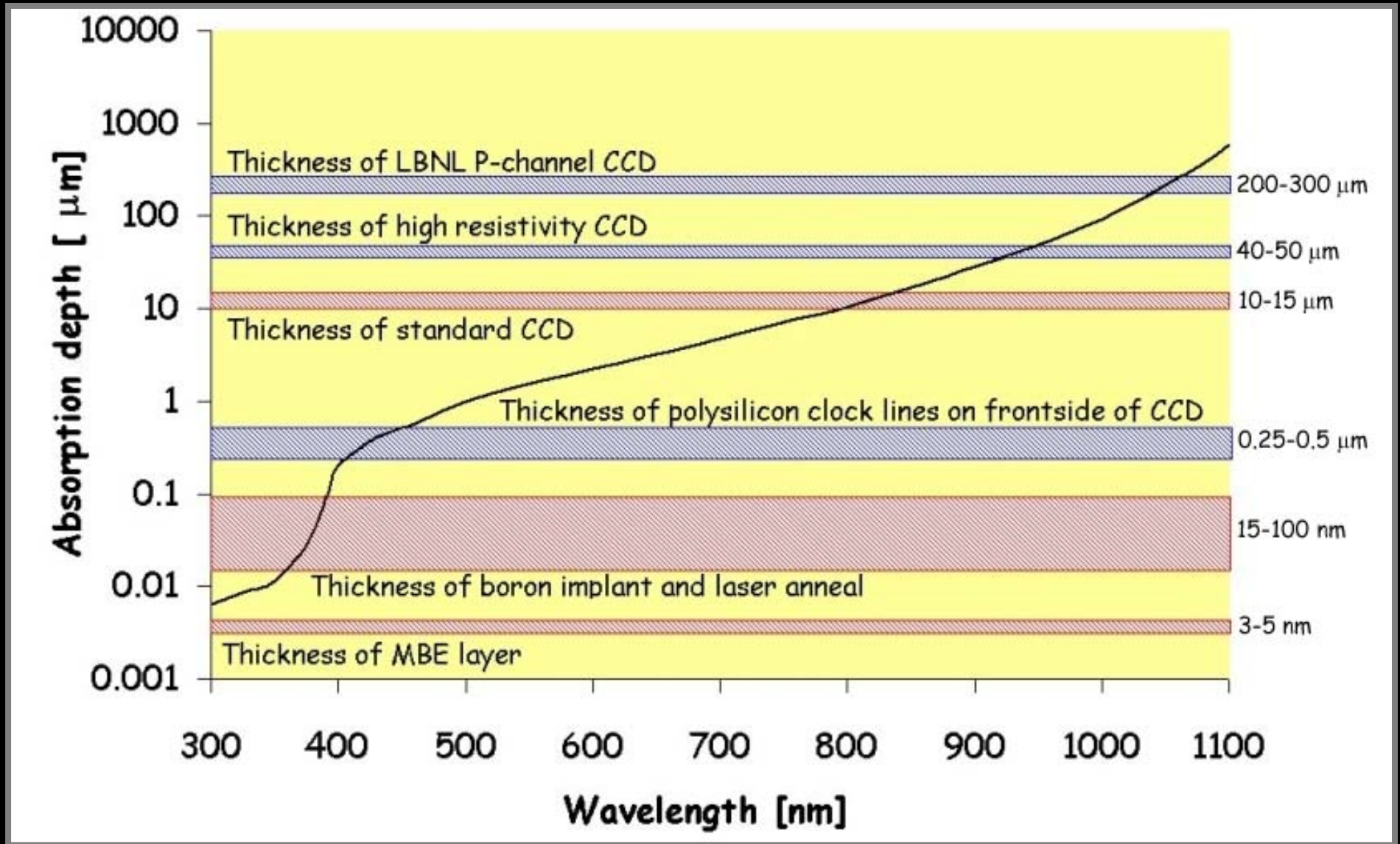
Backside illuminated CCDs have high spectral response...if processed correctly.

Thin to 10-20 microns, and **backsurface treatment** to ensure that photons absorbed near the back surface are collected. Surface treatments include:

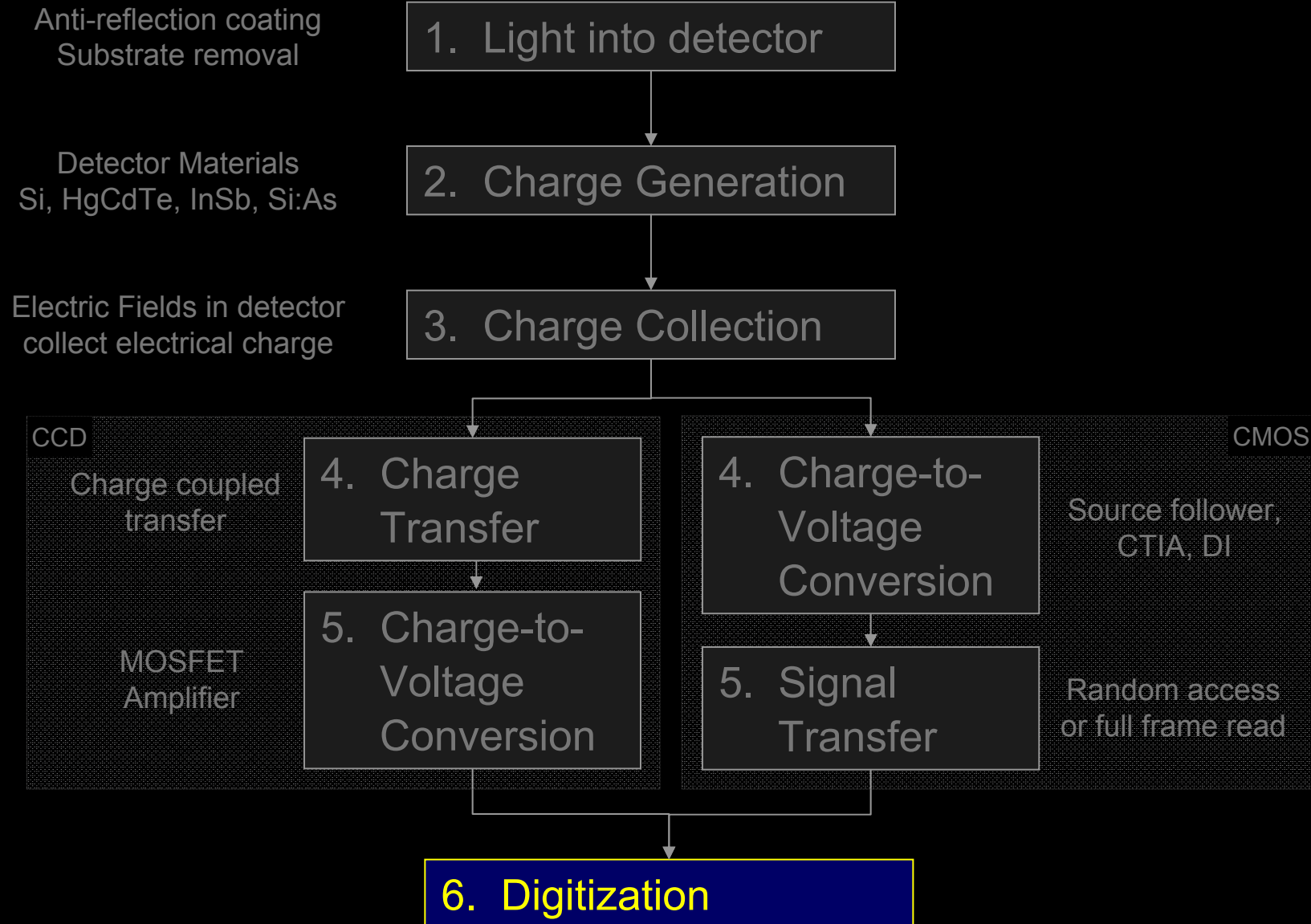
- Ion implantation followed by laser annealing
- Ion implantation followed by furnace annealing
- Chemisorption charging
- Molecular beam epitaxy (MBE) / delta doping

Optical Absorption Depth in Silicon

(a.k.a. "The Beautiful Plot")



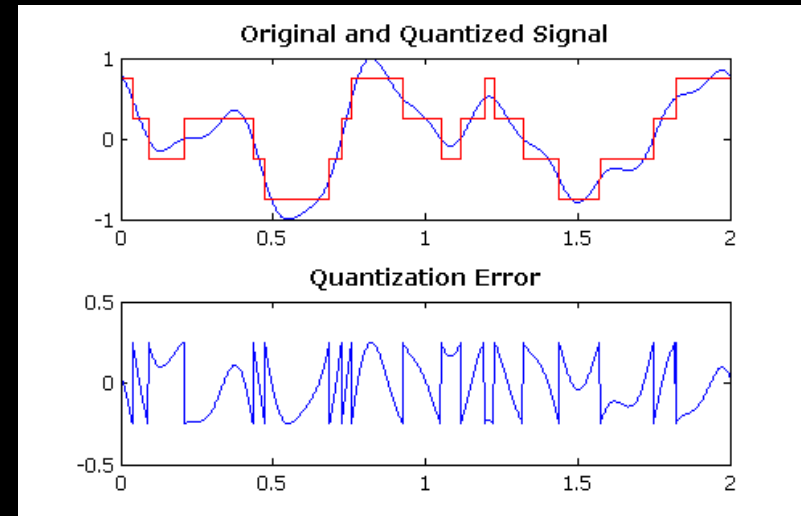
6 steps of optical / IR photon detection



Analog-to-digital converters

“Convert the analog signal (voltage or current) into a digital number”

- Quantization noise of an ADC is $(1/\sqrt{12})$ Least Significant Bit = 0.289 LSB
- Typically set gain of amplifier chain so that quantization noise is much less than readout noise. If readout noise is 4 electrons, set gain so that LSB equals ~ 2 electrons
- 16 bit ADC is most commonly used in astronomy. At ~ 2 electrons per ADU (analog to digital unit), or LSB, full well of a 16 bit ADC will be $\sim 130,000$ electrons; good match to the typical full well of a CCD or Short-Wave IR detector of 100,000 electrons.

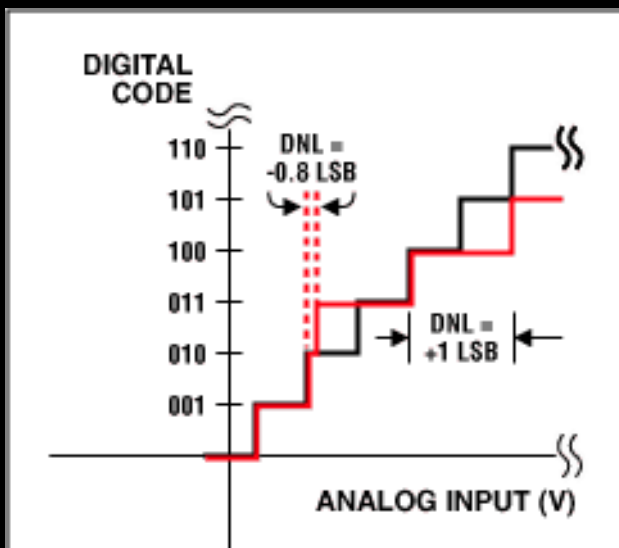


Highly exaggerated quantization noise

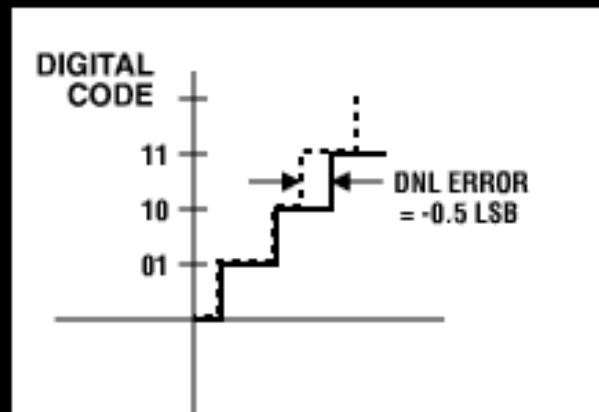
Differential Non-Linearity (DNL)

- DNL describes the distance of an ADC code from its adjacent code.
- It is measured as a change in input voltage magnitude, and then converted to number of Least Significant Bits (LSBs).

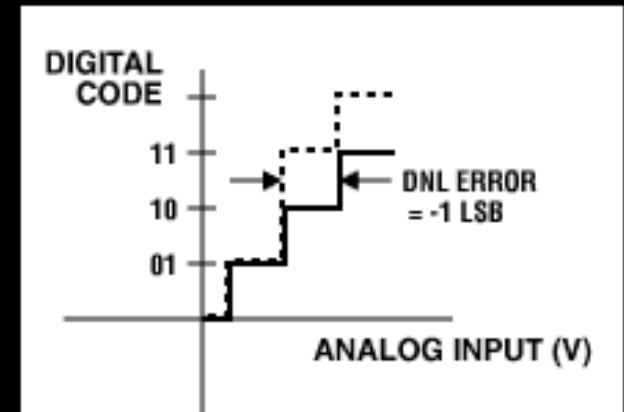
$$DNL = (V_{D+1} - V_D) / V_{LSB-Ideal} - 1$$



Code 100 is increased
DNL = +1



Code 10 is reduced
DNL = -0.5

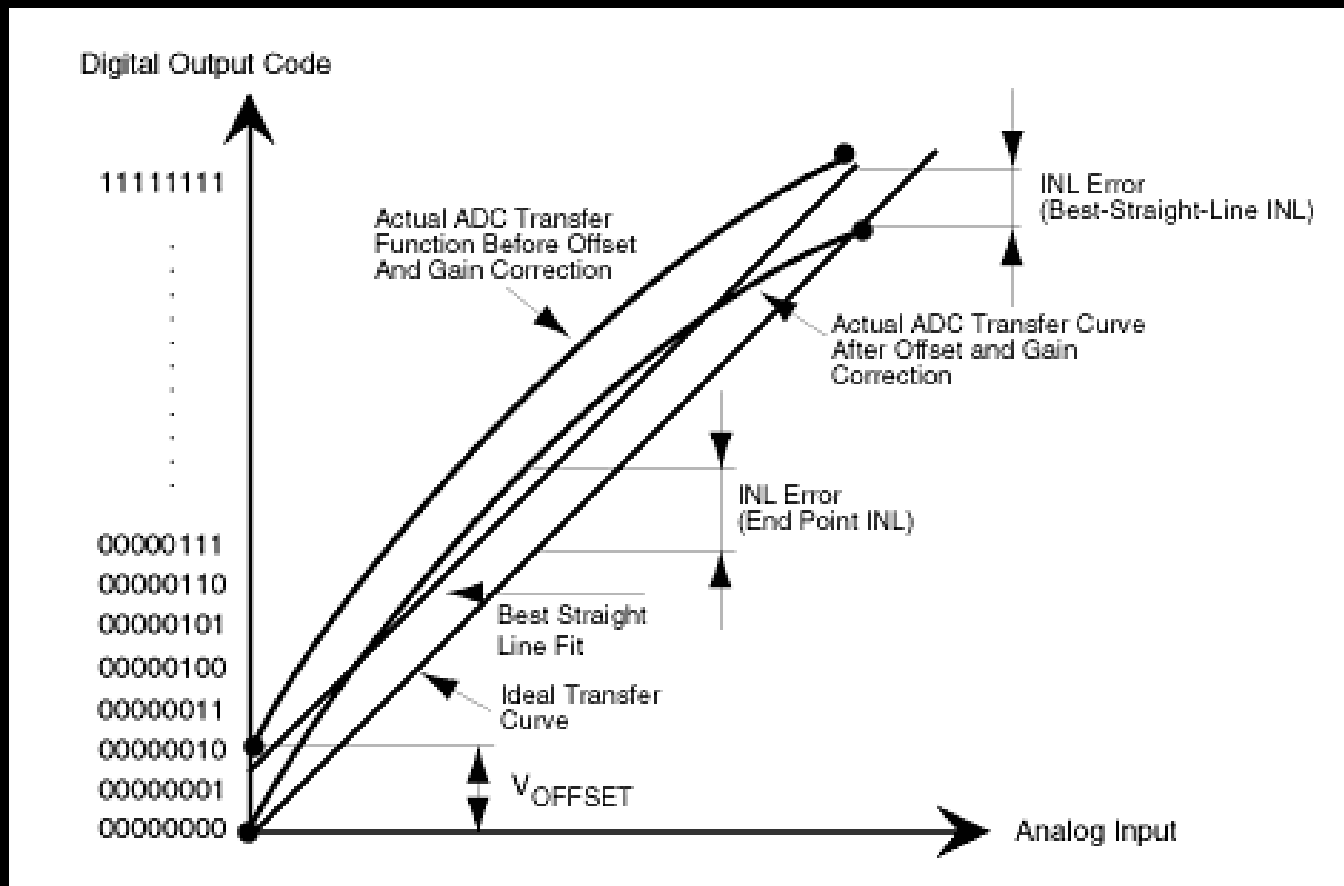


Code 10 is missing
DNL = -1

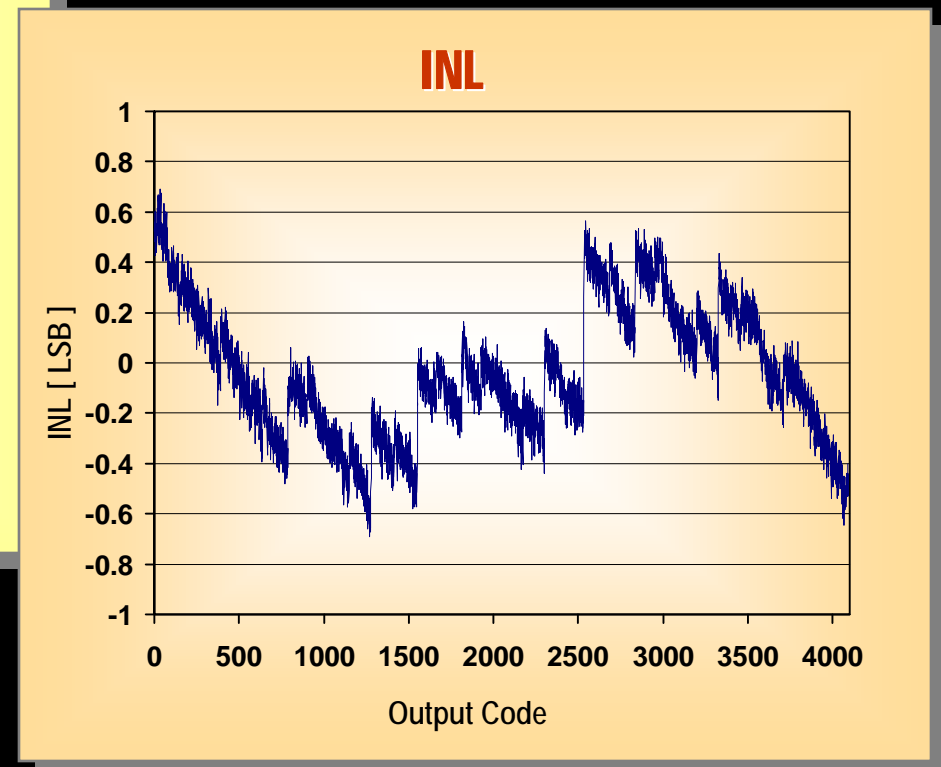
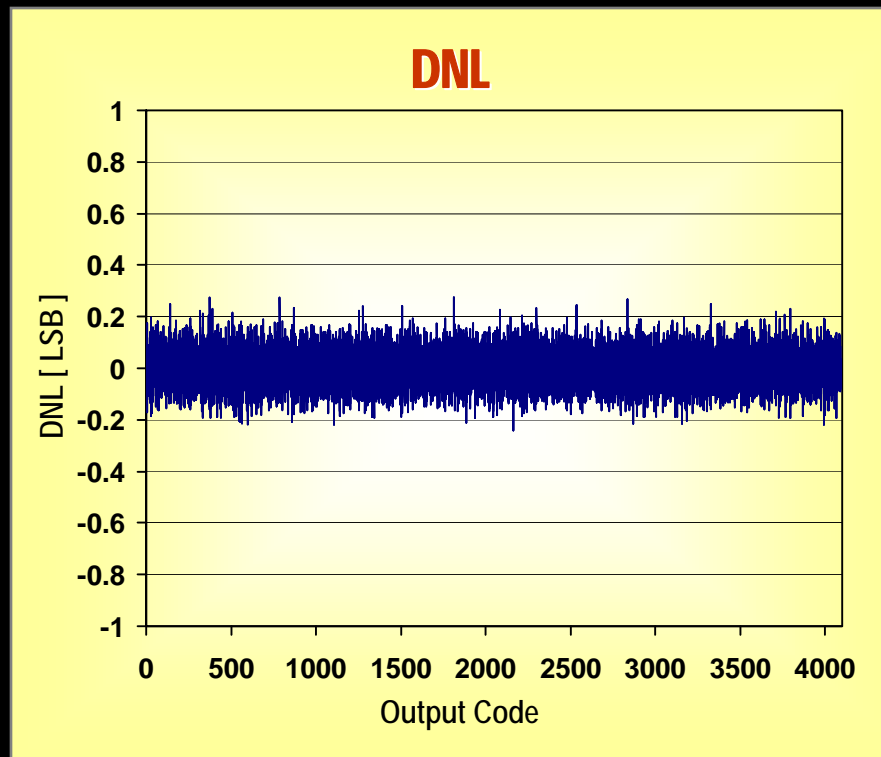
Integral Non-Linearity (INL)

- INL describes the deviation of the ADC transfer function from a straight line
- It can be computed as the integral of the DNL, and is expressed in LSB

$$INL = (V_D - V_{Zero}) / V_{LSB-Ideal} - D$$

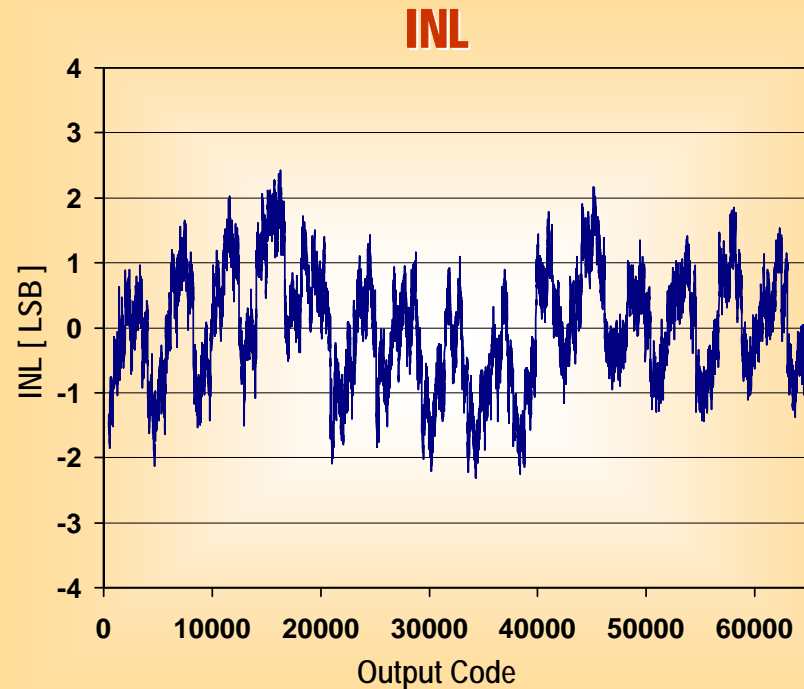
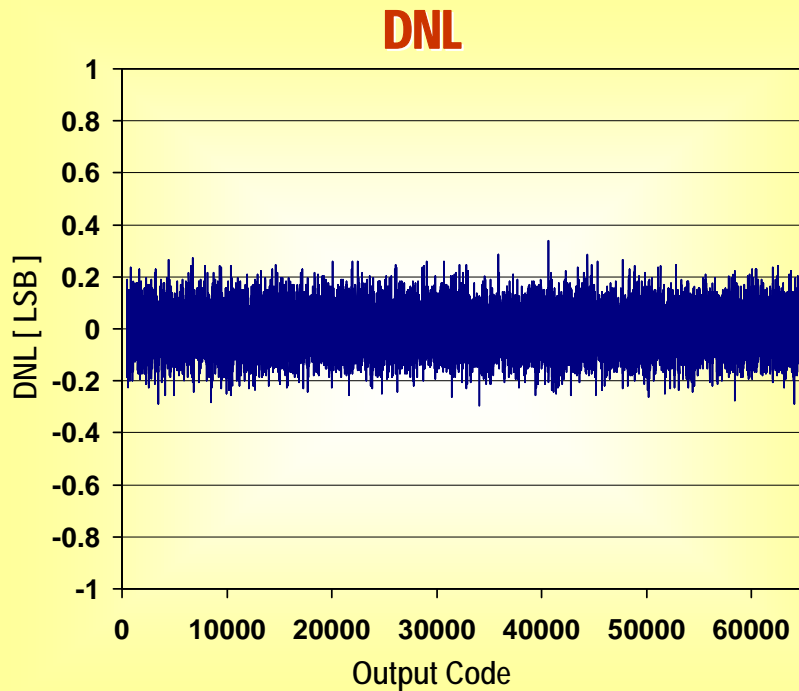


DNL and INL Plots of a 12-bit ADC (from SIDECAR ASIC, at 7.5 MHz rate)



- Differential Non-Linearity: $< \pm 0.3$ LSB
- Integral Non-Linearity: $< \pm 0.7$ LSB

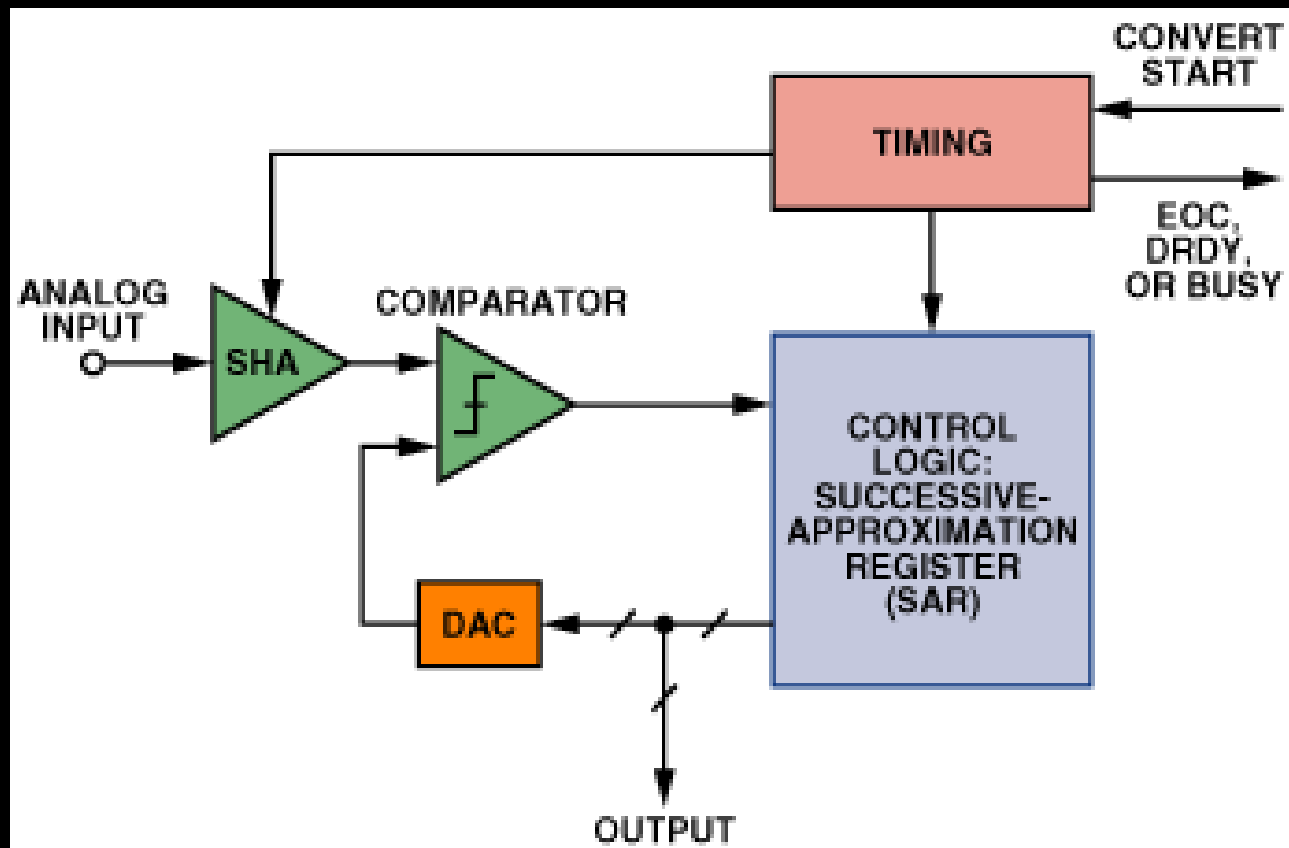
DNL and INL Plots of a 16-bit ADC (from SIDECAR ASIC, at 125 kHz rate)



- Differential Non-Linearity: $< \pm 0.3$ LSB
- Integral Non-Linearity: $< \pm 0.7$ LSB

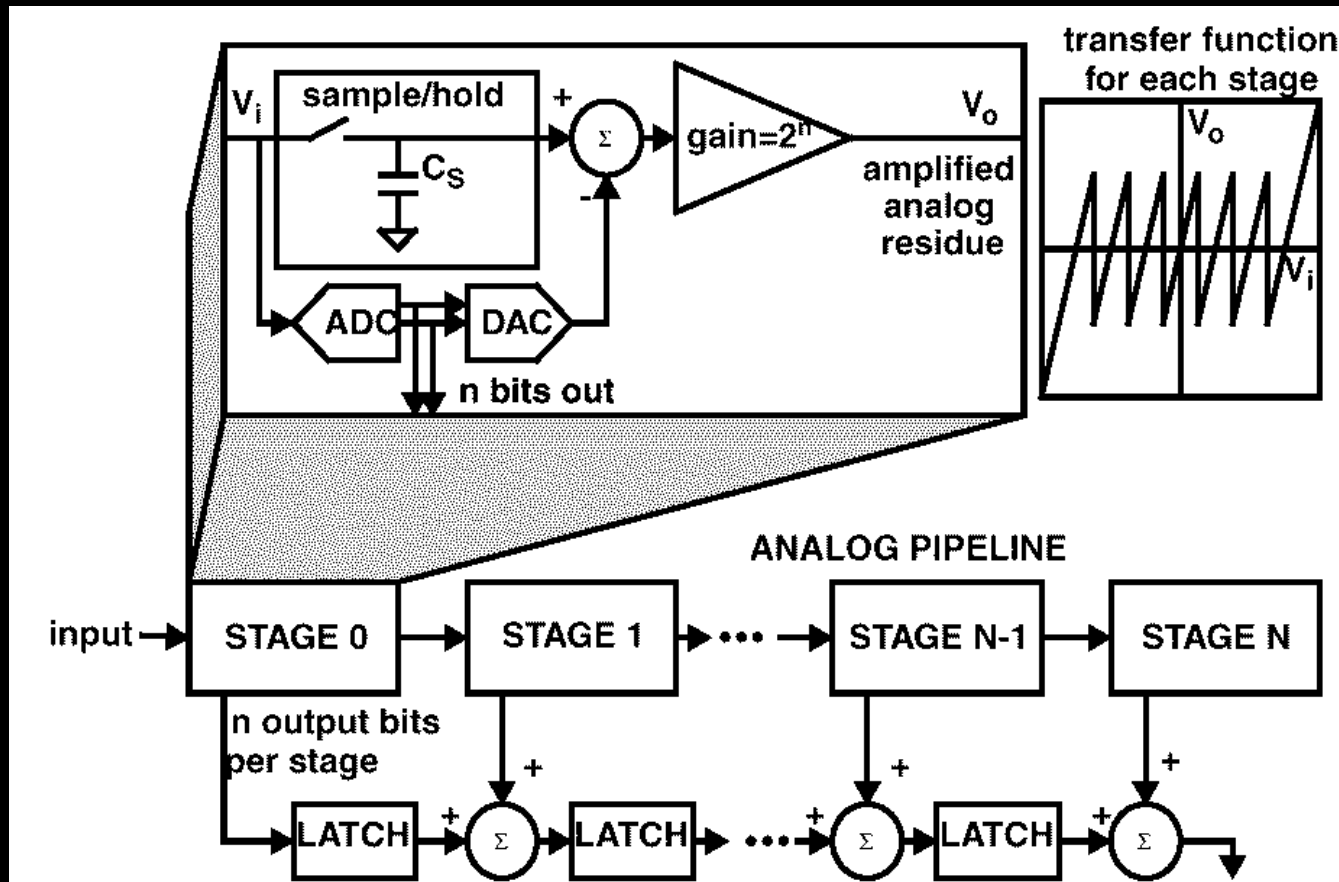
Sample ADC Architectures

Successive Approximation Register (SAR)



Sample ADC Architectures

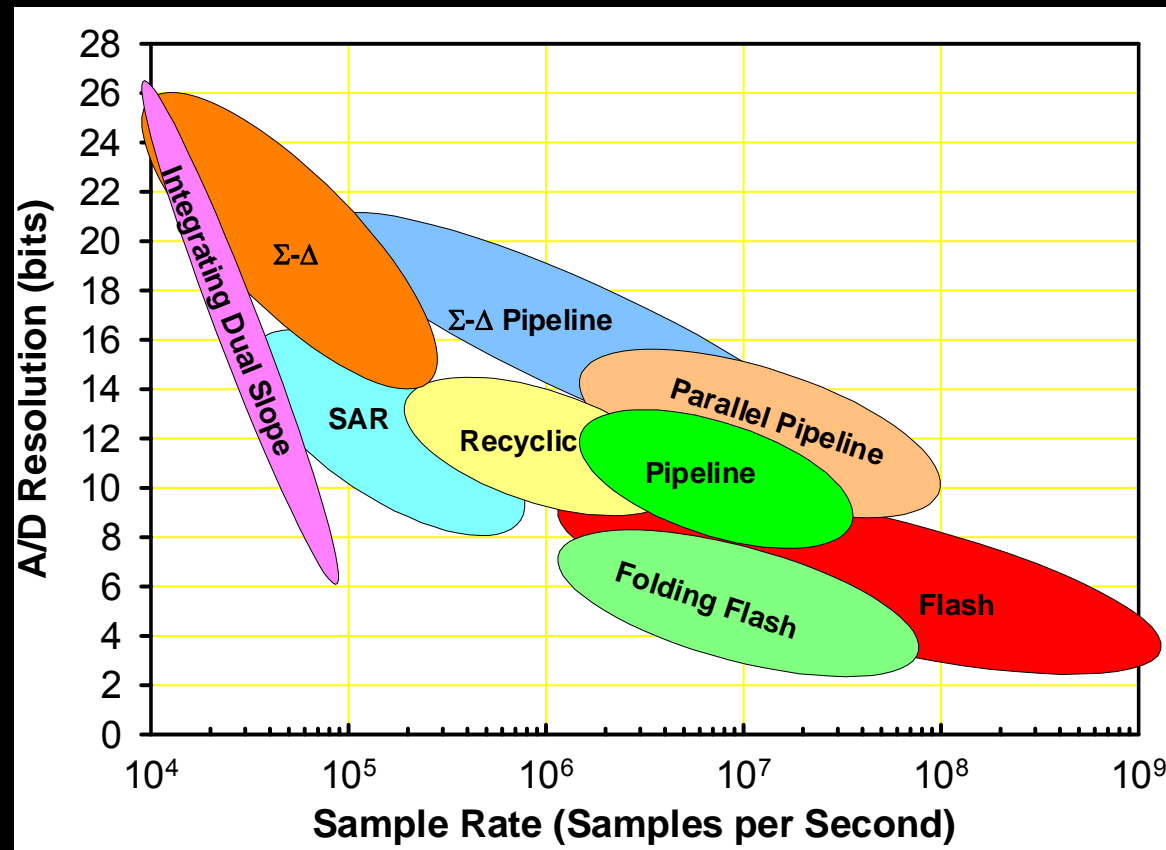
Pipeline ADC



Cleared for Public Release (OSR Case 08-S-0319), but Unpublished. ITAR Restricted – 22 CFR 125.4(b)(13) Applicable

ADC Development Optimized for Applications

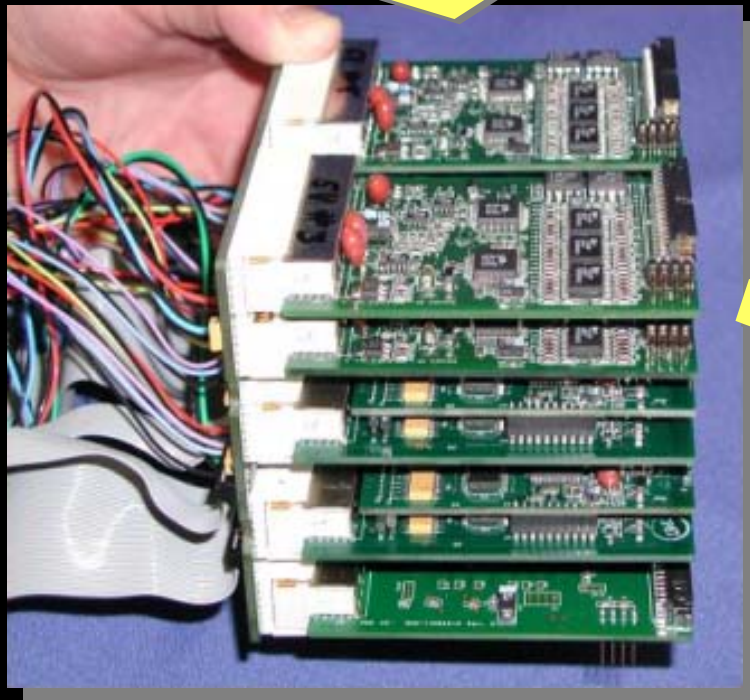
- Depending on resolution, sample rate and power consumption requirement, different architectures for ADCs are used.
- Pipeline ADCs used for video rate applications.
- Successive Approximation Register (SAR) ADCs are used for medium speed, higher resolution applications.
- Sigma-Delta ADCs are used for slow speed, very high resolution applications.



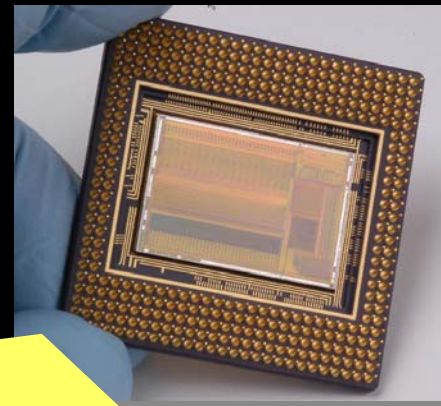
The SIDECAR ASIC

Complete Electronics on a Chip

Replace this



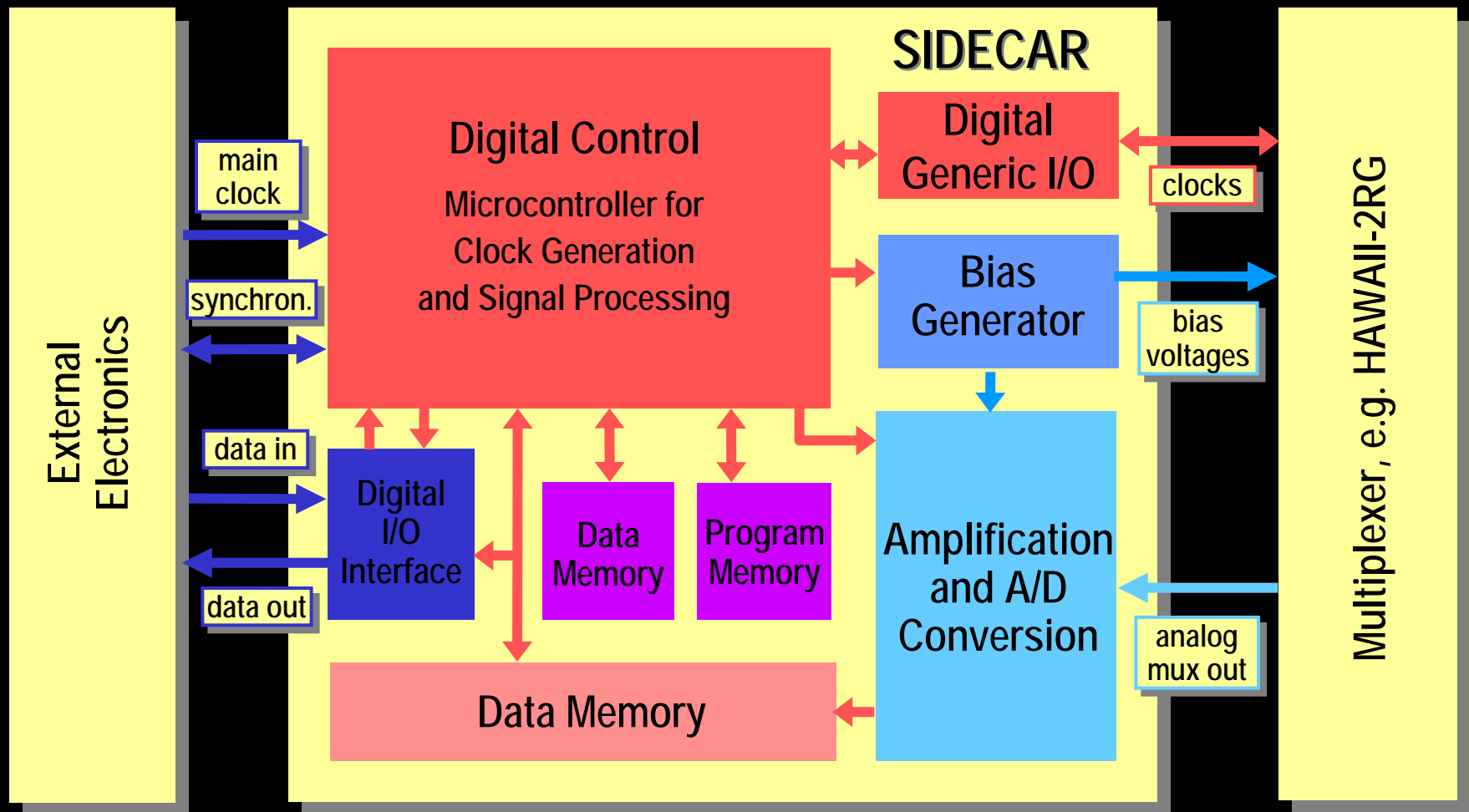
with this!



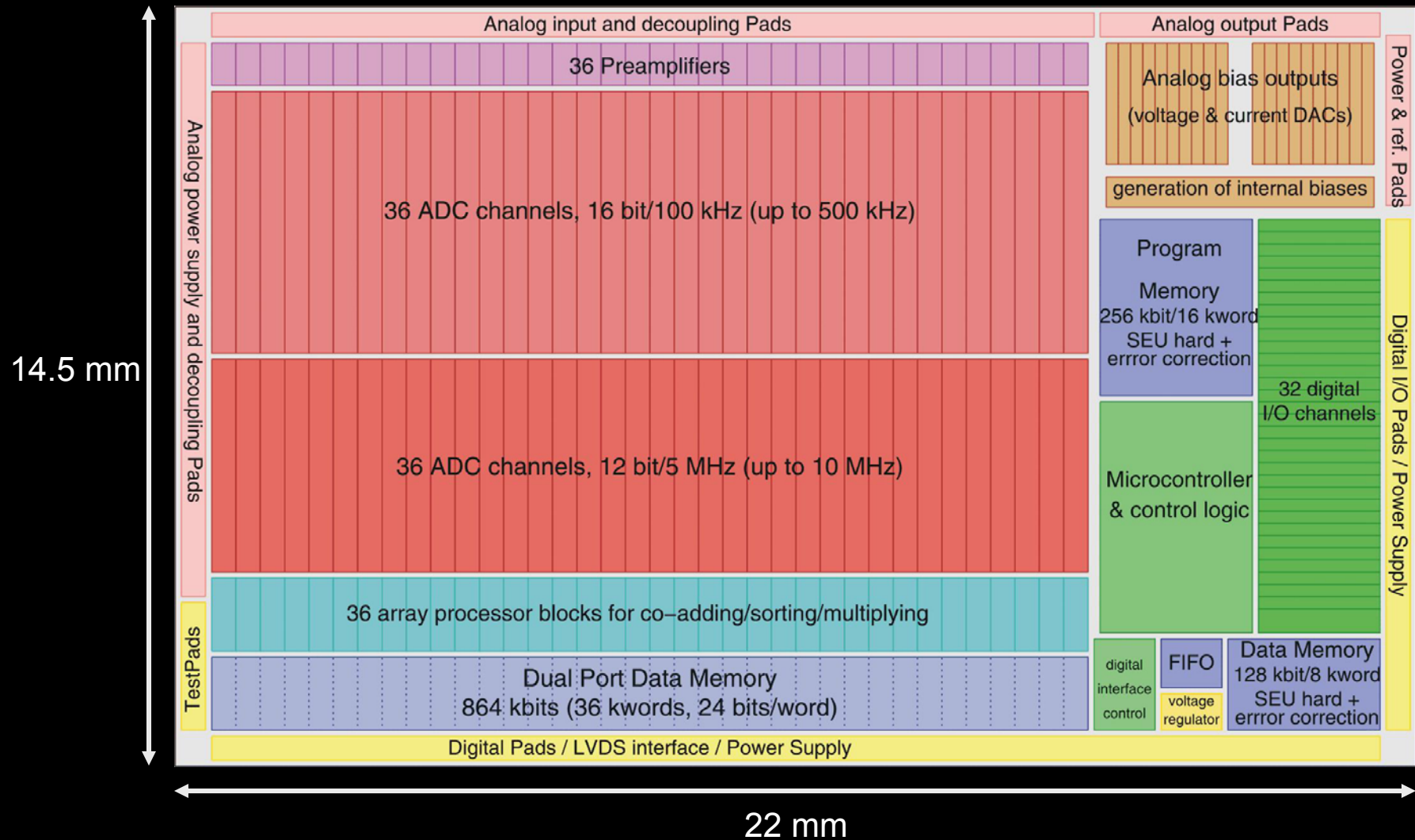
1% volume
1% power
less hassle

SIDECAR: **S**ystem for **I**mage **D**igitization, **E**nhancement, **C**ontrol **A**nd **R**etrieval

SIDECAR ASIC Functionality

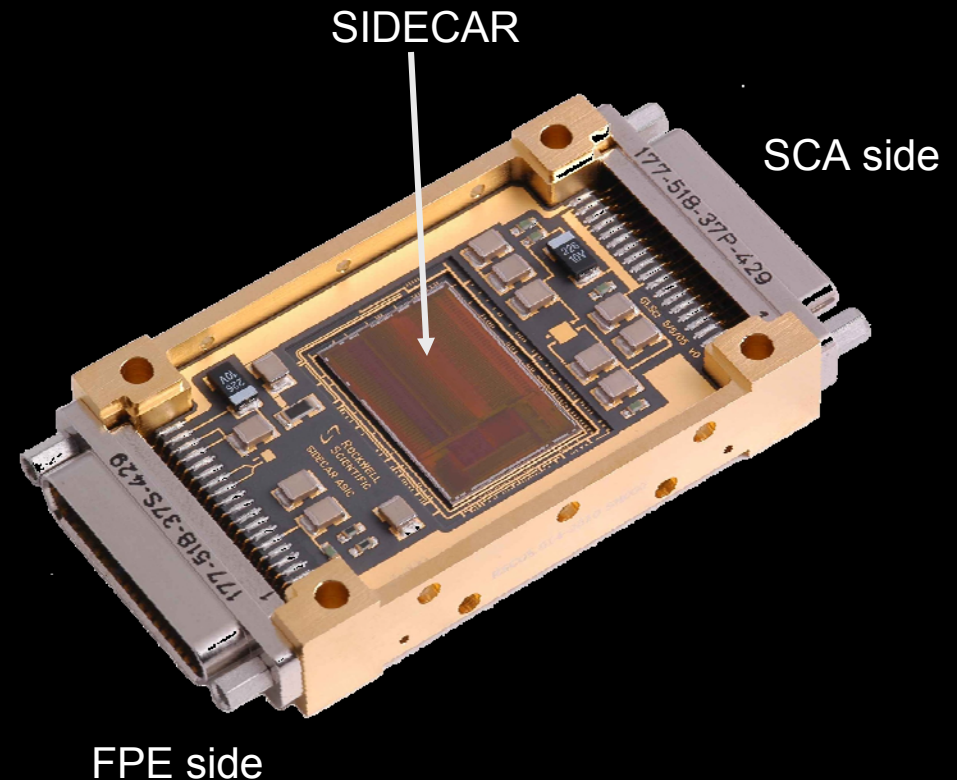


SIDECAR ASIC Floorplan



SIDECAR ASIC Flight Package for JWST

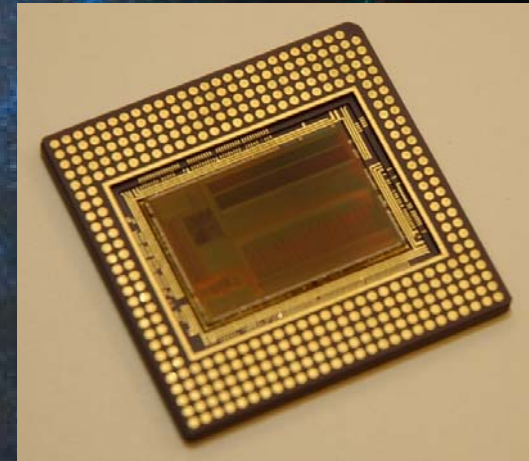
- Ceramic board with ASIC die and decoupling caps
- Invar box with top and bottom lid
- Two 37-pin MDM connectors
 - FPE-to-ASIC connection
 - ASIC-to-SCA connection
- Qualified to NASA Technology Readiness Level 6 (TRL-6)
- 11 mW power when reading out of four ports in parallel, with 16 bit digitization at 100 kHz per port.



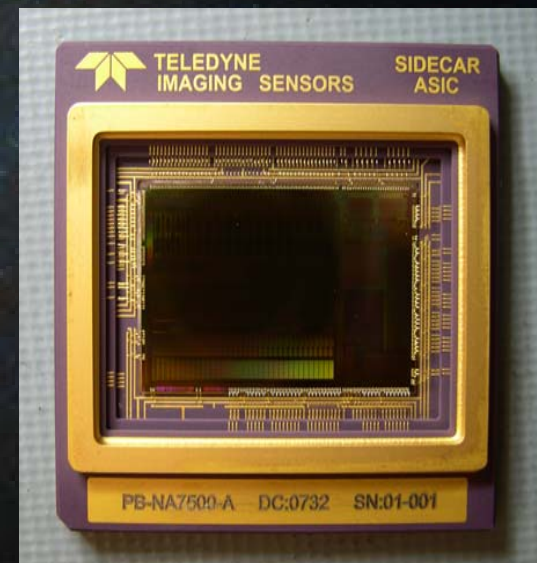
SIDECAR ASIC LGA Package

- Package for board level mounting:
 - 337-pin LGA ceramic carrier
- Currently used for all ground-based applications
- Existing LGA package cannot be hermetically sealed: not enough room to attach the seal ring.
- Modified version is operating on the Hubble Space Telescope:
 - Uses “cavity-up” instead of “cavity-down”
 - Provides large seal ring for hermetic seal
 - Pinout is exactly mirrored compared to original LGA package
 - Used by Hubble Space Telescope Advanced Camera for Surveys (ACS) Repair (image in background is from first light press release)

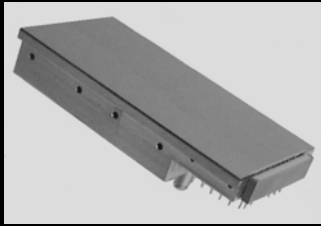
LGA
(old)



LGA
(new)

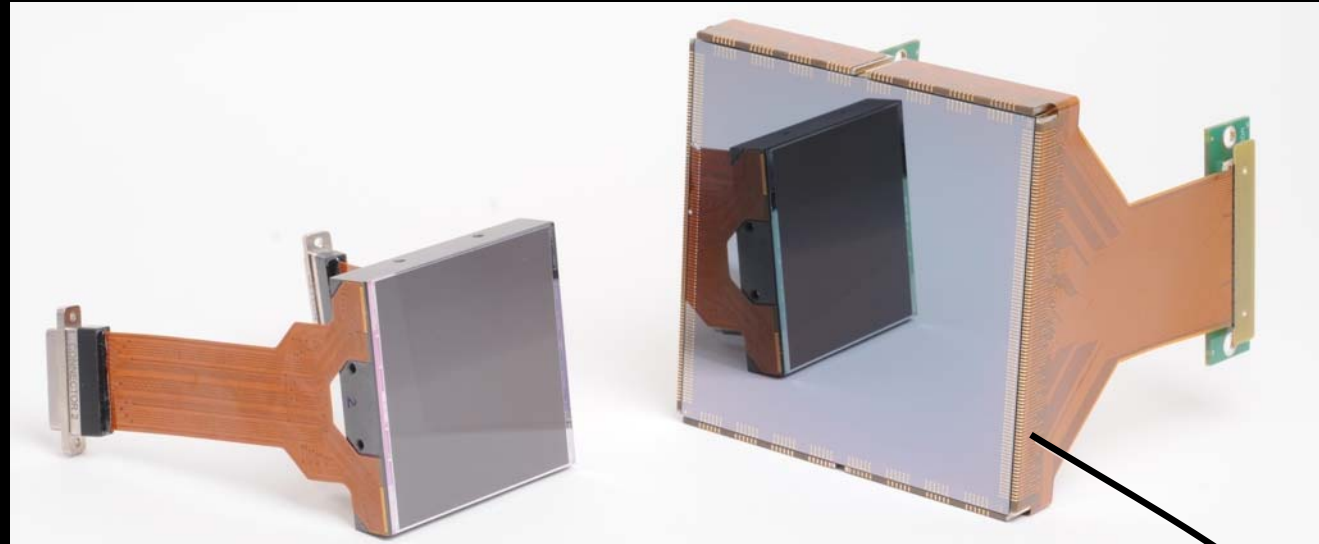


World's Largest Monolithic CCDs



e2v

8.4 million pixels
2048×4096, 15 μm
18.9 cm^2

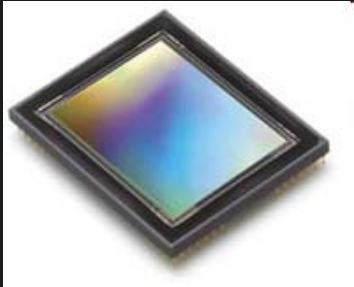


e2v

16.8 million pixels
4096×4096, 15 μm
37.7 cm^2

STA

111.5 million pixels
10,240×10,240, 9 μm
90.3 cm^2

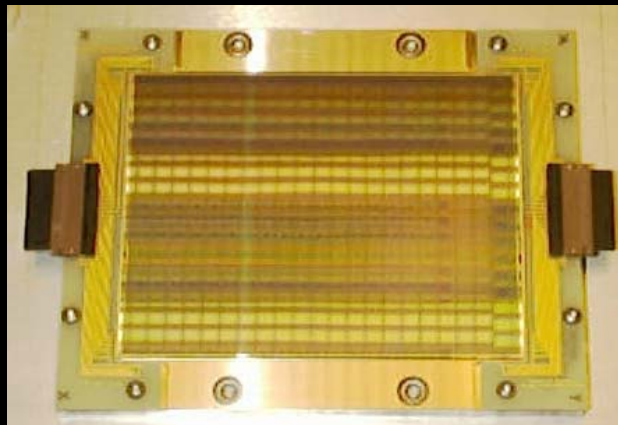


Dalsa

48 million pixels
6000×8000, 6 μm
17.3 cm^2

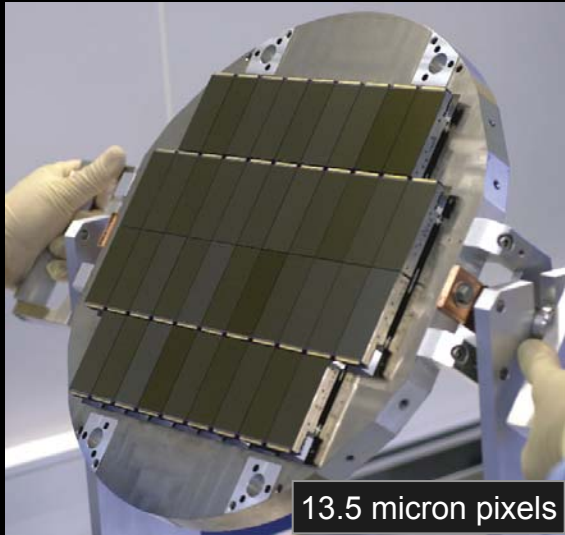
Philips

66.1 million pixels
7168×9216, 12 μm
95.1 cm^2



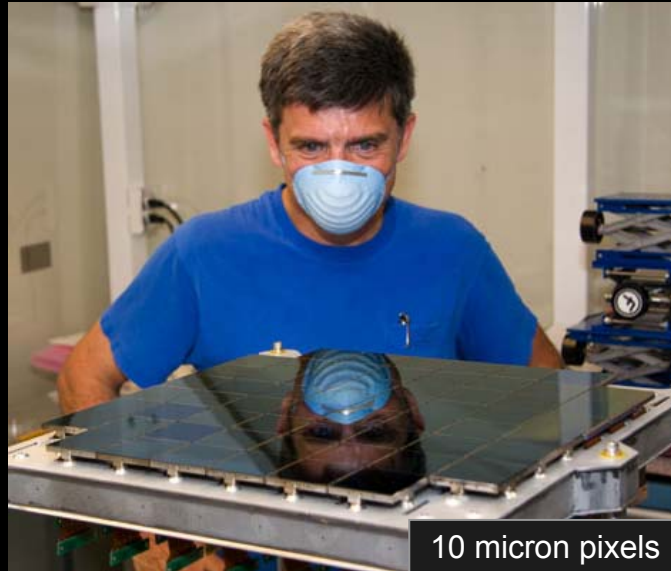
445 Mpixel mosaic

CCD Mosaics



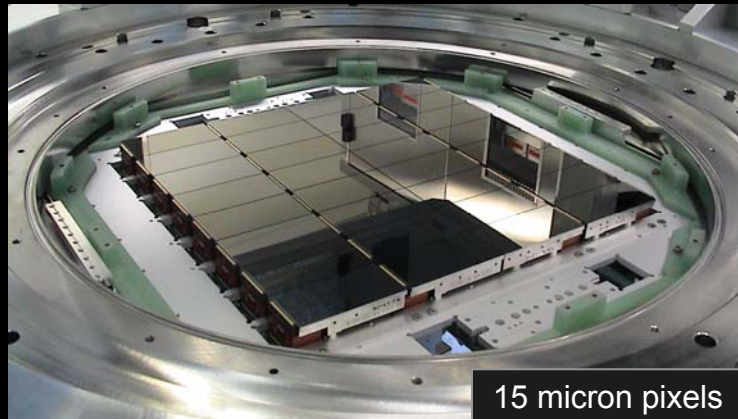
13.5 micron pixels

MegaCam on the CFHT - 378 million pixels



10 micron pixels

Pan-STARRS 1
1,397 million pixels



15 micron pixels

OmegaCam on the VST - 268 million pixels



LSST
3,171 million pixels



10 micron pixels

Growth of CCD mosaics

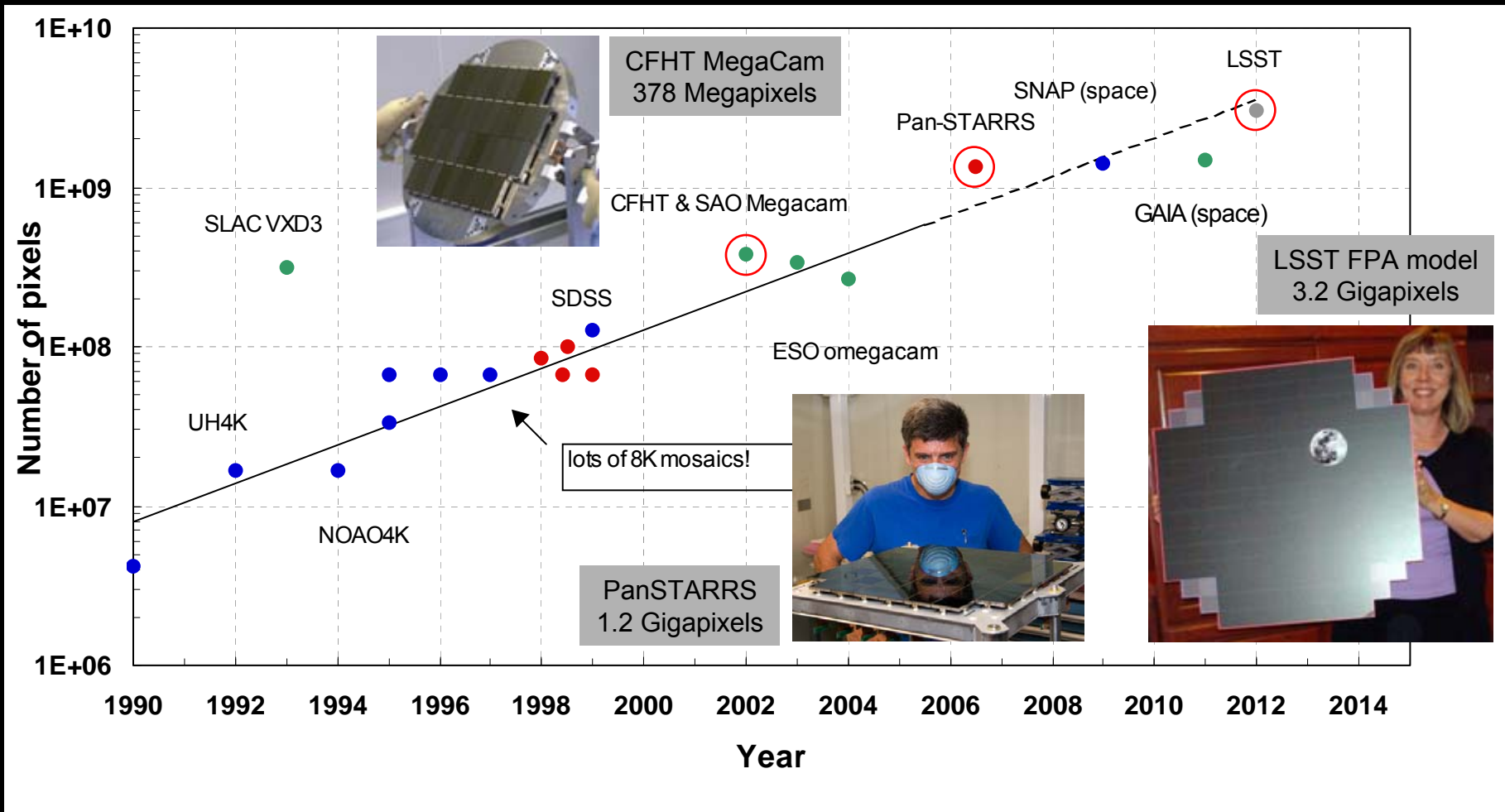
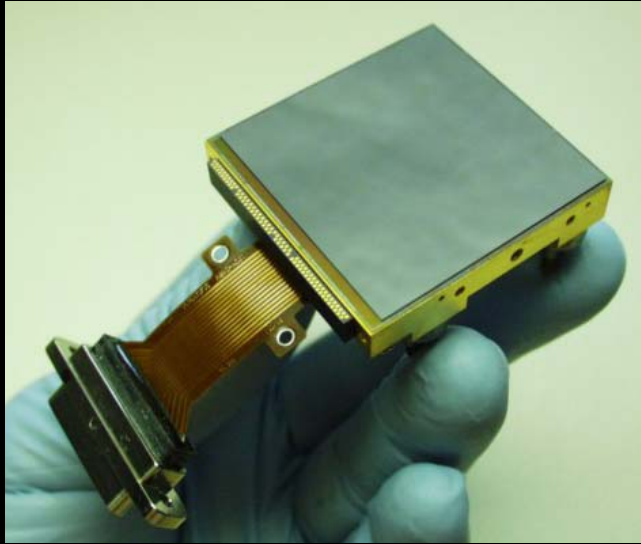


Illustration of large focal plane sizes, from Luppino 'Moore's' law

Focal plane size doubles every 2.5 years

Infrared Mosaics



HgCdTe 2K x 2K, 18 μm pixels

2x2



HgCdTe 4K x 4K mosaic, 18 μm pixels

Teledyne Imaging Sensors

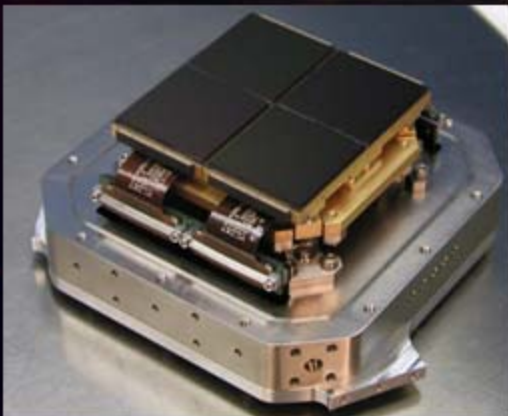
Another 4096 x 4096 pixel IR mosaic comes on-line

July 2007 - First light of HAWK-I (High Acuity, Wide field K-band Imaging)

European Southern Observatory 4096x4096 pixel mosaic of H2RGs

6th operational 4Kx4K mosaic of H2 / H2RGs: ESO, Gemini, CFHT, UH, UKIRT, SOAR

Two more 4Kx4K mosaics to be commissioned in 2010: OCIW, MPIA



Serpens Star Forming Region
1 million year old stars



HAWK-I at Paranal

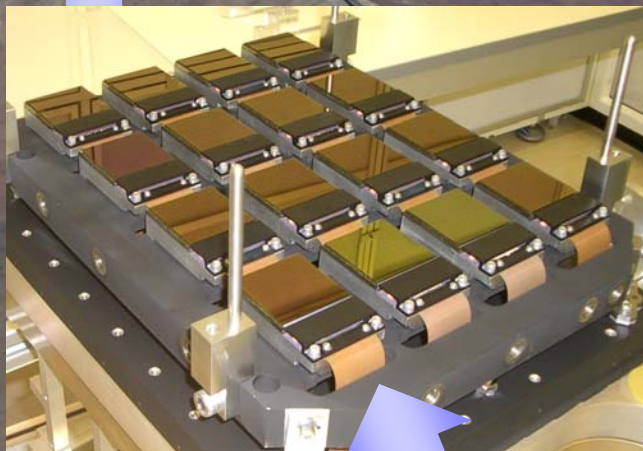
ESO Press Photo 36d/07 (22 August 2007)



VISTA Telescope (ESO)



Mockup of image on sky with Moon



4x4 Mosaic
67 Megapixels

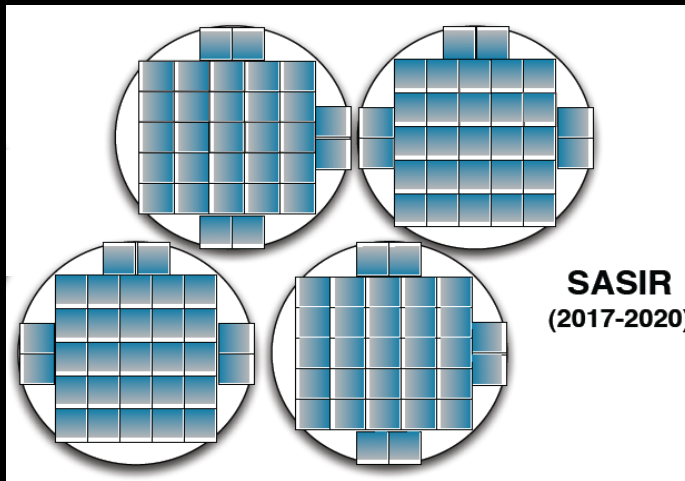
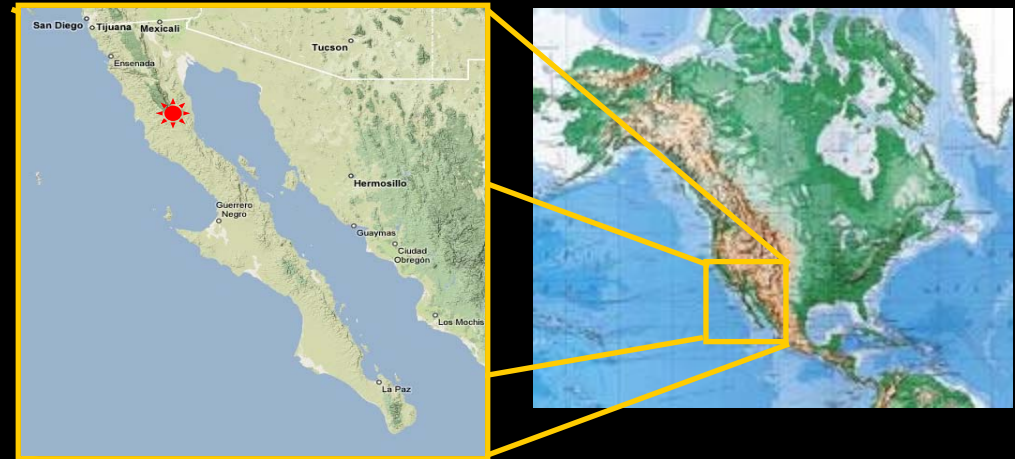


Raytheon Vision Systems

HgCdTe 2K x 2K,
20 μ m pixels



Synoptic All-Sky InfraRed (SASIR) Telescope

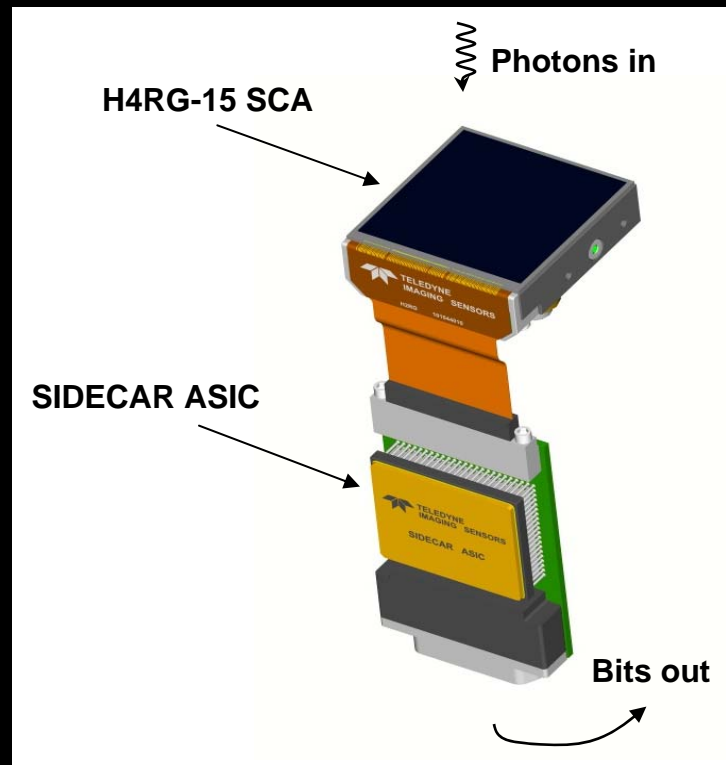


- 6.5-meter primary
- Four color camera
 - Y, J, H, K
- 31 2K×2K IR arrays for each channel
- 520 million IR pixels

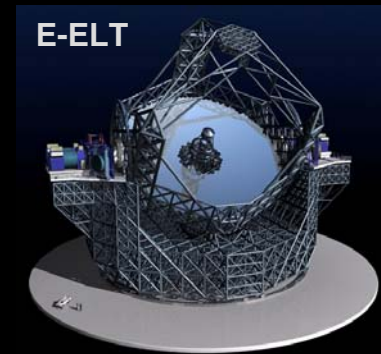
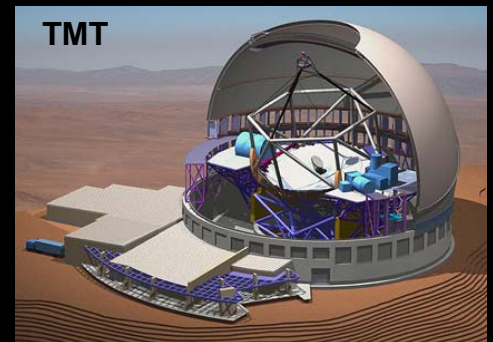


Large IR Astronomy Focal Plane Development

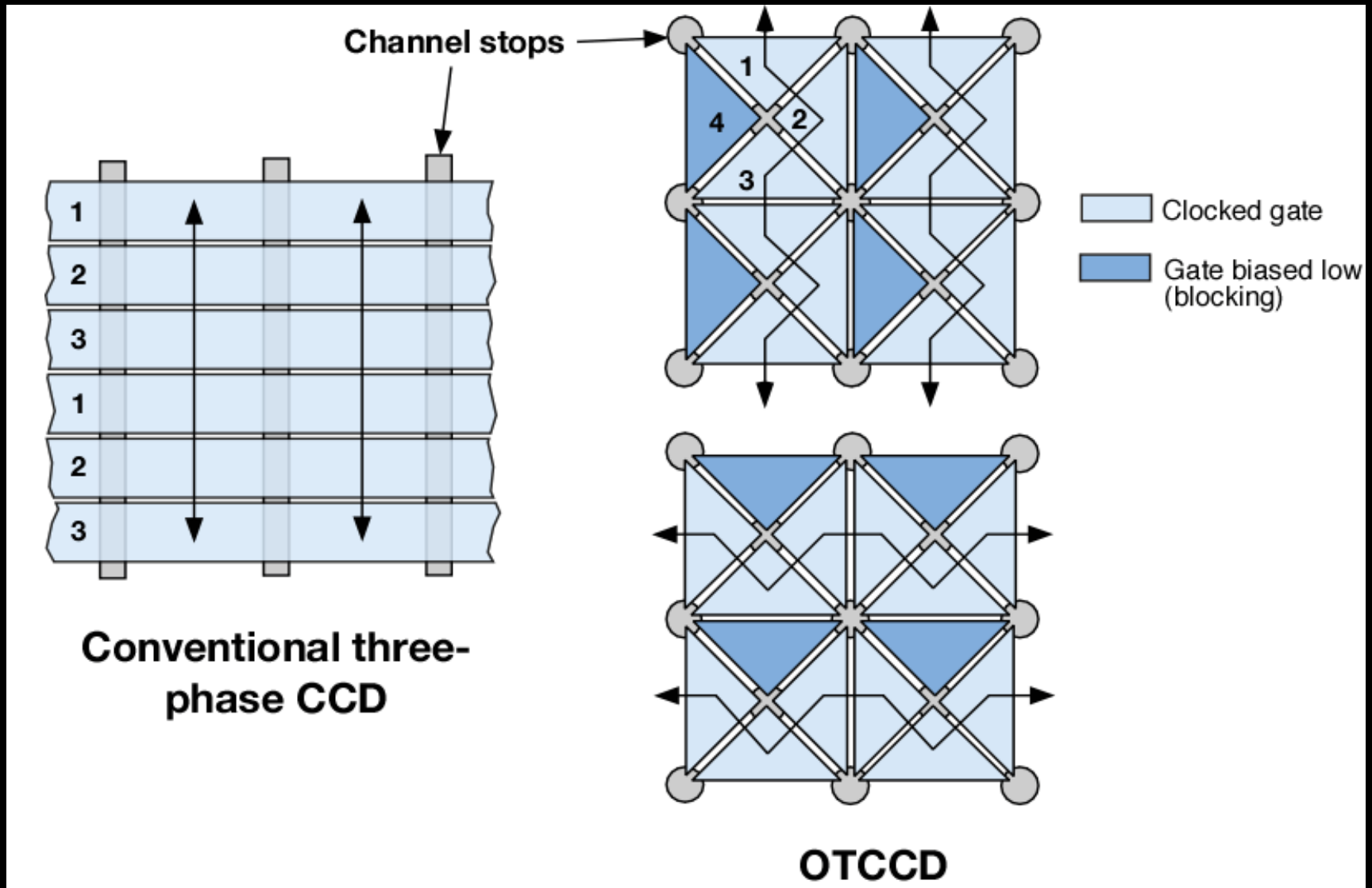
The Next Step: 4096×4096 pixels



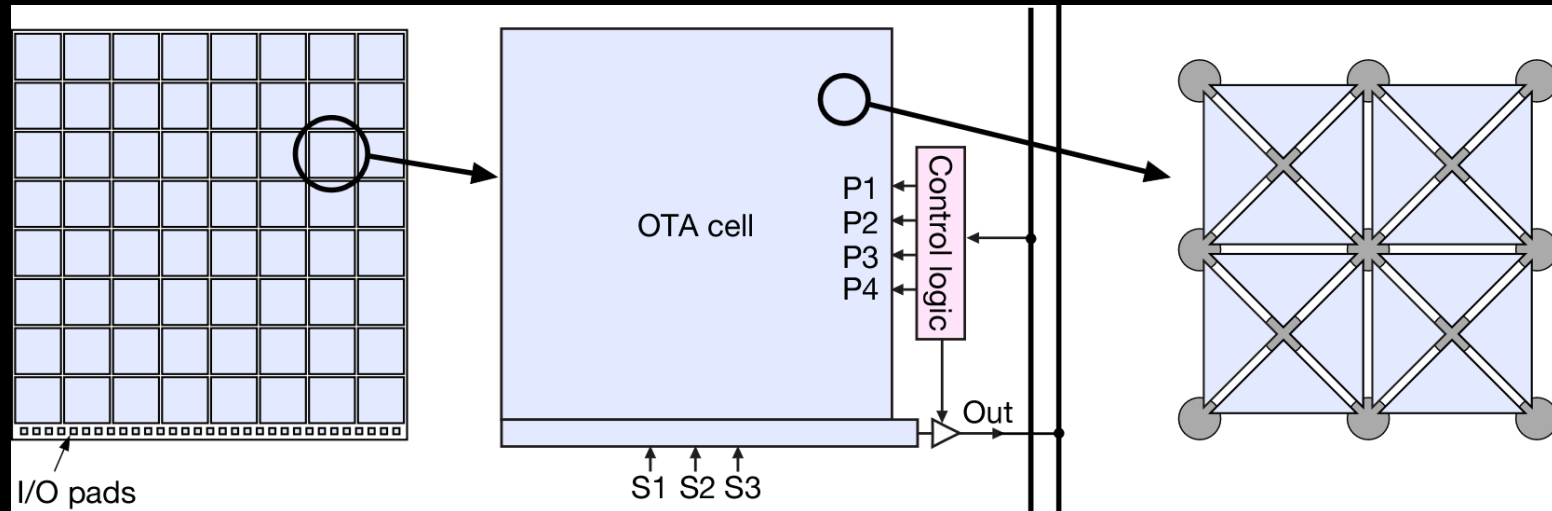
- 4096×4096, 15 μm array
- Design readout circuit for high yield
 - 4 ROICs per 8-inch wafer
- 4-side buttable for large mosaics
- Developed for the Extremely Large Telescopes



Conventional vs. Orthogonal-Transfer CCDs



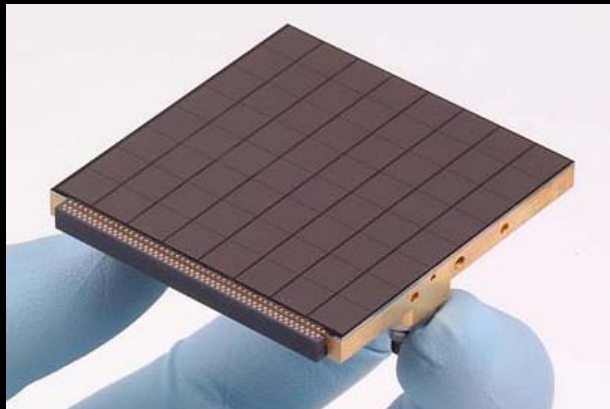
Orthogonal Transfer Array



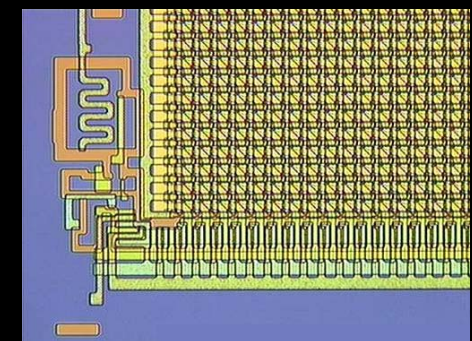
OTA: 8x8 array of OTCCD cells

OTA cell with I/O control

Four-phase OTCCD structure



- **New device paradigm**
 - 2D array of independent OTCCDs
 - Independent clocking and readout of OTCCDs
- **Advantages**
 - Enables spatially varying tip-tilt correction
 - Isolated defective cells tolerable (higher yield)

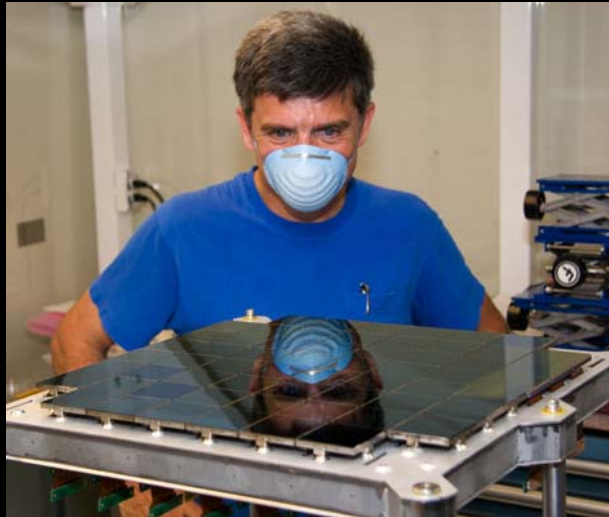


~250 microns

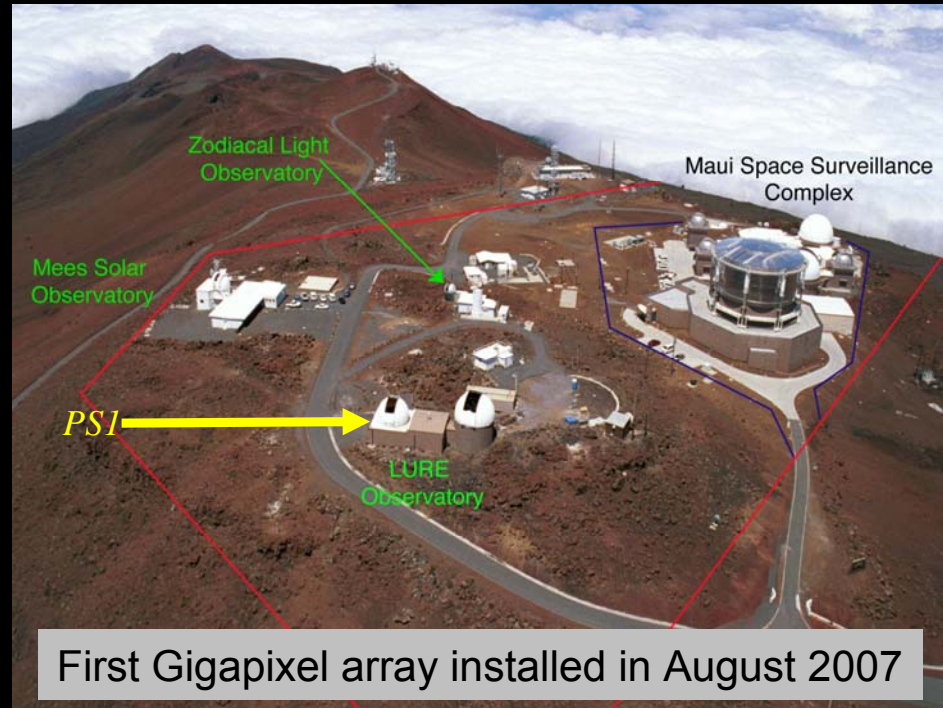
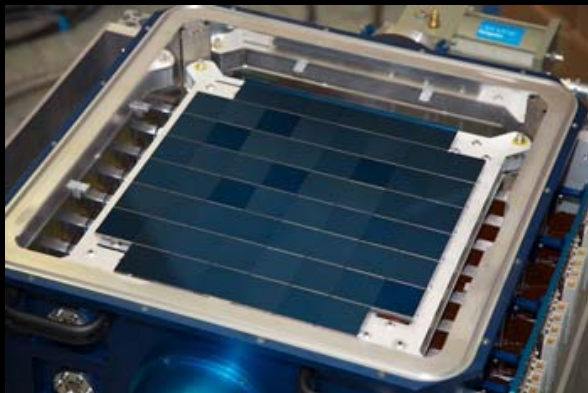
MIT Lincoln Laboratory

Pan-STARRS 1 on Haleakala (Maui)

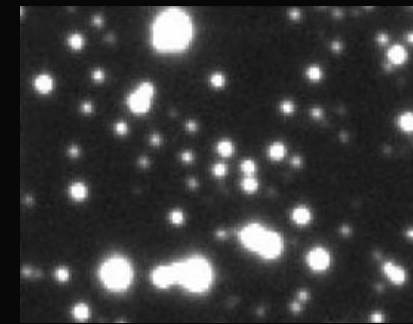
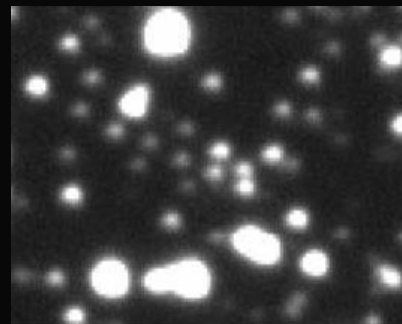
1.4 Gigapixel array of orthogonal transfer CCDs



John Tonry & his masterpiece

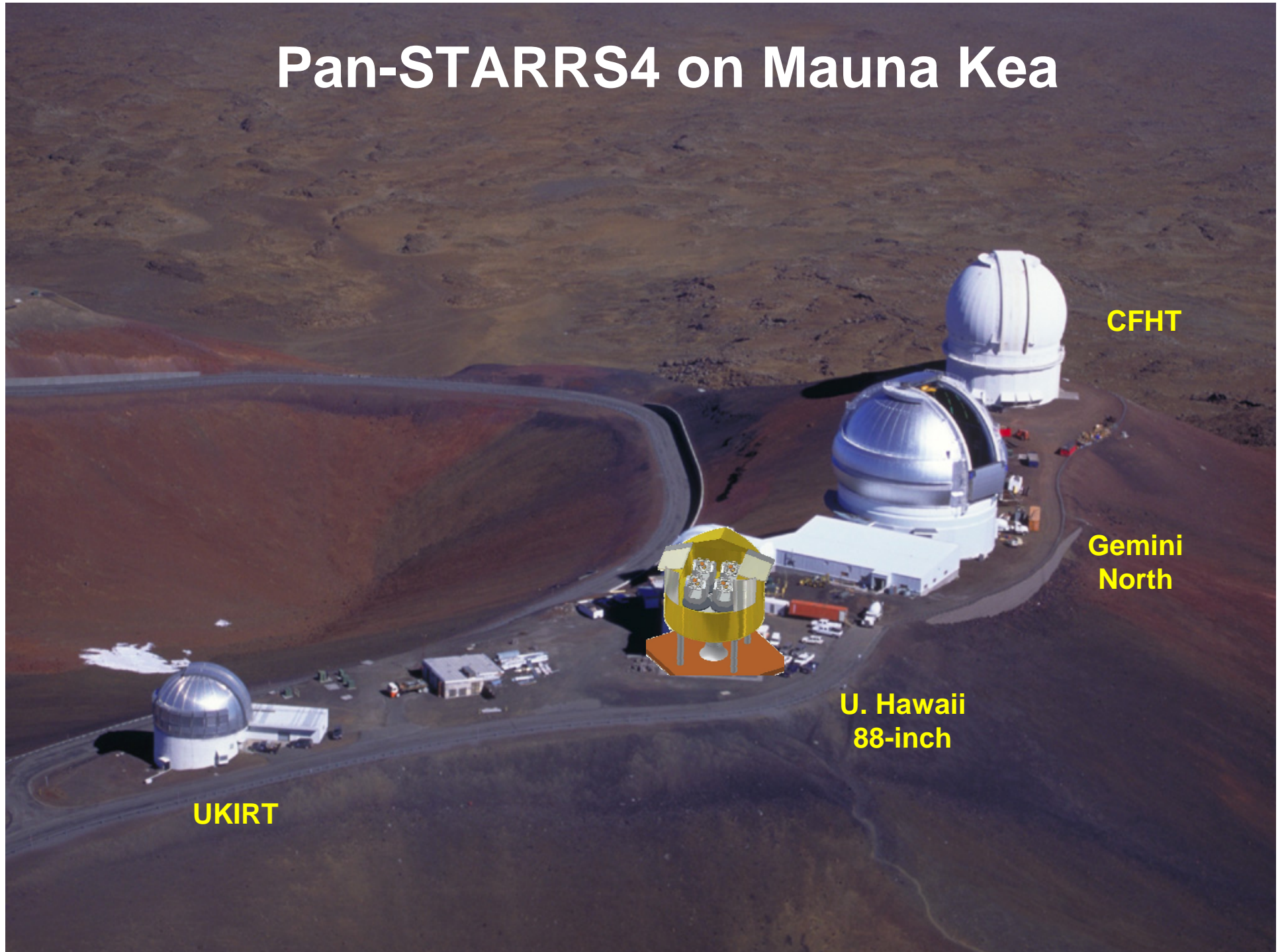


First Gigapixel array installed in August 2007



Improved resolution from OTCCD Tip-Tilt Correction

Pan-STARRS4 on Mauna Kea



UKIRT

U. Hawaii
88-inch

Gemini
North

CFHT

Avalanche Process before Charge-to-Voltage Conversion

Anti-reflection coating
Substrate removal

Detector Materials
Si, HgCdTe, InSb, Si:As

Electric Fields in detector
collect electrical charge

1. Light into detector

2. Charge Generation

3. Charge Collection



Potential for
noiseless
photon counting

CCD

Charge coupled
transfer

MOSFET
Amplifier

4. Charge
Transfer



5. Charge-to-
Voltage
Conversion

6. Digitization

CMOS

Source follower,
CTIA, DI

Random access
or full frame read

4. Charge-to-
Voltage
Conversion

5. Signal
Transfer

Geiger APD Sensor architecture

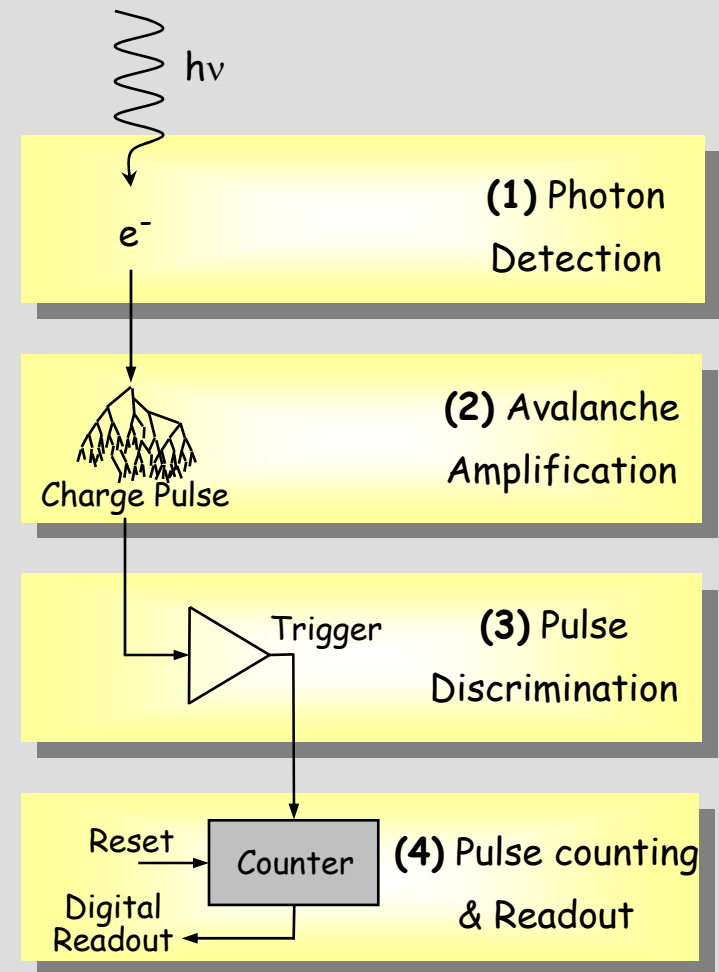
- Four main parts

- 1) Photon detection
- 2) Avalanche amplification (pulse generation)
- 3) Pulse discrimination
- 4) Photon counting and readout circuitry

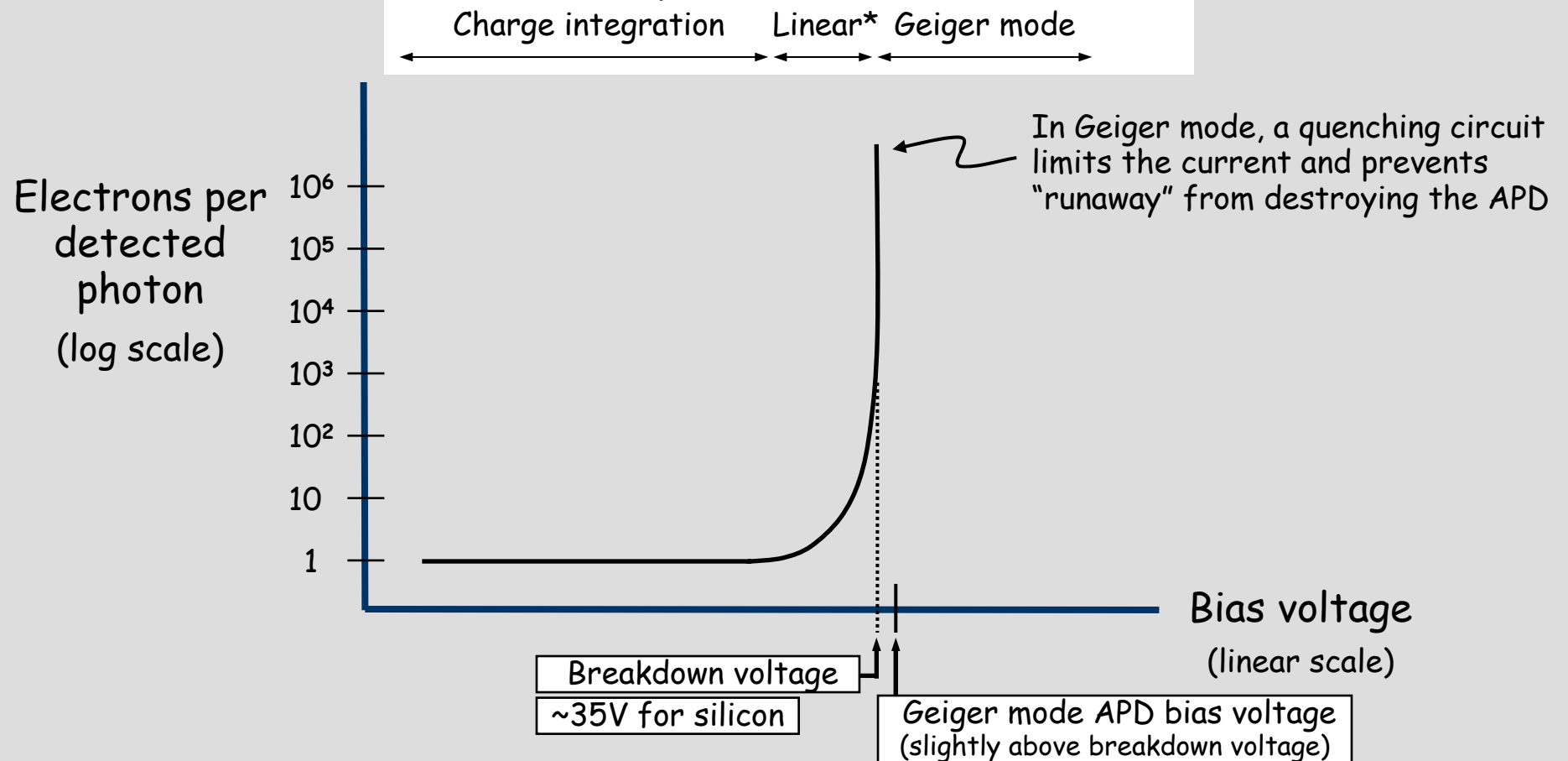
- CMOS circuit used for (3) and (4)

- For (1) and (2) - two options:

- a) Part of CMOS circuit
- b) Put APD into detector material and hybridize to CMOS circuitry



Mode of operation of an APD

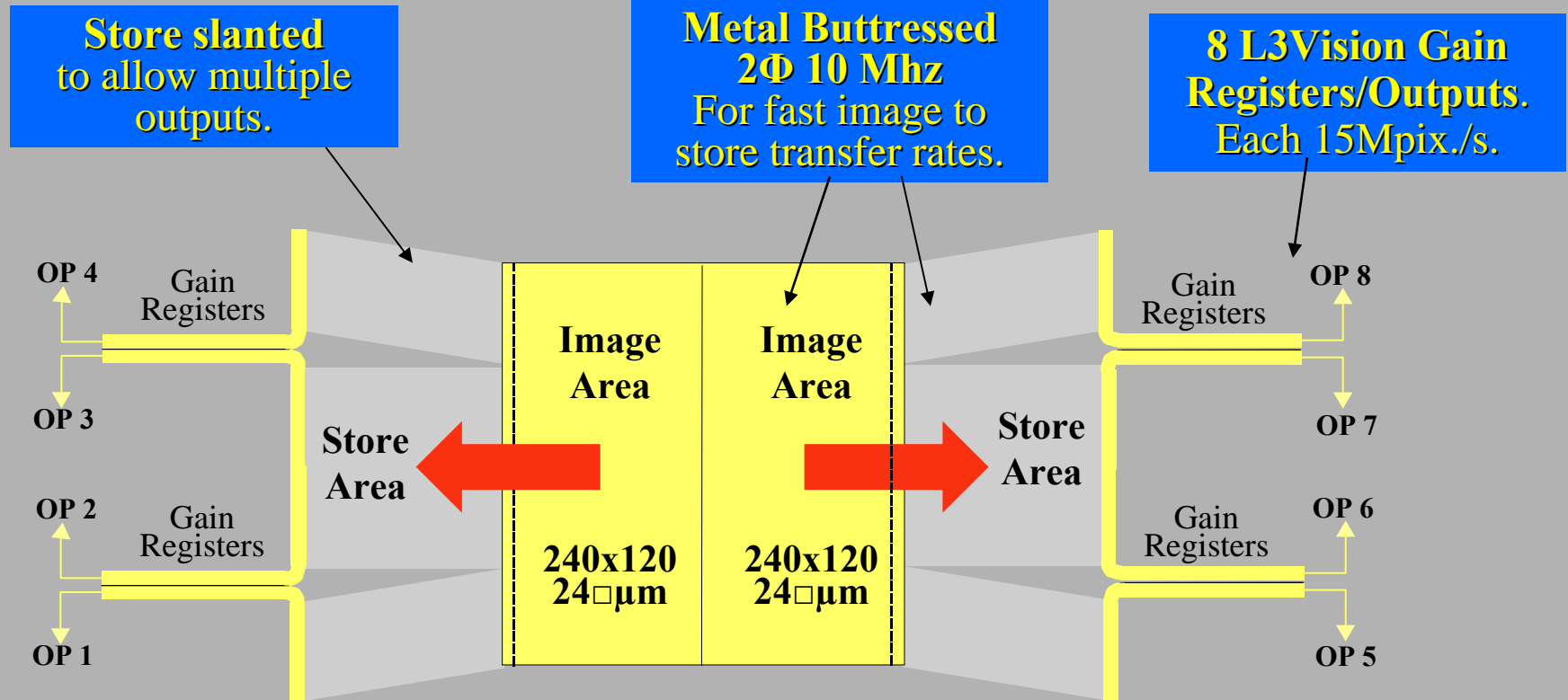


*Linear mode operation of APD

In this mode, the total number of electrons collected in each pixel is a linear function of the number of detected photons.

- However, the amplification process is statistical and there is "excess noise" in linear mode.
- HgCdTe may be a special material with very little excess noise (few %) for avalanching under the appropriate conditions.
 - Electron avalanche HgCdTe (e-APD) with ~5 micron cutoff material ($X \sim 0.33$)
 - Hole avalanche HgCdTe (h APD) with ~1.7 micron cutoff material ($X \sim 0.63$)

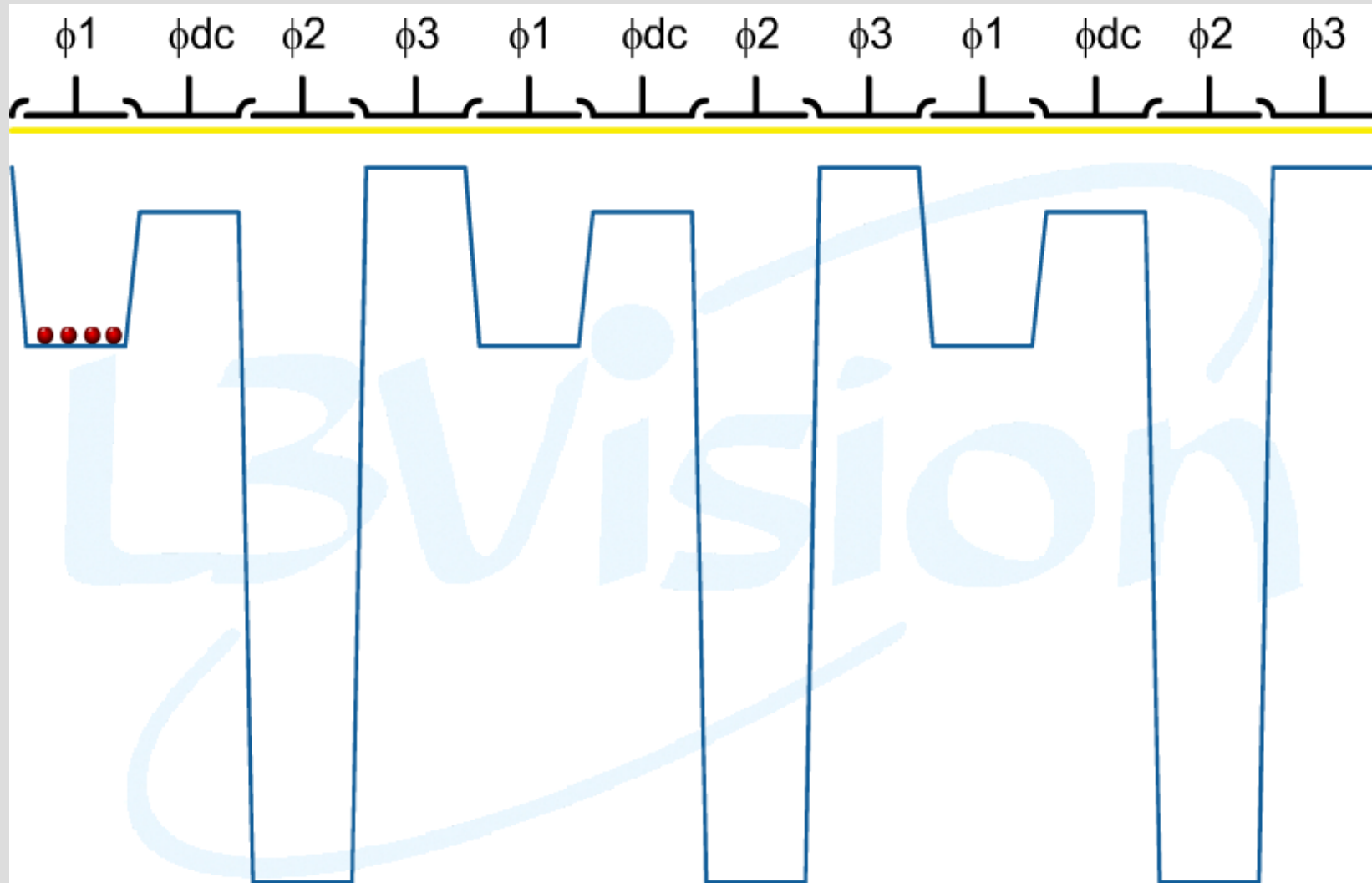
e2v L3CCD - Serial Gain Register



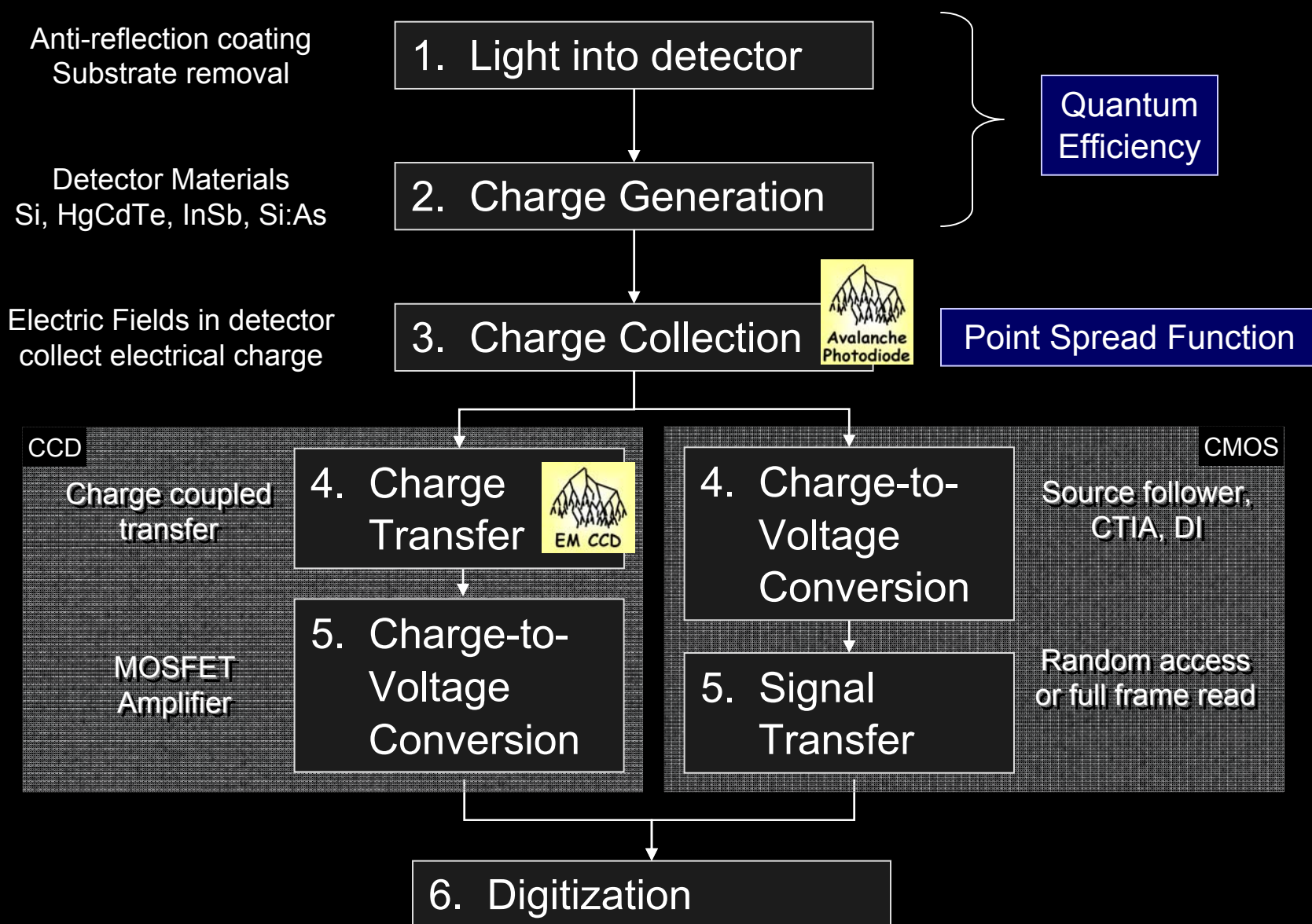
Split frame transfer 8-output back-illuminated e2v L3Vision CCD.

e2v L3Vision Technology

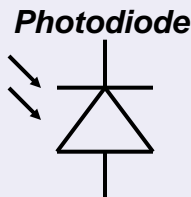
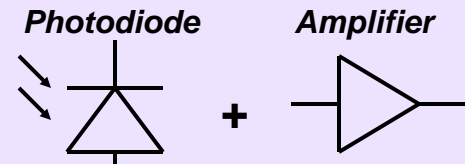
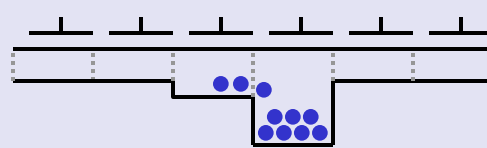
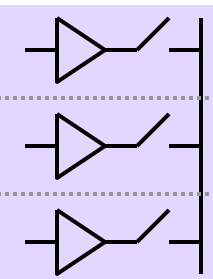
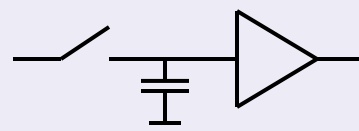
Effective noise
is $\sqrt{2}$ photon noise



6 steps of optical / IR photon detection



CCD / CMOS Comparison

	CCD Approach	CMOS Approach
Pixel	 <p>Charge generation & charge integration</p>	 <p>Charge generation, charge integration & charge-to-voltage conversion</p>
Array Readout	 <p>Charge transfer from pixel to pixel</p>	 <p>Multiplexing of pixel voltages: Successively connect amplifiers to common bus</p>
Sensor Output	 <p>Output amplifier performs charge-to-voltage conversion</p>	<p>Various options possible:</p> <ul style="list-style-type: none"> - no further circuitry (analog out) - add. amplifiers (analog output) - A/D conversion (digital output)

CMOS = Complimentary Metal Oxide Semiconductor

Comparison CMOS vs. CCD for Astronomy

Property	CCD	Hybrid CMOS
Resolution	> 4K x 4K	up to 4K x 4K
Pixel pitch	10 – 20 μm	10 – 40 μm (up to 100 μm if required)
Typical wavelength coverage	400 – 1050 nm	400 – 1050 nm with Si PIN 400 – 18,000 nm with HgCdTe 400 – 5,000 nm with InSb
Noise	Few electrons	Few electrons with multiple sampling
Shutter	Mechanical	Electronic, rolling shutter, snapshot
Power Consumption	High	Typ. 10x lower than CCD
Radiation	Sensitive	Much less susceptible to radiation
Control Electronics	High voltage clocks, at least 2 chips needed	Low voltage only Can be integrated into single chip
Special Modes	Orthogonal Transfer Binning	Windowing, Guide Mode, Random Access, Reference Pixels, Large dynamic range (up the ramp)

- Silicon PIN hybrid detectors have become a serious alternative to CCDs providing a number of advantages, especially for space applications.
- **Backside illuminated monolithic CMOS** which combines the best of CMOS and CCD features will make major strides before the next detector workshop.

Thank you for your attention